Master's thesis

NTNU
Norwegian University of Science and Technology
Faculty of Medicine and Health Sciences
Kavli Institute for Systems Neuroscience

Rikke Bie

# Micro- and mesoscale neuroplasticity of *in vitro* cortical neuronal networks

Master's thesis in Neuroscience

Supervisor: Ioanna Sandvig, Ph. D; Axel Sandvig, Ph. D, M.D.; Ola Huse Ramstad (PhD candidate)

June 2020

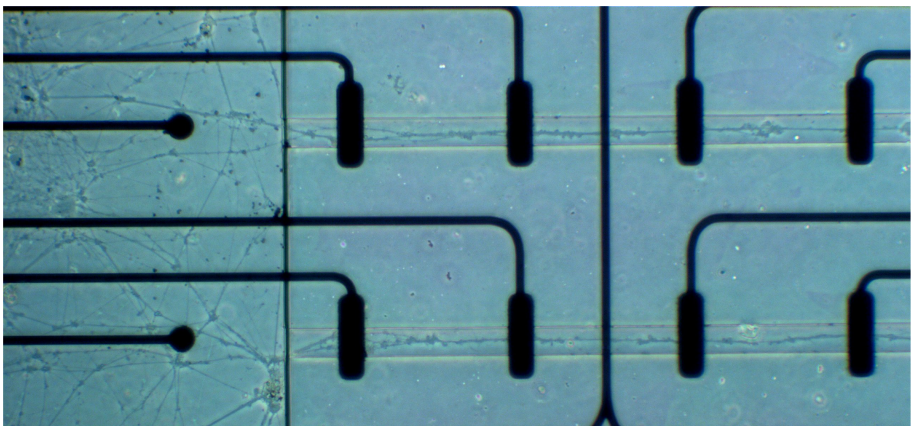

NTNU
Norwegian University of Science and Technology

Rikke Bie

# Micro- and mesoscale neuroplasticity of *in vitro* cortical neuronal networks

Master´s thesis in Neuroscience
Supervisors: Ioanna Sandvig, Ph. D; Axel Sandvig, M.D., Ph. D; Ola Huse Ramstad (PhD candidate)
Trondheim, June 2020

Norwegian University of Science and Technology
Faculty of Medicine and Health Sciences
Kavli Institute for Systems Neuroscience

NTNU
Kunnskap for en bedre verden

## SAMMENDRAG

**Bakgrunn:** Aksonskade er et kjennetegn ved traumatiske skader tilført sentralnervesystemet (CNS). Pasienter lider ofte av langvarige funksjonsnedsettelser som et resultat av den komplekse patofysiologien assosiert med slike skader, og grunnet mangel på en iboende repareringsevne i det voksne CNS. Nevroplastisitet i CNS kan potensielt utnyttes til å reetablere funksjonsfriskhet. En økt forståelse for mekanismene involvert i aksonskade og nevroplastisitet kan gi ny innsikt til potensielle metoder som har som hensikt å begrense nevrodegenerering og metoder som kan oppfordre til funksjonsfriskhet etter skade. Dette kan igjen bidra til utvikling av mer presise og spesifikke rehabiliteringsstrategier/terapier. Ved bruk av en *in vitro* tilnærming kan vi øke vår forståelse av aksonskade og studere spesifikke mekanismer ved nevroplastisitet.

**Mål:** Dette prosjektet var delt inn i tre eksperimenter. Målet for eksperiment 1 var å utforske aspekter ved *in vitro* kortikal aksonskade og evaluere effekter av ekstracellulær stimulering med γ-aminobutyric acid (GABA) etter aksotomi, ved bruk av mikrofluidiske brikker. Målet for eksperiment 2 var å stimulere *in vitro* kortikale nettverk med gjentatt «tetanisk stimulering» (TS) levert gjennom en sentral elektrode på mikroelektrode-matriser (MEAer) for så å estimere nettverkenes nevroplastiske responser. Målene for eksperiment 3 var å spesifikt styrke en bestemt funksjonell forbindelse innen kortikale nettverk kultivert på mikrofludiske MEAer ved levering av elektriske pulser til en presynaptisk så postsynaptisk nettverksnode. I tillegg hadde vi som mål å estimere potensielle endringer i akson-signalisering i respons til den samme stimuleringen.

**Resultater:** Ingen aksoner var observert i mikrokanalene som kobler cellekamrene i de mikrofluidiske brikkene over tre uker med monitorering (eksperiment 1). Kortikale nettverk justerte styrken på spesifikke funksjonelle koblinger etter fokal TS (eksperiment 2). Endringene var svært uforutsigbare ettersom både retningen (potensering vs. depresjon) og omfanget (antall endrede koblinger) av endringene varierte mellom de kortikale nettverkene. Vi fant at aksoner kan øke sin forplantningshastighet og signal amplitude som et resultat av elektrisk stimulering (eksperiment 3). Disse endringene ble observert både rett etter og tre dager etter stimulering. Stimuleringen resulterte i tillegg til en økning i korrelasjon mellom aktiviteten til de to stimulerte nettverksnodene.

**Diskusjon:** Den første delen av diskusjonen fokuserer på potensielle forklaringer på mangelen av aksoner i mikrokanalene (eksperiment 1). Videre diskuteres potensielle forklaringer på de varierte responsene til TS mellom de ulike kortikale nettverkene (eksperiment 2). Med henhold til eksperiment 3 diskuteres ulike mekanismer som kan ligge til grunn for de kort- og langvarige endringene i akson-signalisering etter stimulering, i tillegg til den observerte økningen i korrelert aktivitet mellom de to stimulerte nodene. Funksjonelle betydninger av endringer i akson-signalisering blir også utforsket. Den siste delen av diskusjonen tar for seg betydningen resultatene kan ha i lys av til skade.

**Konklusjon:** Evaluering av potensielle effekter av GABA-stimulering etter *in vitro* kortikal aksotomi gjenstår for fremtidig forsking. Resultatene fra eksperiment 2 understreker kompleksiteten ved nervroplastisitet i CNS, mens eksperiment 3 viser at det er mulig å styrke bestemte funksjonelle koblinger innen et *in vitro* kortikalt nettverk. Resultatene fra eksperiment 3 foreslår i tillegg at aksoner kan være et mål i stimuleringsbaserte rehabiliteringsstrategier. Resultatene fra dette prosjektet er et bidrag til forskning hvis mål er økt forståelse av nevroplastisitet i CNS på mikro- og mesoskala.

## ABSTRACT

**Background:** Axonal injury is a hallmark of traumatic central nervous system (CNS) injuries. Patients often suffer from prolonged functional deficits due to the complex pathophysiology associated with such injuries, as well as due to the lack of intrinsic repair mechanisms in the adult CNS. Importantly, mechanisms of CNS neuroplasticity can potentially be harnessed to promote functional gain. A greater understanding of both CNS axonal injury and neuroplasticity can offer new insights into potential ways of limiting neurodegeneration and promoting functional gain after injury. This, again, can contribute in the development of more accurate and targeted rehabilitation strategies/therapies. One way to increase our understanding of axonal injury and specific mechanisms of neuroplasticity is by using an *in vitro* reductionist approach.

**Aims:** The current project was divided into three experiments. The aim of experiment 1 was to investigate aspects of *in vitro* cortical axonal injury and the effects of extracellular γ-aminobutyric acid (GABA) addition post axotomy, by the use of microfluidic chips. The aim of experiment 2 was to assess the neuroplastic responses of *in vitro* cortical networks to repetitive tetanic stimulation (TS) delivered through one fixed central electrode on microelectrode arrays (MEAs). The aims of experiment 3 were to specifically strengthen targeted functional connections within *in vitro* cortical networks cultured on microfluidic MEAs, by using a paired pulse stimulation protocol, and to assess potential alterations in axonal signalling in response to the same stimulation.

**Results:** No axonal growth was observed within the microtunnels connecting the cell compartments of the microfluidic chips over three weeks of monitoring (experiment 1). Repetitive TS altered the strength of specific functional connections within cortical networks. However, the alterations were highly unpredictable as both the nature (potentiation vs. depression) and the magnitude (nr. of altered connections) varied between the different cortical networks (experiment 2). Both axonal propagation velocity and peak spike amplitude increased as a result of the paired pulse stimulation. The observed alterations were noticed both immediately after stimulation and three days after stimulation. In addition, the paired pulse stimulation resulted in increased correlated activity between the stimulated node pair (experiment 3).

**Discussion:** The first part of the discussion focuses on potential explanations for the lack of axonal growth through the tunnels of the axotomy chip (experiment 1). Next, possible explanations for the observed variability in cortical network responses to TS is explored (experiment 2). In relation to experiment 3, potential mechanisms involved in both the observed short-term and long-term alterations in axonal signalling and the increase in the correlated activity between the stimulated node pair are discussed. Furthermore, the functional effects of altered axonal signalling are considered. The last part of the discussion focuses on the significance of the results within the frame of CNS traumatic injuries.

**Conclusion:** Assessment of the effects of GABA addition after *in vitro* cortical axotomy is left for future investigations. Experiment 2 emphasises the complexity of CNS neuroplasticity, while experiment 3 shows the potential for targeted strengthening of specific connections within a network. In addition, the results from experiment 3 suggests that axons may be a relevant target in stimulation-induced rehabilitation**.** All in all, the current findings add to the body of research aiming to increase our understanding of both micro- and mesoscale neuroplasticity.

## ACKNOWLEDGEMENTS

Firstly, I would like to give a special thanks to my main supervisors Ioanna Sandvig (Ph. D) and Axel Sandvig (Ph. D, M.D.). Thank you for creating a master thesis that allowed me to learn a great deal of research skills and techniques. You've challenged me in critical thinking and offered advice in subjects ranging from planning and executing experiments, to academic writing. Whenever hurdles were met, you amazed me with your positive approach to solving problems. Thank you for your continuous feedback and support throughout this project.

Another big thanks goes to my co-supervisor Ola Huse Ramstad (PhD candidate). Your patience, invaluable knowledge and optimism throughout this project have been greatly appreciated. From teaching me pretty much all the lab skills I know, to answering the thousands of questions I've had, whether face-to-face or over the phone, this wouldn't have been possible without you.

Kristine Heiney (PhD candidate) and Nicolai Winter-Hjelm (MSc student), working together with you on the spike tracking project has been exciting. For all the trying and failing, I feel like it paid off in the end. Your knowledge outside of my area of competence (which you have so openly shared) has been a great resource. You never stopped trying to improve on your ideas, and for that I'm grateful.

To the other PhD candidates in the lab, Vegard Fiskum, Nicholas Christiansen, Ulrich Stefan Bauer, Lars Erik Schiro, Katrine Sjaastad Hansen, Janelle Shari Weir, Christiana Bjørki, and to our lab technician Biljana Arsenic. For your enthusiasm, inspiration, support, question-answering and lunch break chats, thank you all. A special thanks to you Katrine, for taking the time to read my drafts, give feedback, provide help with figure making, and for discussions during city walks - you made it all so much more fun.

To the two other neuroscience master students in the lab, Anna Mikalsen Kollstrøm and Marit Trones Rem, the road of ups and downs has been easier with you there. Thank you for being there to celebrate the successes and for sharing countless hours of frustrations over endless cups of coffee. I wish you both all the best on whatever path you choose.

And then, my family. Thank you for supporting me, not only throughout this master´s, but in my journey to get here, both inside and out of education. Your unconditional love and support mean the world, and it has been assuring to know that you're never more than a phone call away.

My friends in Trondheim, thank you for helping me unwind with boardgames, conversations over good food, hikes, city walks, dancing. You helped me keep my sanity.

Thank you, Ia, for always picking up the phone, for listening, for your rationality, your kindness, your ability to keep me grounded, and for always cheering on me from the sideline. In addition, thank you for helping me write the Norwegian abstract of this thesis.

To Jake, thank you for believing in me, reminding me of the importance of taking breaks, and for listening to my frustrations and for helping me see solutions when I have lost all fate. Most importantly, thank you for making me laugh! Your support throughout this past year has been invaluable.

# TABLE OF CONTENTS

# TABLE OF FIGURES

# TABLE OF TABLES

## ABBREVIATIONS

| | |
|---|---|
| AAD | Acute axonal degeneration |
| AxIS | Axion´s Integrated Studio Software |
| CA1 | Cortical area 1 |
| CNS | Central nervous system |
| D-MEM | Dulbecco´s modified eagle medium |
| D-PBS | Dulbecco´s phosphate buffered saline |
| EPSP | Excitatory postsynaptic potential |
| GABA | γ-aminobutyric acid |
| GAD | Glutamate decarboxylase |
| GS | Goat serum |
| HEPES | 4-(2-hydroxyethyl)-1-piperazineethanesulfonic acid |
| IPSP | Inhibitory postsynaptic potential |
| LTD | Long-term depression |
| LTP | Long-term potentiation |
| MAI | Myelin-associated inhibitor |
| MEA | Microelectrode array |
| NF-H | Neurofilament heavy |
| NMDA | N-methyl-D-aspartate |
| PDMS | Polydimethylsiloxane |
| PEDOT | Poly(3,4-ethylenedioxythiophene) |
| PEI | Polyethyleneimine |
| PenStrep | Penicillin/Streptomycin |
| PFA | Paraformaldehyde |
| PLO | Poly-L-ornithine |
| Post Stim | Post stimulation |
| Pre Stim | Pre stimulation |
| Pt | Platinum |
| PV | Propagation velocity |
| ROS | Reactive oxygen species |
| SCI | Spinal cord injury |
| SD | Standard deviation |
| SNR | Signal-to-noise ratio |
| STC | Spike-tracking chip |
| STDP | Spike-timing dependent plasticity |
| TAI | Traumatic axonal injury |
| TBI | Traumatic brain injury |
| TS | Tetanic stimulation |
| 3 Days Post Stim | Three days post stimulation |

# 1. INTRODUCTION

## 1.1. CENTRAL NERVOUS SYSTEM DEVELOPMENT AND NEURONAL NETWORKS

The organization of the human brain, with billions of neurons and glial cells[1], and trillions of connections between the neurons, is thought to emerge through self-organization principles that together form complex neuronal networks[2]. The study of central nervous system (CNS) connectivity concerns anatomical pathways, and interactions and communication between specific elements of the CNS. These elements can roughly be described on three levels: (i) individual neurons (microscale); (ii) neuronal populations (mesoscale); or (iii) distinct brain regions (macroscale)[3–5].

Two main types of neurons inhabit the human cortex (the outermost part of the brain): excitatory projection neurons and inhibitory interneurons, representing approximately 80% and 20% of all cortical neurons, respectively[6]. Projection neurons are typically glutamatergic in nature and project within and among various areas of the cortex and other areas of the CNS, such as the spinal cord. Interneurons, on the other hand, are GABAergic (GABA = γ-aminobutyric acid) and play an essential role in modulating cortical network activity by forming local connections within cortical microcircuits[7]. Brain function and information flow depend on communication among neurons organized in local and widely distributed interconnected neuronal networks. Physically connecting the individual neurons, networks, and brain regions are the axons; long projections sent out of single neurons responsible for the propagation of information from the cell body to the axon terminal[8].

During CNS development, newborn neurons migrate to their target location which positions them such that they can be integrated within the CNS circuitry. During or after the migration phase, neurons extend neurites, i.e. dendrites and axons, to establish physical connections with other neurons. The neuron´s longest neurite, the axon, establishes connections through axonal growth and guidance. A specialized structure at the tip of the axon, called a growth cone, navigates to find its appropriate destination by responding to electrical, chemical, and structural guidance cues in its environment[9–12]. The guidance cues, which can be either attractive or repulsive and long or short distance in nature, react with receptors on the growth cone surface, which through signalling engages the growth cone´s dynamical cytoskeleton to move forward and turn when appropriate (**Figure 1**)[9,11]. When the axon reaches its target, i.e. another neuron, the growth cone transforms into a presynaptic terminal and a synapse is formed[13]. Synapses are anatomically identifiable intracellular junctions between neurons where information is transferred from a presynaptic to a postsynaptic neuron. The synapse can be electrical[14], which refers to a direct propagation of the electrical stimulus (i.e. the action potential), or more commonly, chemical; the electrical impulse is transmitted indirectly through the release of neurotransmitters into the synaptic cleft (the small space adjacent to the postsynaptic neuron), which then react with receptors located on the postsynaptic neuron [13]. Initially, the developing nervous system fosters a relatively high number of synapses. However, through a process of synaptic pruning during postnatal development, synapses are selectively lost. The phenomenon of synaptic pruning is thought to fine-tune neuronal networks in an activity-dependent manner by strengthening functional connections, while excess connections are lost[15–17].

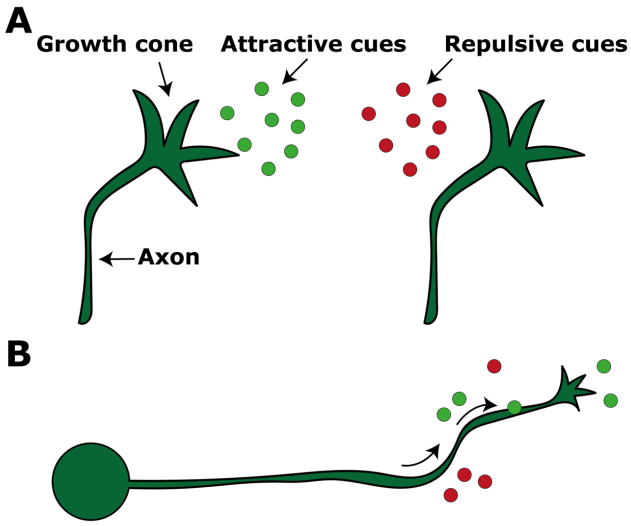


**FIGURE 1. FUNCTION OF GROWTH CONE DURING AXONAL NAVIGATION.**

**A)** Growth cone responses to attractive (light green) and repulsive (red) cues present in its environment. **B)** An example of how a growth cone might navigate when encountering a combination of attractive and repulsive cues in its environment. Whether a growth cone is attracted or repulsed by a specific guidance cue is dependent on which types of receptors that are expressed on its surface (not shown). The figure is adapted from [18].

Network wiring during development can roughly be divided into (i) activity-independent and (ii) activity-dependent processes[2,17,19]. The activity-independent part relies mostly on genetics and can be viewed as establishing a foundation on which activity-dependent processes can take place. For example, developmental synapse formation is thought to be largely independent of neuronal activity, while the process of synaptic pruning is activity-dependent[15,17]. Spontaneous electrical activity in the nervous system emerges early in embryogenesis, and both self-generated and experience-dependent (i.e. from sensory experience) activity patterns modulate and fine-tune the neuronal networks[2,20].

Neuroplasticity; the nervous systems ability to alter its structure and/or function in response to changes in its internal and/or external environment, including injury[21,22], is an essential part of network self-organization, influencing the wiring and rewiring of neuronal networks throughout development[23,24]. In addition, neuroplasticity is a feature that persist into adulthood. In fact, activity-dependent plasticity is an essential player in how we are able to acquire new knowledge and skills and remember facts and experiences throughout life, which occur through e.g. a remodelling of neuronal circuits, remapping of functional areas, modulation of synaptic strength or by a removal or addition of new connections[21,25–27]. Furthermore, the ability of the CNS to plastically alter its structure and function in response to injury can restore lost functionality to some degree[21,27].

Even though the adult CNS is capable of modifications in response to injury, a traumatic injury to the adult CNS often results in devastating long-lasting functional deficits for the patients in question. Complete functional recovery is often limited due to a combination of the CNS´s complex pathophysiologies and the limited regeneration capacity of the adult CNS axons[28–30]. In the following section, the reader will be introduced to traumatic injuries to the brain and spinal cord, with a specific focus on one aspect associated with these types of injuries, namely axonal injury.

## 1.2. AXONAL INJURY

As axons are vital players in signal transmission and network connectivity, axonal damage is an injury to the substrate of which all neuronal networks communicate. Axonal injury is a pathological hallmark of traumatic injuries to the brain and spinal cord[31]. Traumatic brain injury (TBI) is defined as an "alteration in brain function, or other evidence of brain pathology, caused by an external force"[32]. Traumatic events, such as motor vehicle accidents or falls, can cause high-velocity translational or rotational forces to act upon the brain [29,33]. Consequently, a varying degree of brain damage occurs, which may result in long-term cognitive and behavioural deficits. Traumatic axonal injury (TAI), a pathoanatomical subgroup of TBI, refers to TBIs where axonal injury is the most prominent component. The initial mechanical injury-forces shear and stretch axons resulting in primary axotomy (i.e. complete transaction of axons) or partial damage to axons[33]. During brain trauma, axonal injury is dependent on both the magnitude and the rate of the insult, with primary axotomy only happening in the most severe cases[34]. In fact, primary axotomy is not regarded as a common component of TAI. More often, TAI is gradual, with the initial axonal injury further triggering molecular pathways resulting in secondary axotomy and axonal degeneration over an extended time course, including the degeneration of axons not initially attacked by the insult[34].

In TBI, where injury can impact any part of the skull, the damage and the resulting symptoms are highly variable. In contrast, traumatic spinal cord injury (SCI) results in less diverse, yet still devastating, symptoms; including a varying degree of motor and sensory dysfunction. The location and severity of the injury determine the clinical outcome of SCI, and injuries at the cervical level are the most common[35]. Often, SCI is a result of a displacement of the vertebrae column and/or disk leading to mechanical depression of surrounding tissue[31]. Most SCIs are anatomically incomplete, i.e. some anatomical connectivity between the brain and the spinal cord is spared, even after severe injuries associated with complete loss of function below the injury site[31].

Both TBI and SCI involve a primary and a secondary injury phase. The primary injury is a direct result of the initial impact force. Immediately after a traumatic insult to the CNS, local axons, blood vessels and cell membranes are damaged and disrupted. This leads to local vasospasm, ischemia, ionic imbalance, cell necrosis and neurotransmitter accumulation[30,33,35,36]. The initial loss of local blood supply and cell necrosis trigger secondary mechanisms ultimately leading to further tissue damage. The secondary injury shares several mechanisms with the primary injury, but also include, though not exclusively, the formation of free radicals (causing oxidative stress), lipid peroxidation (i.e. cell membrane destruction), excitotoxicity, apoptosis (programmed cell death), demyelination of surviving axons, Wallerian degeneration, and the formation of a glial lesion scar[30,33,35,36]. The diverse biochemical and physiological changes associated with the secondary injury can continue for weeks to months. As a consequence, the lesion site expands, and restorative processes are limited[30]. A few of the secondary injury mechanism involved in both TBI and SCI, i.e. axonal degeneration, excitotoxicity and oxidative stress will be discussed in further detail below.

### 1.2.1. AXONAL DEGENERATION

The elaborate axonal cytoskeleton (i.e. microtubules, neurofilaments and actin filaments) ensures that axons can withstand some degree of stretch, compression, tension and torsion[37]. However, a traumatic insult to axons can result in axonal degeneration. While

apoptosis leads to the death of the entire neuron, axonal degeneration may or may not lead to the death of the soma, suggesting separate neuron intrinsic signalling pathways responsible for axonal degeneration and apoptosis[37]. Although the rate, cause and some underlying molecular pathways of axonal degeneration might differ between various CNS injuries and diseases[38,39], several hallmarks are shared, such as axonal transport impairments, microtubule disassembly, mitochondria dysfunction, axonal swelling, and the fragmentation of the axonal cytoskeleton[38,40].

Axonal transection (i.e. axotomy) might be the simplest model for studying axonal degeneration. Following axotomy, axonal degeneration can be classified based on the localization of the axon in spatial relation to the injury; the segment of the axon between soma and the injury site is referred to as proximal, while the segment from the injury site onwards is referred to as distal[38,40]. Simply put, axonal degeneration involves at least three different morphologically and temporally distinct phases[40] (**FIGURE 2**). The first of these phases is acute axonal degeneration (AAD), in which the first 200-300µm of the axon, on either side of the lesion site, fragments[41]. The AAD phase is followed by a period of stability; the distal axon´s morphology remains intact with the ability to conduct action potentials upon stimulation (i.e. latent Wallerian degeneration)[42]. Lastly, the entire distal part of the axon undergoes rapid fragmentation known as Wallerian degeneration[43]. In rodent axons, the three phases are completed by 12-24h *in vitro*, and by 24-48h *in vivo* (reviewed in [40]).

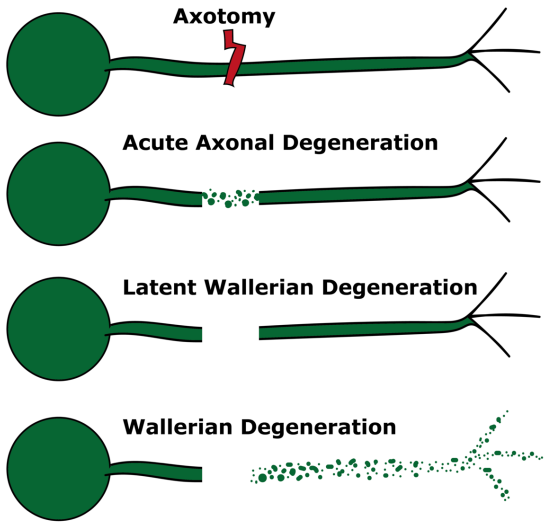


**FIGURE 2. PHASES OF AXONAL DEGENERATION AFTER AXOTOMY.**

Immediately after axotomy, the first 200-300µm of the axon, on either side of the lesion site, fragments (acute axonal degeneration). Next, there is a period of stability, the distal axon´s morphology stays intact, and the distal axon can conduct action potentials upon stimulation (latent Wallerian degeneration). Finally, the entire distal segment of the axon rapidly fragments (Wallerian degeneration).

The mechanisms of downstream cellular events after axonal injury are not completely understood. However, axonal injury is associated with changes in axolemma ion concentrations. Injury-induced sodium influx can result in axonal swelling, while an increase in intra-axonal calcium levels has been linked with initiating axonal degeneration, as calcium can lead to cytoskeleton breakdown through the activation of calpains, which cleave neurofilament- and microtubule-associated components[38,40,44]. Both calcium influx

at the lesion site and calcium release from intracellular stores have been reported to be involved in the AAD phase and in Wallerian degeneration[37,38].

Both primary axotomy and a partial damage to the axonal cytoskeleton disrupt axonal transport; the transport of proteins and materials from the soma to the axon and vice versa. Axonal transport is important for axonal energy homeostasis and optimal functioning[45], and disturbance can lead to accumulation of transport proteins within the swelled areas of the axon[44], causing axonal malfunctioning. Interestingly, not only physical injury, but also disruption of axonal transport alone has been reported to trigger Wallerian-like degeneration (reviewed in [38]), emphasising the importance of soma support for axonal functioning. In fact, secondary axotomy can result from disruption of axonal transport; the initial injury might disturb the axon cytoskeleton, leading to axonal swelling and the accumulation of transport proteins. This again, can cause disconnection and finally Wallerian degeneration[46].

### 1.2.2. HYPEREXCITABILITY, EXCITOTOXICITY AND OXIDATIVE STRESS

As previously mentioned, glutamate and GABA are the primary excitatory and inhibitory neurotransmitters in the brain, respectively[7]. Balancing the excitatory and inhibitory inputs to CNS neuronal networks is thought to be essential for circuit stability and function. On one hand, glutamate signalling is linked with synaptic plasticity; the strengthening and weakening of synaptic coupling[47]. On the other hand, a massive increase of extracellular glutamate levels in and around the lesion site is reported to occur soon after spinal cord and head trauma[30,48]. Excess extracellular glutamate, in addition to a loss of inhibitory control due to e.g. injury-induced loss of inhibitory interneurons, can disrupt the excitatory-inhibitory input ratio to surviving neuronal circuits, and ultimately lead to hyperexcitability (i.e. enhanced excitatory neuronal activity)[48].

Hyperexcitability and excess extracellular glutamate is further linked with excitotoxicity[49]. An acute increase in extracellular glutamate levels after injury can overstimulate glutamate receptors leading to secondary processes that may ultimately result in neuronal death[50] (summarized in **Figure 3**). One glutamate receptor that has received particular attention in relation to excitotoxicity is the ionotropic N-methyl-D-aspartate (NMDA) receptor, as this receptor is highly permeable to calcium[50]. NMDA receptor overactivation can lead to excess intracellular calcium which further activates calcium-dependent enzymes leading to lipid peroxidation, and protein and DNA damage. Additionally, excess intracellular calcium can cause mitochondria calcium overload resulting in mitochondria dysfunction, as well as oxidative stress[49].

Oxidative stress can be defined as "an imbalance between free radical production and endogen antioxidant systems"[51]. Reactive oxygen species (ROS), a subgroup of free radicals, can form when specific molecules interact with oxygen. As the main cellular consumers of oxygen, the mitochondria is recognized as the major production source of ROS[52,53], and unless properly regulated, ROS can initiate chain reactions leading to toxic effects. An imbalance in the intracellular free radical-antioxidant ratio can cause lipid, protein and nuclei acids damage leading to necrosis, and/or apoptosis through mitochondria release of pro-apoptotic factors[51,52].

The electrophysiological responses to axotomy have not been studied extensively, however, a few *in vitro* studies have reported altered neuronal excitability after axotomy.

For example, transection of cultured Aplysia mechanosensory nerves led to hyperexcitability in the injured neurons, dependent on specific neuron-intrinsic signalling pathways[54]. In relation to mammalian CNS neurons, Nagendran and colleagues[55] found that axotomy of hippocampal neurons induces retrograde spine loss followed by a specific loss of presynaptic inhibitory, but not excitatory, inputs. Furthermore, they reported an increase in presynaptic glutamate release 48h post injury. Thus, both a reduction in inhibitory inputs and an increase in glutamate release seem likely to contribute to enhanced excitation after *in vitro* axotomy.

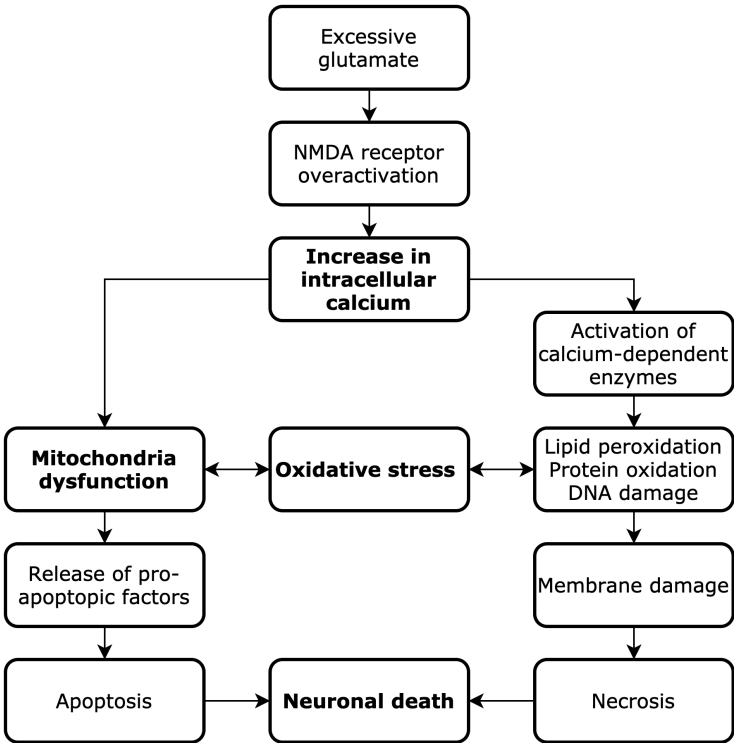


**FIGURE 3. MAIN CELLULAR MECHANISMS INDUCED BY NMDA RECEPTOR OVERACTIVATION IN CNS NEURONS.**

The overactivation of NMDA receptors leads to an increase in intracellular calcium, which may cause mitochondrial dysfunction and oxidative stress. This can further trigger intracellular processes which can lead to neuronal death by necrosis and/or apoptosis.

### 1.2.3. GABA AS A POTENTIAL NEUROPROTECTIVE NEUROTRANSMITTER

Up until this point, we have seen that CNS axonal injury can lead to secondary injury mechanisms which may cause prolonged axonal and neuronal degeneration. One potential way of reducing neuronal degeneration after CNS injury would be to limit glutamate-mediated excitotoxicity, and this may be achieved by blocking NMDA receptor activity post injury. However, NMDA receptor antagonists have proven ineffective, and even neurotoxic in clinical trials of stroke and TBI, possibly due to the functional diversity of NMDA receptor signalling (reviewed in [56]). A different approach would be to try and balance out the enhanced excitability by increasing GABAergic neurotransmission.

Two main subtypes of GABA receptors exist; the ionotropic $GABA_A$ receptor and the metabotropic $GABA_B$ receptor[57]. When activated by GABA, $GABA_A$ receptors cause fast inhibitory transmission by the direct opening of chlorine ion channels, hence causing postsynaptic hyperpolarization[58]. $GABA_B$ receptors, on the other hand, are associated with slower inhibitory transmission and have a much broader range of effects when activated. The binding of GABA leads to the release of associated G-protein subunits which trigger

intracellular signalling eventually leading to the activation of postsynaptic potassium channels, and/or the inhibition of presynaptic calcium channels. Presynaptic calcium inhibition reduces the amount of neurotransmitter release, while postsynaptic activation of potassium channels leads to neuronal hyperpolarization as membrane potassium conductance increases[58]. Thus, enhancing $GABA_A$ and $GABA_B$ receptor signal transmission can potentially balance out the shift in the excitatory-inhibitory ratio of neuronal network input associated with CNS injury, by increasing inhibitory neurotransmission and/or by reducing excitatory neurotransmission. In fact, experimentally increasing GABAergic signalling after CNS injury have been reported to be neuroprotective in the case of for example (i) restoring ischemia-depleted neuronal energy levels to normal in *ex vivo* hippocampal slice cultures[59]; and (ii) increase neuronal survival after induced excitotoxicity in *ex vivo* spinal cord slice circuits[60] and (iii) increase neuronal survival after induced cerebral ischemia in *in vivo* mouse hippocampal cortical area 1 (CA1) neurons[61]. As far as the author knows, no studies have looked specifically at the effects of increased GABAergic signalling after mammalian CNS axotomy.

### 1.2.4. AXONAL REGENERATION

Another factor that plays an important part in the prolonged functional deficits associated with CNS trauma, is the lack of successful adult CNS axonal regeneration. In contrast to developing axons, most adult CNS axons cannot grow back to their target after injury[62]. Axonal regeneration can be defined as regrowth occurring from the injured tip of a damaged axon[63]. However, successful axonal regeneration after injury depends on several factors; first, the axon must survive, then, it must find permissive growth cues, receive proper trophic support, elongate towards appropriate targets, and make functional connections[63]. Therefore, promoting axonal regeneration alone does not ensure the establishment of functional connections with intact target neural circuity.

The failure of adult CNS axonal regeneration is attributed to both neuron intrinsic and extrinsic factors. Adult neurons lack the expression of essential genes, termed regeneration-associated genes, linked with embryonic growth, and instead express several genes that restrict growth[62,64]. In addition, the expression of axonal guidance cues is inapt in the adult CNS[62]. However, understanding the interplay between the many neuron intrinsic and extrinsic factors, responsible for successful embryonic axonal growth, but failed adult CNS axonal regeneration, is extremely challenging. In addition, not all processes involved in adult axonal regeneration are present during development. For example, many extracellular factors that directly limit/inhibit axonal growth are injury-dependent, such as inhibitory factors associated with the glial scar[65], increasing the complexity of adult regeneration.

Among the extrinsic factors is the glial scar that forms after a traumatic CNS injury. The glial scar composites both glial - mainly astrocytes, but also reactive microglia and glial precursor cells - and fibrotic components[65]. The glial scar is linked with preventing axonal regeneration, both by acting as a physical barrier and by the production of inhibitory molecules[65]. Other extrinsic barriers for axonal growth, including axonal regeneration, are myelin associated inhibitors (MAIs); inhibitors within CNS myelin sheaths and inhibitors located on the membrane of oligodendrocytes (a type of glial cell within the CNS)[63]. In healthy networks, myelination provides insulation and rapid signal propagation along axons, and myelin associated inhibitors (MAIs) minimize plasticity and structural

remodelling that could interfere with proper circuits function. After injury, these molecules continue to restrict plastic and regenerative processes[63,66].

Further complicating adult CNS regeneration; as neurons mature, some of their intrinsic regenerative ability is lost. For example, cortical neurons harvested from day 18 embryonic rat brains are at the developmental stage where they begin projecting axons into other areas of the CNS. When these neurons are plated in culture, they quickly start growing projections and form connections. Axotomy at this stage results in regeneration (defined as successful formation of a new growth cone and subsequent axonal elongation) in most cases. However, as the culture is left to grow over several weeks, the neurons grow long projections, develop synapses and become spontaneously electrically active. In addition, gene expression is altered and resembles an adult pattern. When the axons of these neurons are cut, regeneration is unlikely[64,67]. This illustrates that there is a clear distinction between growth-competent developmental CNS axons, and active, electrically transmitting axons.

### 1.2.5. MODELLING AXONAL INJURY *IN VITRO*

Though there is no doubt that *in vivo* animal models of CNS injury have given us invaluable insights into the pathophysiology of such injuries and the potentials for recovery, the *in vivo* environment is highly complex which can limit tissue accessibility, and the presence of uncontrollable variables can potentially reduce reproducibility[68]. In addition, *in vivo* experiments are often time-consuming, labour-demanding and can be resource intensive[44]. Though *in vitro* models of CNS injury are unable to mimic every aspect of what´s happening *in vivo*, such models have been reported to be able to reproduce many of the post-traumatic processes associated with mechanical injury *in vivo*, including excitotoxicity, free radical generation, and lipid and cytoskeleton disruption[68]. As such, *in vitro* models can complement *in vivo* models by offering a reductionist approach with increased control over experimental variables; thus, aspects of an injury can be investigated in detail.

If wanting to manipulate neuronal subcomponents or investigate molecular and cellular mechanisms that affect specific parts of the neuron differently, which is often the case with neuronal injury, conventional cell culture models are insufficient; they lack the ability to segregate neuronal subcellular components (axons from soma), and does not offer control over cellular microenvironments[69]. The incorporation of microfabrication techniques in the study of biological systems has allowed for the development of platforms useful for studying and manipulating CNS neuronal networks, namely microfluidics[70,71]. Microfluidics take advantage of soft-lithography techniques in the fabrication of specific culture devices, i.e. microfluidic chips. These chips, often consisting of a set of micro-sized compartments connected by microtunnels/channels, offer both spatial control over neuronal subcomponents and/or subpopulations, as well as guidance of neuronal growth.

Due to their ability to spatially segregate neuronal soma from axons, microfluidic chips have proven useful in studying axonal injury, as specific designs can accommodate different methods of injury, such as axon stretch injury, chemical axonal injury, laser-based axotomy and vacuum-assisted axotomy (reviewed in [72]). Furthermore, microfluidic chips allow for fluidic isolation if a minute volume difference between the compartments is created[70]. Thus, a high experimental control over neuronal microenvironments can be achieved.

## 1.3. FUNCTIONAL CONNECTIVITY AND NEUROPLASTICITY

When studying CNS connectivity, we often talk about both structural and functional connectivity. Structural connectivity encompasses the physical connections (synapses/axons/white matter tracts) between defined elements of a neuronal network (neurons/clusters of neurons/brain regions), while functional connectivity is a measure of the statistical dependencies, i.e. the correlation or coherence between the activity, of the defined elements[3,4,73]. Understanding how adaptive function emerges from the structural architecture of the brain has been, and still is, a challenge faced by neuroscientists. On one hand, the structural architecture of a neuronal network limits the possible functional connections that can occur[74]. On the other hand, measures of functional connectivity may not reflect direct anatomical connections, but also interactions between two anatomically distinct nodes[4] (**FIGURE 4**). In an attempt to reveal the dynamic patterns of functional and structural connectivity within neuronal networks, graph theory; a branch of mathematics which provides a set of tools for the study of complex networks, has been integrated with neuroscience. In graph theory, a set of nodes and edges describe the principle elements of a system and their interrelations, respectively[74].

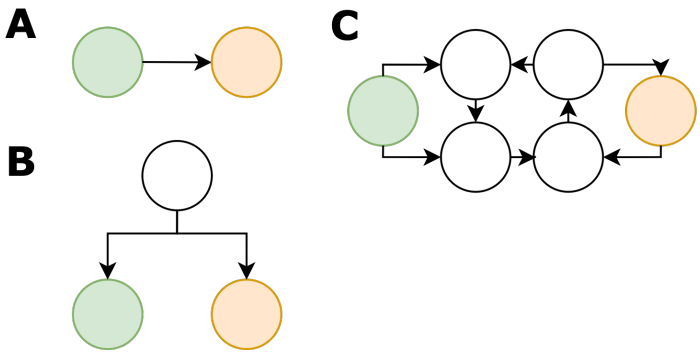


**FIGURE 4. FUNCTIONAL CONNECTIVITY DOES NOT SHARE A 1:1 RELATIONSHIP WITH ANATOMICAL CONNECTIVITY.**

Node 1 (green) and 2 (orange) are functionally connected. **A)** The measured functional connection between node 1 and 2 reflects direct anatomical connectivity. **B)** The measured functional connection between node 1 and 2 reflects common input from a third node (white). **C)** Node 1 and 2 are anatomically connected through multiple synapses, however a functional connection between the two nodes might still be measured. The figure is adapted from[75].

The spatiotemporal organization of the adult CNS, or its pattern of structural and functional connectivity, is not fixed, but highly dynamic throughout life. This is illustrated by the concept of neuroplasticity. Neuroplasticity can occur at different levels of the nervous system´s organization. Plasticity at the macroscale encompasses changes in the spatiotemporal pattern of activity between different brain regions, while plasticity at the mesoscale involve modifications of connections between and within distinct neuronal populations. At the microscale, plasticity occurs at the cellular and subcellular level as structural and functional modifications of neurons and synapses[21]. The structural connectivity of neuronal networks is thought to be relatively stable on short time scales, but prone to plastic changes on longer time scales (hours to days). The functional connectivity of a network, on the other hand, can be modulated on the scale of tens or hundreds of milliseconds, as indicated by the rapid changes in the pattern of brain activity in response to sensory stimuli[3].

A traumatic injury to the CNS, disrupts both the structural and the functional connectivity of neuronal networks, and the specific area(s) and extent of damage will influence both the resulting functional deficits and potentials for recovery. Importantly, neuroplasticity

can contribute to functional recovery after CNS injury. There is usually some spontaneous recovery of function over the first several months after both TBI and SCI[76–78]. This spontaneous functional gain is commonly attributed to an injury-induced reorganization of connectivity within spared neuronal circuits, associated with mechanisms such as injury-induced axonal sprouting[77,78]. In contrast to axonal regeneration, axonal sprouting (i.e. collateral growth from surviving axons) can occur spontaneously both within the spinal cord and in the cortex after trauma[21,76,79,80]. While axonal regeneration involves restoring original anatomical connections, axonal sprouting may provide an indirect route, reconnecting pools of neurons that communicated before the injury through multiple synapses (**FIGURE 5**).

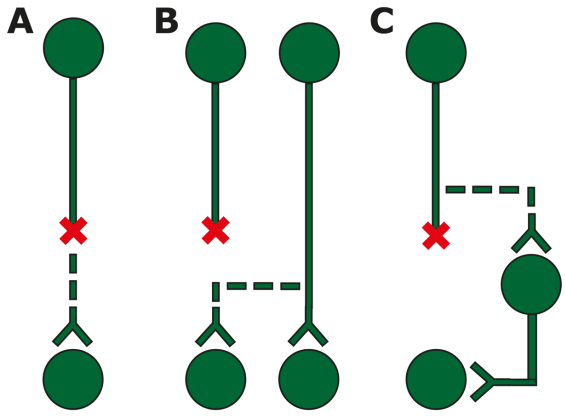


**FIGURE 5. AXONAL REGENERATION VS. AXONAL SPROUTING.**

Axonal injury is indicated by the red cross, while new axonal growth is indicated by the dashed line. **A)** Illustrates axonal regeneration where new growth occurring from the tip of the injured axon establishes contact with the original target neuron. **B)** Illustrates compensating axonal sprouting from a nearby uninjured axon. **C)** Illustrates axonal sprouting from the injured axon which establishes indirect contact with the original target neuron.

The spontaneous improvement in function described above is, however, often insufficient. Importantly, targeted rehabilitation training after an incomplete SCI or after TBI, such as cognitive or behavioural task-specific training, which involves repetitive training on a particular task, can advance functional recovery even further[81–83]. For example, in monkeys, behavioural training encouraging specific forelimb movements can result in a larger area of primary motor cortex devoted to that specific task[84]. Neuronal circuit reorganization and subsequent functional improvement in response to training are built on the idea that coordinated neuronal activity triggered by training results in functional gain, while inactivity results in functional loss. This emphasises the idea that experience may promote recovery by interacting with the plastic CNS environment (i.e. experience-dependent plasticity). Furthermore, this opens up for the possibility that lost function, as a consequence of traumatic CNS injury, could potentially be restored by harnessing endogenous CNS plasticity mechanisms, and that re-establishing lost structural connectivity (through e.g. axonal regeneration) not necessarily is required in all instances. It should, however, be noted that not all neuroplasticity is adaptive[21], thus, interventions that aimlessly try to promote plasticity after injury may not result in functional gain. In the following sections, mechanisms of neuroplasticity at the micro- and mesoscale will be discussed, and there will be an emphasis on how we can study neuroplasticity by the use of *in vitro* neuronal networks.

### 1.3.1. SYNAPTIC PLASTICITY

During synaptic transmission, a presynaptic neuron communicates with a postsynaptic neuron within close vicinity, either through an electrical current or the release of neurotransmitters[13,14]. This again, alters the membrane potential of the postsynaptic neuron, with reference to its resting membrane potential; a temporary depolarization of the postsynaptic membrane is referred to as an excitatory postsynaptic potential (EPSP), while a temporary hyperpolarization is referred to as an inhibitory postsynaptic potential (IPSP). If the sum of EPSPs and IPSPs, within a set time-window, favours depolarization and exceeds a certain threshold, an action potential is generated.

One of, if not *the* most fundamental form of functional plasticity is the activity-dependent change in synaptic strength, commonly known as Hebbian plasticity. Donald Hebb hypothesized that correlated pre- and postsynaptic activity, i.e. if one neuron persistently takes part in the firing of another neuron, or if two neurons are steadily excited together, this increases the strength of connection between the two[85]. Hebb´s hypothesis got strong experimental support in 1973, when Bliss and Lømo found evidence for long-term potentiation (LTP) in the rabbit hippocampus[25]. Bliss and Lømo delivered high frequency electrical stimulation, or tetanic stimulation (TS), to the hippocampal prefrontal path which synapses with neurons in the dentate area. Extracellular recordings of field potentials from neurons in the dentate area revealed an increase in the amplitude of the recorded population EPSP to test stimuli post TS, and this increase could last for several hours. Not mentioned by Hebb, but now regarded as an important aspect of Hebbian plasticity is the weakening of synaptic strength between neurons, or long-term depression (LTD), discovered in the cerebellum[86]. In general, high frequency neuronal activity results in the strengthening of neuronal connections (LTP) while prolonged low frequency neuronal activity leads to the weakening of neuronal connections (LTD)[25,86] (exemplified in **FIGURE 6**). Mechanisms of LTP/LTD have been widely studied in the hippocampus[25,87–89] but have also been reported to occur in pathways throughout the brain, including cortical pathways[90].

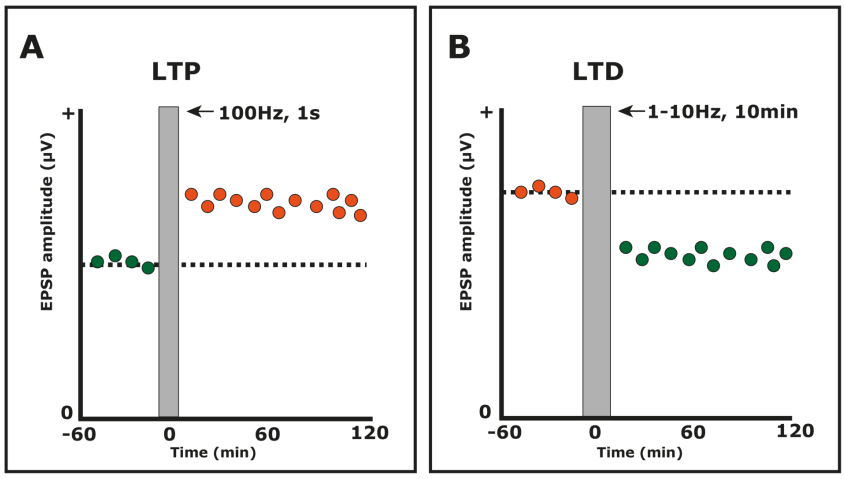


**FIGURE 6. HEBBIAN PLASTICITY: LONG-TERM POTENTIATION AND DEPRESSION.**

**A)** Example of long-term potentiation. The figure illustrates an increase in the recorded EPSP amplitude to test stimuli after presynaptic TS (100Hz), with the effect lasting for >2h. **B)** Example of long-term depression. The figure illustrates a decrease in EPSP slope to test stimuli after prolonged low frequency (1-10Hz) presynaptic stimulation, with the effect lasting for >2h.

Another mechanism of synaptic plasticity highlights the importance of the temporal order of pre- and postsynaptic activation. By varying the relative spiking of weak and strong input from the entorhinal cortex to the dentate gyrus in rats, Levy and Steward[91] found that LTP was induced when strong input was activated at the same time or preceded the weak input by as much as 20ms. LTD, on the other hand, was induced when the temporal order was reversed. Several *in vitro* studies have verified the importance of the timing of pre- and postsynaptic firing for inducing LTP/LTD[92–94]. In such spike-timing dependent plasticity (STDP), it is thought that information can be carried by the precise timing of spikes which subsequently gets stored at synapses as LTP/LTD. Interestingly, it has been shown that structural modifications, such as the formation or elimination of axonal or dendritic trees, accompany LTP/LTD of synaptic strength, indicating a link between synaptic structure and function[21].

Notably, alterations in synaptic strength can occur at both long (hours to days, as discussed above) and short (milliseconds to minutes) timescales. While long-term plasticity lasting for more than several hours depend on the synthesis of new proteins, such as the synthesis of new postsynaptic receptors, short-term plasticity is a rapid and transient activity-dependent modulation of synaptic strength, which can happen due to mechanism causing e.g. an immediate alteration in the amount of presynaptic neurotransmitter release[26,95,96]. Unlike long-term synaptic plasticity, which is thought to be important for learning, memory and recovery after injury, mechanisms of short-term plasticity can directly influence neuronal network computation and information processing[95].

### 1.3.2. AXONAL PLASTICITY

Axons have traditionally been thought of as stable conduits for action potentials to travel, however, recent studies have shown that the computational and functional role of single axons are much more complex[97–102]. For example, low frequency electrical stimulation can induce short-term changes in the axonal propagation velocity (PV) of cultured rat cortical neurons[100]. Furthermore, repeated high frequency stimulation of mossy fibre boutons in rat hippocampal slices can broaden the shape and increase the amplitude of the action potential at the presynaptic terminal (reviewed in [102]). Functional changes at the level of the axon interfere with synaptic coupling; both the shape of the presynaptic action potential and axonal PV is of great importance in determining the timing of synaptic transmission, which again can influence synaptic plasticity[8,103]. In addition, a broadened action potential at the presynaptic terminal will influence the amount of presynaptic neurotransmitter release, thus influence the signal strength[8,103].

### 1.3.3. STUDYING NEURONAL NETWORK DYNAMICS *IN VITRO* USING MICROELECTRODE ARRAYS

As alterations in EPSP strength only have a functional effect if it causes alterations in neuronal firing, Marder and Buonomano[104] proposed that when investigating synaptic plasticity, not only alterations in EPSPs should be considered, but also alterations in the firing pattern of and between neurons. Even though synaptic connectivity and functional connectivity do not share a one-to-one relationship, synaptic connectivity and functional connectivity are related (**Figure 4**). Thus, modifications of synaptic connectivity should also reveal themselves as alterations in the measured functional connectivity between defined network nodes. A widely used method for studying the functional dynamics of neuronal assemblies is by coupling dissociated neurons onto MEAs.

The MEA platform usually consists of a culture chamber where neuronal networks can grow on an insulating surface embedded with an array of microelectrodes. When a neuron generates an action potential, ions travel across its membrane through ion channels. The flow of ions creates an electric field, i.e. voltage change, which can be picked up by microelectrodes in close enough vicinity to the neuron[105]. The MEA platform allows for non-invasive extracellular recordings of neuronal activity from multiple sites in a network simultaneously. Thus, dynamic network behaviour can be captured, as repeated recordings from the same neurons and networks can be carried out over an extended time period (i.e. months)[106].

MEAs can detect both extracellular action potentials, i.e. spikes, in the frequency band of 300-3000Hz, and local field potentials in the frequency band of 1-300Hz[107]. The spatial signal resolution is determined by the number, spacing and the receptive field of the microelectrodes. Commercially available MEAs usually have 60-120 electrodes, 10-50μm diameter each, with an inter-electrode spacing ranging from 100-500μm[106,108]. In addition to passive observation, MEAs allow for active influence as neuronal activity can be perturbed, i.e. electrical stimulation can be delivered using the microelectrodes and/or chemical compounds can be delivered in the culture chamber[106,107].

Importantly, *in vitro* neuronal networks recapitulate two important aspects of *in vivo* development; self-organization and the emergence of spontaneous network activity. Only a few hours after plating, neurites in search for synaptic contact starts extending from the neuron soma, and in line with *in vivo* network development, the initial self-organization phase is largely activity-independent. Within the first week *in vitro*, the networks start eliciting spontaneous activity, and network organization becomes increasingly more activity-dependent[109]. The initial phase of network development is characterized by random and asynchronized spiking from individual neurons, suggesting that neurons within the network are mostly uncoupled. Around the second week *in vitro*, network activity becomes more synchronized; spikes tend to cluster into bursts (i.e. groups of spikes in rapid succession) and the bursting appears quite regular, occurring simultaneously across most of the MEA electrodes[108–110]. This phase is associated with an increase in neurite elongation and the formation of functional synapses. After this, a richer pattern of network activity emerges, characterized by a non-periodic and synchronized complex pattern of spiking and bursting. This activity pattern is maintained for months and represents a "mature" network state[108,109].

### 1.3.4. FUNCTIONAL CONNECTIVITY AND NEUROPLASTICITY *IN VITRO*

Marom and Shahaf[108] stated that two universals of learning and memory exist in neuronal systems: "(i) an extensive functional connectivity that enables a large repertoire of possible responses to stimuli; and (ii) sensitivity of the functional connectivity to activity, allowing for selection of adaptive responses". In the current study, we are particularly interested in (ii), i.e. how specific activity patterns may plastically alter the functional connectivity within neuronal networks. As dissociated cortical neurons cultured on MEAs self-organize into networks with random connectivity (with minimal predefined constraints) and exhibit emergent activity, this model is particularly advantageous when wanting to investigate such universal mechanisms[108].

When studying mechanisms of neuroplasticity of *in vitro* neuronal networks, there are some experimental issues that need to be addressed. Firstly, the spontaneous activity patterns expressed by neuronal networks are highly variable between similarly prepared cultures and can even vary within the same network at different recording days[110,111]. Secondly, *in vitro* neuronal networks do not experience sensory stimuli which can activate neuronal circuits and drive behaviour *in vivo*. Thus, comparing the activity patterns between different *in vitro* neuronal networks, and identifying the "behavioural output" of such networks are challenging. However, this can partly be overcome if we consider electrical stimuli as artificial sensory inputs, and recorded signals in response to stimulation as motor outputs. Such considerations have led to the development of plasticity protocols, where electrical stimuli with varying features (i.e. pulse amplitude, stimulation frequency etc.) are delivered to one or several electrodes on the MEA[112–115], and network responses to such stimuli are regarded as "behavioural output". Notably, such stimulation protocols are inspired by and also used to evoke plastic responses *in vivo* (e.g. reference [25]).

One of the first groups to report plastic alterations in network functional connectivity in response to electrical stimulation was Maeda and colleagues[113]. They found that the delivery of a tetanic stimuli to one or several electrodes on the MEA induced plastic changes in the activity recorded from the cultured network. The plastic changes occurred as a modulation in the spontaneous bursting rate, number of spikes per burst, and by an alteration in the probability of evoking bursts by test pulses. A year later, a highly interesting study was published by Jimbo and colleagues[112]. They applied a test stimulus pulse to all sites of a 64-electrode MEA both pre and post TS, and the total number of spikes generated by the test stimulus from identified single neurons within the network was counted. Interestingly, depending on the site of the test stimuli, the neuronal population responded homogenously – either by increasing their firing (i.e. potentiation) or by decreasing their firing (i.e. depression) after TS. For a specific neuron, the response was heterogenous, it increased and decreased its firing rate depending on the test-stimulation site. Jimbo and colleagues concluded that "potentiation or depression is pathway specific, not neuron-specific". Furthermore, both prolonged low-frequency stimulation (<1Hz), conducted through a single or multiple sites[115], and TS (20Hz) coupled to prolonged low frequency stimulation (≤1Hz)[114], have been reported to induce modifications in the functional connectivity of dissociated neuronal networks. The studies described above all indicate that electrical stimulation can modify, or plastically alter, the underlying activity pattern/functional connectivity of *in vitro* neuronal networks, i.e. neuronal networks can develop into new dynamical states depending on the features of the electrical stimulus.

In recent years, MEA technology has been integrated with microfluidics (i.e. microfluidic MEA), which in addition to spatial segregation of neuronal subcomponents and subpopulations, allow for the recording and stimulation of functionally connected modular neuronal networks. Microfluidic MEAs have for example been used to study the functional connectivity between interconnected subpopulations of neurons in different cell compartments[116,117], or between subpopulations of neurons with unidirectional synaptic connections[118]. In addition, if electrodes are aligned within microtunnels of the microfluidic device, isolated axons can be targeted and axonal information processing (such as axonal PV and spike shape) and axonal plasticity can be investigated in detail[97–100]. In addition, as spikes travelling along axons can be detected by the electrodes within the microtunnels, signal directionality can be determined. This raises the possibility of studying specific

mechanisms of neuroplasticity, such as STDP, by targeted and temporally ordered electrical stimulation of pre- and postsynaptic clusters of neurons (i.e. paired pulse stimulation).

## 1.4. FINAL NOTE

*In vitro* models of neuronal injury allow the researcher to reduce the complexity of injury mechanisms *in vivo*. As a consequence, aspects of an injury can be investigated in detail. Microfluidic chips, which spatially segregate neuronal soma from axons and are designed specifically to enable targeted axotomy, are useful tools if interested in investigating one aspect of neuronal injury, namely axonal injury. Furthermore, *in vitro* models of neuronal networks that enable electrical recording and stimulation of axons, neurons and networks, can reduce the complexity of neuronal network mechanisms in the brain and offer an approach to study specific components of neuroplasticity. A great deal of studies investigating mechanisms of neuroplasticity have focused on long-term and short-term plasticity at the microscale. In this project, we are interested in investigating how such plasticity mechanisms are expressed not only on a microscale, but also on a network level (i.e. mesoscale). As mentioned, CNS neuroplasticity is thought to facilitate some spontaneous recovery after injury, and behavioural and/or cognitive training can enhance functional gain even further. However, a great challenge lies in understanding which exact mechanisms and which specific functional and structural changes are essential for recovery. We believe that an *in vitro* reductionist approach can help increase our understanding of adult CNS axonal injury and mechanisms of neuroplasticity. This again can potentially contribute to the development of improved therapeutic and rehabilitation strategies for patients suffering from traumatic CNS injuries, such as TBI and SCI.

## 2. AIMS AND OBJECTIVES

The current project was based on the underlying idea that a greater understanding of aspects and processes involved in traumatic CNS injuries, as well as an increased understanding of mechanisms of neuroplasticity, can help facilitate the development of interventions that potentially can limit neuronal degeneration and promote functional recovery after injury. The project was divided into three main experiments. Experiment 1 focused on cortical neuronal responses to *in vitro* axotomy, as well as the effects of GABA addition post axotomy. Experiment 2 concerned investigating cortical functional neuroplasticity at the mesoscale, while experiment 3 explored cortical functional neuroplasticity at the microscale. Experiment 2 and 3 were both based on the underlying assumption that certain types of activity patterns might alter functional connectivity. The main objectives and research question for each experiment are listed below.

**The main objectives of experiment 1 were:**

i) Establish viable *in vitro* cortical neuronal networks on custom-designed microfluidic chips
ii) Perform *in vitro* axotomy and assess cortical neuronal injury-responses, i.e. cell viability, oxidative stress response and axon regenerative response
iii) Chemically perturb cortical networks with extracellular GABA immediately after axotomy, and assess cell viability, oxidative stress response and axon regenerative response

Main research question:

*Can extracellular GABA stimulation offer neuroprotection, i.e. increase neuronal survival and reduce neuronal oxidative stress response, after* in vitro *cortical axotomy?*

**The main objectives of experiment 2 were:**

(i) Establish viable *in vitro* cortical neuronal networks on MEAs
(ii) Electrically stimulate the cortical networks with focal TS and assess the neuroplastic response

Main research question:

*Does the functional connection strength between defined cortical network nodes (i.e. clusters of neurons) alter as a result of repetitive focal TS?*

**The main objectives of experiment 3 were:**

(i) Establish viable *in vitro* cortical neuronal networks on custom-designed microfluidic MEAs with embedded topography
(ii) Electrically stimulate the cortical neuronal networks with targeted and temporally ordered pre- and postsynaptic electrical stimulation (i.e. paired pulse stimulation) and assess the neuroplastic response

Main research question:

*Does targeted paired pulse stimulation (i) induce alterations in axonal signalling and (ii) strengthen the connection between the stimulated node pair?*

# 3. MATERIALS AND METHODS

## 3.1. CELL CULTURE DEVICES

### 3.1.1. THE AXOTOMY CHIP (EXPERIMENT 1)

For the study of cortical neuronal responses to *in vitro* axotomy, in custom-designed microfluidic chips were fabricated, and hereafter, these chips will be referred to as axotomy chips. The axotomy chip is composed of three cell compartments (Ø 5mm) connected by 52 microtunnels (see **FIGURE 7** for axotomy chip design). The size of the tunnels; 10μm in width and 5μm in height, ensures that only neurites (dendrites and axons), and not cell somata, can enter the tunnels, while the tunnel length of 500μm restricts dendrites from growing all the way through the tunnels and into the subsequent cell compartment[71]. Axotomy microchannels (width = 50μm) run perpendicular to the tunnels and allow for the transection of axons elongating through the tunnels, by the introduction of one or several air bubbles, which run from the inlet to the outlet opening of the axotomy channels[119,120]. Most of each cell compartment is not enclosed in the chip, but open on top, which allows for easy seeding access, and media and reagent handling[121]. Fluidic isolation of the cell body microenvironments can be established by creating a hydrostatic pressure difference between the chambers. A slight difference in media volume between the cell compartments creates a continuous flow between the compartments that counteracts diffusion[70].

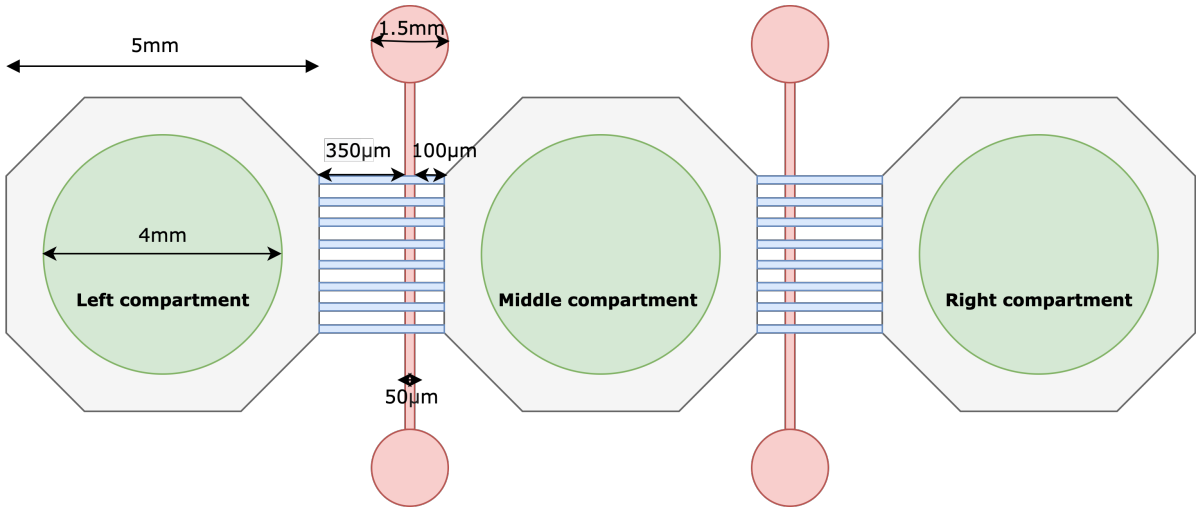


**FIGURE 7. AXOTOMY CHIP DESIGN.**

The axotomy chip is composed of three octagonal shaped cell compartments (left, middle and right) of Ø 5mm (grey) each. A Ø 4mm opening (green) within each compartment allows for easy cell seeding and reagent handling. Neurites, but not somata, can enter and elongate into 52 tunnels (blue) which connect the left and right outer compartments with the middle compartment, respectively (only 8 tunnels are illustrated in the figure for easy visualisation). Two axotomy channels of 50μm in width (red) are located perpendicular to the tunnels, and the axotomy channel inlet and outlet are Ø 1.5mm (also red). The distance from the edge of the outer compartment/tunnel entrance to the axotomy channel is 350μm, and the distance from the axotomy channel to the edge of the middle compartment is 100μm. The length of each tunnel is 500μm. The figure is not to scale.

The axotomy chips were fabricated in polydimethylsiloxane (PDMS) at NTNU NanoLab, by PhD candidate Vegard Fiskum, using standard soft lithography techniques and were assembled on glass coverslips (details can be found in [121]).

### 3.1.2. THE MEA PLATE (EXPERIMENT 2)

*In vitro* cortical neuronal networks were established on commercially available MEAs for the study of cortical network plasticity in response to targeted electrical stimulation. The CytoView MEA plate (*M384-tMEA-6B, Axion Biosystems*) holds six separate wells containing 64 electrodes each, tightly spaced in an 8x8 grid in the culture surface of each well (**FIGURE 8**). The electrodes are made of poly(3,4-ethylenedioxythiophene), or PEDOT, are 50μm in diameter, and the inter-electrode spacing is 300μm. Neuronal networks are grown on top of the electrodes on a SU-8 insolation layer. All the 64 electrodes have the ability of both recording and stimulating. The plate has built-in humidity reservoirs which prevent evaporation, and the bottom of the plate is transparent which allows for easy visualization of neuronal networks throughout the course of the experiment. The plate allows for the maintenance of multiple cultures at the same time, contained to one device. Thus, the plate maintains the same underlying properties, such as environment, for all cultures.

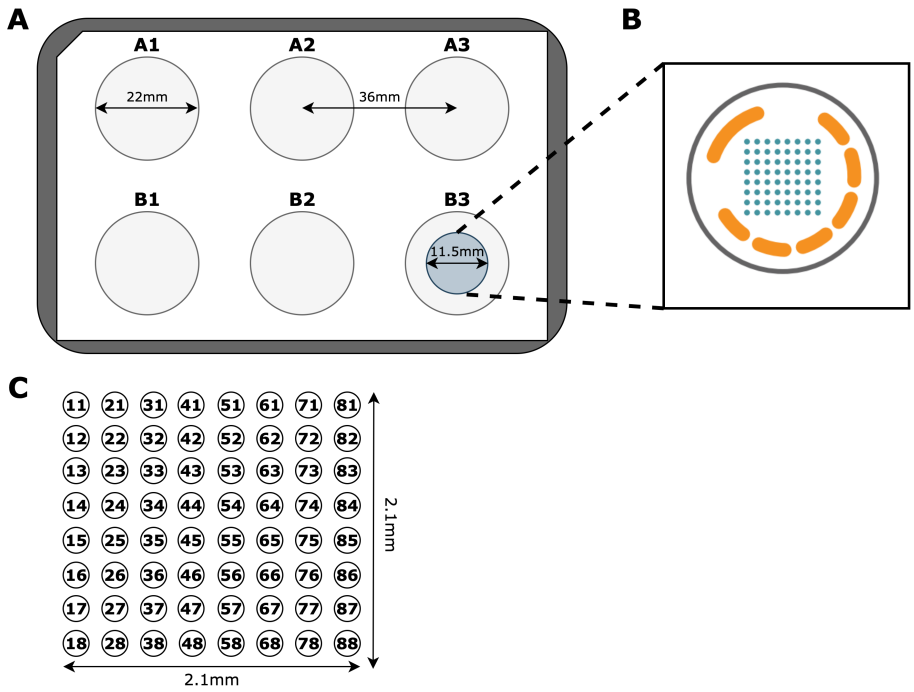


**FIGURE 8. THE MEA PLATE.**

**A)** The CytoView MEA plate holds six wells (light grey) with a well-well distance of 36mm. The wells are named according to their position on the plate, i.e. top row = A1-A3, bottom row =B1-B3. The top well diameter is 22mm. The area around the wells (white) is composed of numerous small reservoirs that can be filled with water to prevent evaporation (not shown in the figure). The bottom well diameter is 11.5mm (exemplified in well B3). **B)** Illustrates the bottom well area. 64 electrodes (small blue circles) are arranged in an 8x8 grid in the centre of each well. Electrode grounds are shown in orange. The image is reprinted from Axion Biosystems Cytoview MEA Flyer 2018. **C)** Electrodes are numbered according to their position in the grid; first number = column number, second number = row number. The recording area of each well is 2.1mm x 2.1mm.

The Maestro Pro MEA system (*Axion Biosystems*) allows for extracellular recordings from neurons cultured over and in close vicinity to the electrodes in all plate wells simultaneously. In addition, the system allows for electrical neuronal stimulation. An inbuilt heating system keeps temperatures at 37°C, and a 360° shower distributes $CO_2$ evenly across the plate during recordings and stimulations. A single button initiates plate docking, environmental control, and MEA plate recognition which gets logging based on the plate´s unique barcode. Axion´s Integrated Studio Software (AxIS) helps setup the

experiment, and stimulation designs can be made with drag-and-drop interface by AxIS Stimulation Studio. In addition, simple data analyses, such as spike and burst detection, can be done directly in AxIS.

### 3.1.3. THE SPIKE TRACKING CHIP (EXPERIMENT 3)

Microfluidic chips with microelectrode interface were custom-designed for the study of neuroplastic responses to targeted and temporally ordered pre- and postsynaptic stimulation. These chips will be referred to as spike-tracking chips (STCs). The process of making the STCs was similar to the axotomy chips, however, the PDMS chip was aligned onto a 60-electrode microelectrode array (MEA) (see [120] for information on chip alignment onto MEA). The microelectrode platform was built on a glass substrate with appropriate dimensions for the MEA2100 System™ (*Multi Channel Systems*) for recordings and stimulations (**FIGURE 9B**). The STCs were fabricated at NTNU NanoLab by MSc student Nicolai Winter-Hjelm.

The STC allows for the growth of *in vitro* neuronal networks on top of electrodes on a silicon nitrate insulation layer. The chip consists of two cell compartments (Ø 5mm) connected by eight microtunnels of 30μm width, 5μm height and 800μm length (see **FIGURE 9A** for STC design and electrode arrangement). As with the axotomy chip, only neurites, but not somata, can enter the tunnels. The chip holds 60 electrodes; 59 recording electrodes and one split internal reference electrode which does not record or stimulate.

To ensure selectivity, electrodes should preferably be small enough in size such that they can communicate with single, or small pools of, neurons. However, reducing the electrode size causes an increase in electrode impedance, and high electrode impedance is linked with low signal-to-noise ratio (SNR)[122]. Microelectrodes are commonly made of metallic conductors, such as e.g. titanium nitride or platinum (Pt)[107]. Improving the performance of micro-sized electrodes, with respect to lowering the impedance, can be achieved by maximizing the electrode surface area by the additional deposition of a material that offers a roughened electrode surface area, such as Pt-black[107,123]. With the goal of improving the performance of micro-sized electrodes, two types of STCs were made; one with all the 60 electrodes made of Pt-black, and one with a combination of Pt (29) and Pt-black (31) electrodes. The two different STC types have the same design and electrode arrangement (**FIGURE 9A)**. The majority of the electrodes (48) are placed in the eight tunnels and right in front of the tunnel entrances (i.e. in the active zones), to enable detection of spikes moving along axons in the tunnels, and to facilitate stimulation of pre- and postsynaptic neuronal network nodes, respectively. The remaining recording electrodes (11) are divided between the two cell compartments. The internal reference electrode is split, i.e. one reference electrode is placed in each compartment, however, they are both connected to the same contact pad on the MEA. The electrodes in the cell compartments are circular in shape, while the electrodes in the tunnels are oval (electrode size, Ø ~30μm). Electrodes where made oval within the tunnels to facilitate easier chip alignment onto the electrodes.

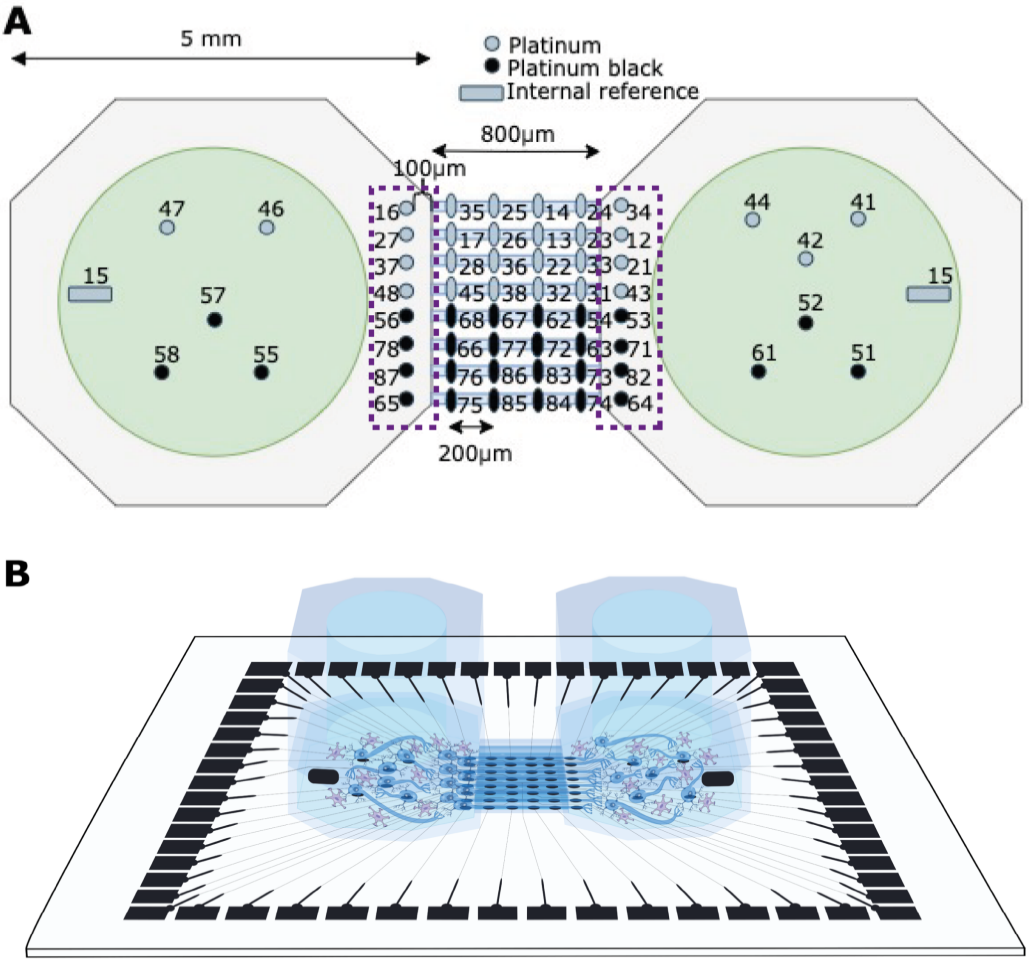


**FIGURE 9. SPIKE TRACKING CHIP DESIGN.**

**A)** The spike-tracking chip (STC) is composed of two octagonal shaped cell compartments of Ø 5mm (grey), connected by eight tunnels (blue). A Ø 4mm opening (green) allows for easy seeding and reagent handling. The chip holds 59 recording electrodes and one split internal reference electrode (electrode numbering is shown in the figure). Four recording electrodes span the length of each tunnel, with an inter-electrode distance of 200µm, resulting in a total of 32 recording electrodes within the tunnels. The electrodes in the tunnels are oval in shape, in contrast to the circular electrodes in the compartments. One recording electrode is located 100µm away from each of the compartment-tunnel intersections, in the active zones (indicated by purple dashed bars). The remaining 11 recording electrodes are split between the two cell compartments, with five and six electrodes in each compartment, respectively. Two types of STCs were made: On of the types holds 31 Pt-black electrodes (black circles and ovals) and 29 Pt electrodes (grey circles and ovals), including the internal reference. The second type has the same design and electrode arrangement as shown in the figure, however, all recording electrodes are made of Pt. **B)** 3D illustration of chip alignment onto the MEA (illustration is made by Nicolai Winter-Hjelm, MSc student). Figure (A) is not to scale.

Using the MEA2100 System™ (*Multi Channel Systems*), extracellular recordings or selective stimulation of individual electrodes, or specific groups of electrodes, can be carried out on the STC. Individual electrodes can be recorded from or stimulated at any given time. The MEA2100 System™ consists of two main devices; an interface board with an integrated signal processor and a MEA IT60 headstage which has integrated amplification, a signal processor, an analog-to-digital converter and a stimulus generator. In addition, the system allows for temperature control, thus, temperatures can be kept constant at 37°C during recordings and stimulations.

### 3.1.4. THE IBIDI CHIP

*In vitro* neuronal networks were grown on a glass slide with eight removable silicone wells (*80841, IBIDI®*) for the purpose of immunocytochemistry (ICC). The device will be referred to as an IBIDI. The culture area of each well is 12mm x 7.75mm (93mm$^2$) and the well height is 8.0mm. The glass slide is 26mm in length, 76mm in width and 1mm in height.

## 3.2. CELL CULTURES

### 3.2.1. COATING

In the current project, cortical neuronal networks were cultured on eight axotomy chips, in three wells of one MEA plate, on six STCs (STC 1-3 had Pt-black electrodes only, while STC 4-6 had a combination of Pt and Pt-black electrodes) and in all eight wells of one IBIDI.

The axotomy chips and the STCs were UV-sterilized overnight in a laminar flow hood before coating. The cell compartments and axotomy microchannels of all chips, as well as all the IBIDI wells, were coated with 0.01% poly-L-ornithine solution (PLO) (*Sigma Aldrich*), and left overnight in the fridge (4°C). An uneven volume of PLO coating was applied between the cell compartments of each chip to promote flow, such that the coating also reached the microtunnels. 200μL PLO coating was used per well of the IBIDI. The next day, PLO coating was aspirated, and the cell compartments, axotomy microchannels and IBIDI wells were rinsed three times with distilled water. Next, natural mouse laminin (20μg/mL, *Thermo Fisher Scientific*) diluted in Dulbecco´s phosphate buffered saline, free of calcium and magnesium (D-PBS-/-, *Sigma Aldrich*), was added to all cell compartments, axotomy microchannels and IBIDI wells. As with the PLO coating, the laminin solution was distributed with a minute volume difference between the compartments. 200μL laminin solution was used per well of the IBIDI. The chips and IBIDI were left in a humidified air incubator (37°C, 5% $CO_2$, 0% $O^2$) for two hours prior seeding. The laminin solution was removed right before seeding and replaced with fresh pre-warmed cell media.

Three wells of one MEA plate were coated with 210μL of 0.05% Polyethyleneimine (PEI, *Polysciences*) diluted in 4-(2-hydroxyethyl)-1-piperazineethanesulfonic acid (HEPES, *Thermo Fisher Scientific*). The plate reservoirs were filled with distilled water to prevent evaporation, and the plate was left in a humidified incubator (37°C, 5% $CO_2$, 0% $O^2$) overnight. The next day, the water was removed from the reservoirs, and the PEI coating was removed from the wells. The wells were then washed four times with 1mL of distilled water. After removing the last wash, the plate was left to air dry in room temperature in a laminar flow hood. 15 days later, the wells were coated with 210μL laminin solution, consisting of natural mouse laminin (20μg/mL, *Thermo Fisher Scientific*) diluted in D-PBS-/- (*Sigma Aldrich*). The plate was then left in the fridge (4°C) for two days. Two hours before cell thawing and seeding, the plate was left in room temperature in a laminar flow hood. The laminin solution was removed right before seeding.

### 3.2.2. CELL SEEDING AND MAINTANENCE

All culture devices were seeded with Rat Primary Cortical Astrocytes (*N7745-100, Thermo Fisher Scientific*) and Rat Primary Cortical Neurons (*A10840-01, Thermo Fisher Scientific*). Cortical neurons were co-cultured with astrocytes, as astrocytes have been reported to enhance neuronal attachment, survival and growth *in vitro*[124]. ***TABLE 1*** contains an overview

of the number of astrocytes and cortical neurons seeded in each cell compartment/well and cortical neuron density (neurons/mm$^2$) with respect to the different culture devices.

Astrocytes (passage number 3) were seeded as a feeding layer in each of the individual cell compartments of all eight axotomy chips, all six STCs, and all eight IBIDI wells. The axotomy chips and IBIDI wells were seeded on the same day, while the STCs were seeded at a later stage. The thawing and seeding of astrocytes were done in accordance with Invitrogen™ protocol (*MAN0001679, Thermo Fisher Scientific*). The astrocyte media consisted of 83% Dulbecco´s modified eagle medium (D-MEM, high glucose), 15% fetal bovine serum (FBS) and 2% penicillin/streptomycin (PenStrep) (all from *Thermo Fisher Scientific)*. To count the astrocytes, Trypan Blue (*Thermo Fisher Scientific*) and the Countess™ II Automated Cell Counter (*Thermo Fisher Scientific*) were used.

Two days after seeding the astrocytes, cortical neurons were seeded on top of the feeding layer (0 days *in vitro* = 0DIV). The left and right cell compartment (see **Figure 7**), but not the middle compartment, of six axotomy chips (axotomy chip 1-6) were seeded with cortical neurons. All three compartments of the two remaining axotomy chips (axotomy chip 7 and 8), both compartments of all six STCs, and all IBIDI wells were seeded with cortical neurons. The culture devices were seeded at different days; however, the procedure was the same; $10^6$ cortical neurons were thawed, and the thawing and seeding were mostly done in accordance with Gilbco™ protocol (*MAN0001574*, *Thermo Fisher Scientific*). The cortical neuronal media consisted of 95% Neurobasal™ Plus, 2% B27™ Plus Supplement (50X), 1% GlutaMax Supplement and 2% PenStrep (all from *Thermo Fisher Scientific*). In contrast with the protocol, Rock Inhibitor (*Y-27632, Sigma Aldrich*) (100X) was added to the media during thawing to promote a higher neuronal survival rate. In addition, 500μL, not 2mL, cortical neuronal media were added to the cell suspension after thawing. This was done to increase the number of neurons/mL to make seeding in small chip cell compartments feasible. The cell compartments of the axotomy chips and the STCs were seeded with 30μL and 45μL cell suspension, respectively, and were topped up with pre-warmed cortical neuronal media right after seeding (to a total of ~40μL media/axotomy chip compartment and ~80μL media/STC compartment). All of the axotomy microchannels were filled with pre-warmed cortical media, and for the axotomy chips containing only astrocytes in the middle compartment, astrocyte media were replaced with cortical neuronal media. Each IBIDI well was filled with pre-warmed cortical neuronal media prior seeding, and after seeding, each well contained a total of 300μL media. 50% of the media were changed five hours after seeding, as well as the next day. Then, 50% of the media were changed every 2-3 days until the cultures were terminated.

Three wells of the MEA plate (well A1, A3 and B2, see **Figure 8A**) were seeded with a co-culture of astrocytes (passage number 3) and cortical neurons, with an astrocyte-cortical neuron ratio of 1:10. Astrocytes were thawed in accordance with Invitrogen™ protocol (*MAN0001679, Thermo Fisher Scientific*), but after centrifugation, the astrocytes were resuspended in 1mL pre-warmed cortical neuronal media supplemented with Rock Inhibitor (*Y-27632, Sigma Aldrich*) (100X). The astrocytes were then counted using Trypan Blue and the Countess™ II Automated Cell Counter (*Thermo Fisher Scientific*). The total number of astrocytes (100 000 astrocytes) needed to make up an astrocyte-neuron ratio of 1:10 equalled 321μL astrocyte cell suspension, and 321μL cell suspension was transferred to a sterile 15mL tube. Next, 679μL cortical neuronal media were dropwise added (1 drop/second) to the astrocyte cell suspension, such that the cell suspension equalled a volume of 1mL. Then, $10^6$ cortical neurons were thawed and transferred to a

sterile 15mL tube. The astrocyte cell suspension (1mL) was dropwise added to the tube containing the cortical neurons. The cell suspension, now containing both astrocytes and cortical neurons, was resuspended slowly. 374.4μL cell suspension was seeded on top of the middle electrode area of each of the three wells, and the plate reservoirs were filled with pre-warmed distilled water to limit evaporation. The plate was left in a humidified air incubator (37°C, 5% $CO_2$, 0% $O^2$) for one hour. Then, the wells were topped up with pre-warmed cortical neuronal media such that each well contained a total of 1mL. 50% of the media (500μL) were changed five hours after seeding, the next day, two days after seeding, and five days after seeding. Then, 50% of the media were changes once a week until the cultures were terminated.

**TABLE 1.** OVERVIEW OF NUMBER OF CELLS SEEDED IN EACH WELL/COMPARTMENT AND CORTICAL NEURON DENSITY WITH RESPECT TO THE DIFFERENT CULTURE DEVICES.

| CULTURE DEVICE | ASTROCYTES PER WELL/ COMPARTMENT | CORTICAL NEURONS PER WELL/ COMPARTMENT | WELL AREA ($MM^2$) | CORTICAL NEURON DENSITY (NEURONS PER $MM^2$) |
|---|---|---|---|---|
| AXOTOMY CHIP | 2 000 | 20 000 | 12.6 | 1 587.30 |
| SPIKE-TRACKING CHIP | 2 000 | 30 000 | 12.6 | 2 380.95 |
| MEA PLATE | 18 700 | 187 200 | 104 | 1 800 |
| IBIDI CHIP | 5000 | 60 000 | 93 | 645.16 |

All axotomy chips and all STCs were kept in Petri dishes together with a small-sized dish filled with 3mL distilled water to prevent evaporation. The Petri dishes were sealed with Parafilm, and the cortical networks cultured on the chips and on the IBIDI were kept in a humidified air incubator (37°C, 5% $CO_2$, 0% $O^2$) over the experimental time frame. The chips and IBIDI were only removed from the incubator during media change, imaging and recording/stimulation. The MEA plate was left in a humidifier air incubator (37°C, 5% $CO_2$, 0% $O^2$) for the first 14DIV. For the rest of the experimental time frame, the MEA plate was left in the Maestro Pro MEA system, which was set to maintain 37°C and 5% $CO_2$. The MEA plate was only removed from the incubator/Maestro Pro MEA system during media change and imaging.

### 3.3. IMMUNOCYTOCHEMISTRY

Immunoassay was performed on cortical networks of 22DIV cultured in the IBIDI and on four axotomy chips (axotomy chip 2, 6, 7 and 8). The IBIDI wells and the cell compartments of the axotomy chips were washed with D-PBS-/- (*Sigma Aldrich*) before fixed with 4% paraformaldehyde (PFA) (*Sigma Aldrich*). After 15 min, the PFA was aspirated and samples were washed three times with D-PBS (15 min wait between each wash). The samples were stored in D-PBS for three weeks in the fridge (4°C). Next, a block, made by diluting 5% goat serum (GS) (*Sigma Aldrich*) and 0.3% Triton X (*Sigma Aldrich*) in D-PBS, was added to each cell compartment and left for two hours to avoid non-specific binding of antibodies. After removing the block, a solution with primary antibodies was added to each well/cell compartment. The primary antibody solution was made by diluting primaries, 1% GS and 0.1% Triton X in D-PBS. The primary antibodies used for the IBIDI were rabbit anti-neurofilament heavy (*ab8135, Abcam*) at a dilution ratio of 1:1000 and mouse anti-GAD65 (GAD = glutamate decarboxylase) (*ab26113, Abcam*) at a dilution-ratio of 1:500. The primary antibodies used for the axotomy chips were rabbit anti-neurofilament heavy (*ab8135, Abcam*) at a dilution ratio of 1:1000, and mouse anti-synaptophysin (*ab8049, Abcam*) at a dilution ratio of 1:50. The samples were left overnight in the fridge (4°C) on a rotating plate, in Petri dishes sealed with Parafilm.

The next day, three consecutive washes with D-PBS were performed on the fixed cells in room temperature. Then, secondary antibodies were added to each well/compartment and left for two hours in the dark to visualize the immunolabeling. The secondary antibody solution was made by diluting secondaries, 1% GS and 0.1% Triton X in D-PBS. All secondary antibodies had a dilution ratio of 1:1000. The secondary antibodies used were goat-anti-rabbit 647 Alexa Flour and goat-anti-mouse 488 Alexa Flour. Hoescht (*Thermo Fisher Scientific*), diluted at 1:5000 in D-PBS, was added to each well and chip compartment five minutes before the two hours had passed, to visualize cell nuclei. Next, the samples were washed two times with D-PBS, and one time with distilled water (15 min wait between each wash). For the axotomy chips, the last wash was left in. For the IBIDI wells, after removing the last wash, the silicon wells were removed. Two drops of Mounting Medium with DAPI - Aqueous, Fluoroshield (*ab104139*, *Abcam*) were added to the glass slide containing the samples, before mounting a rectangular coverslip on top of the glass slide. All samples were stored in the dark, in the fridge (4°C) until imaging the next day. During all steps of the immunocytochemistry (ICC) process, a minute volume difference between the three compartments of each axotomy chip was kept, to promote flow through the microtunnels (i.e. the middle compartment was filled with ~10μL more fluid than the two outer compartments). For the ICC on the IBIDI, all fluids, i.e. washes, PFA fixation, block solution, primary solution, secondary solution and Hoescht solution, were added at 200μL/well.

## 3.4. ELECTROPHYSIOLOGY (EXPERIMENT 2)

### 3.4.1. RECORDING

Before docking the MEA plate in the Maestro Pro MEA system, the plate environment was set to be kept at 37°C and 5% $CO_2$. During recordings/stimulation, spikes were detected with the inbuilt adaptive threshold method (see AxIS Navigator 2.0 User Guide, *Axion Biosystems*). The amplitude threshold is specific for each individual electrode and was set to +/- 7 standard deviations (SD). Data was recorded with a sampling rate of 12.5 kHz, and the electrophysiological activity was filtered with a Butterworth filter (high pass cutoff at 200Hz). All three cortical networks were recorded/stimulated simultaneously. At 55DIV, the cortical network activity was recorded for 1h. At 56DIV, a 1h baseline recording was performed before TS was delivered for 30min (see stimulation protocol below). Cortical network activity was recorded during the stimulation period, and for 30min after ended stimulation.

### 3.4.2. STIMULATION

One arbitrary central electrode on the MEA, i.e. electrode 44 (see **FIGURE 8**), was selected for delivering TS. All three cortical networks received identical stimulation; stimulation pulses were delivered at 100Hz every 10s for 30 min. The stimulation pulse was biphasic (positive first, +/- 100mV, phase duration 200μs) (**FIGURE 10**).

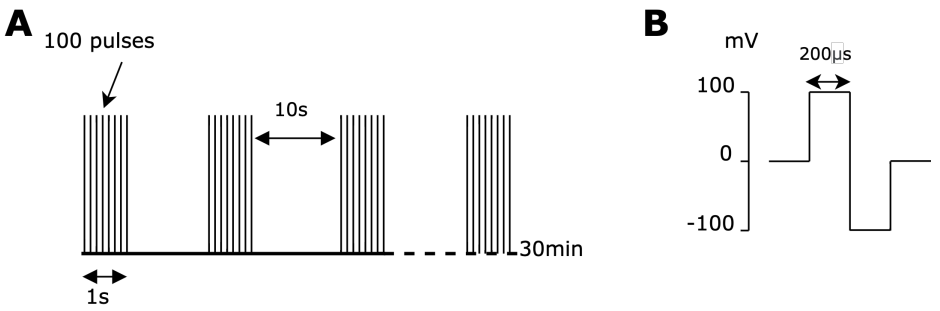


**FIGURE 10. STIMULATION PROTOCOL FOR CORTICAL NETWORKS CULTURED ON THE MEA PLATE.**

**A)** Stimulation pulses were delivered at 100Hz, with an inter-stimulation interval of 10s. Stimulation was applied for a duration of 30 min. **B)** The stimulation pulse was biphasic (positive first, +/- 100mV, phase duration 200µs).

### 3.4.3. DATA ANALYSIS

The data analysis was done in MATLAB in collaboration with Ola Huse Ramstad (PhD candidate). Cross-correlations comparing the spike train data (i.e. the spike times captured by each individual electrode) for every possible electrode pair on the MEA were performed to assess (i) the stability of functional connection strengths over 1h of spontaneous activity; and (ii) whether TS induced alterations in functional connectivity strengths within the cortical networks. The cross-correlations were performed with 10ms time bins, with a time offset up to +/-100ms. For each electrode pair, an average correlation was calculated. The difference in the average correlation between every electrode pair on the MEA pre stimulation (averaged of 1h) vs. post stimulation (averaged over 30min) was then taken by subtracting the average correlation of each electrode pair pre stimulation from post stimulation. The difference in average correlation between every electrode pair, between the first 30min and the second 30min of a 1h recording of spontaneous activity, was calculated in the same way for the network stability analysis. "Significant" alterations in functional connections strengths were defined based on this stability test (see **RESULTS**). The estimated difference in average correlation between the electrode pairs pre and post stimulation was further used to extract the number of significantly altered connections after TS for each cortical network (if the results revealed a significant difference in autocorrelations, these were excluded). The presented raster plots were generated in MATLAB.

## 3.5. ELECTROPHYSIOLOGY (EXPERIMENT 3)

### 3.5.1. RECORDING

To prevent the cortical networks cultured on the STCs from air exposure, a custom-designed Teflon membrane cap was used to cover the STCs during recordings and stimulation. Recordings were done on one STC at a time. After placing the STC in the MEA IT60 Headstage, data acquisition was started. A 5 min time lapse was allowed before starting the recording to compensate for voltage drift in the system. Data was recorded with a sampling rate of 20kHz, and the recorded activity was filtered with a Butterworth filter (high pass cutoff at 200Hz). The cortical networks were recorded for 15 min at different DIV, within a time frame of 13-29DIV. During recordings, the temperature was set to be kept at 37°C.

### 3.5.2. STIMULATION

When the cortical networks cultured on the STCs reached 26DIV, a 15min long baseline recording was performed on all six STC (STC 1-6, as described above). Data analysis on

this baseline recording was used to tailor the paired pulse stimulation protocols, and the data analysis was done in MATLAB by the use of the μSpikeHunter software[125]. μSpikeHunter has been developed specifically for identifying travelling spikes moving along axons cultured in microfluidic chips. μSpikeHunter allows for (i) detection of travelling spikes in the recorded data; (ii) determination of the directionality of the travelling spikes; (iii) estimation of axonal propagation velocity (PV); and (iv) spike sorting.

In μSpikeHunter, negative phase detection and an amplitude threshold of +/- 5 SD were defined for spike detection. Spike events (i.e. spikes travelling across all four electrodes within a microtunnel) were detected by manually choosing the start and end electrode, which corresponds to the two outer most electrodes in the microtunnel of interest. Next, the time range for analysis was set to include the entire 15min of each recording, and a list of all spike events within the chosen microtunnel was generated. To identify signals generated from single neurons/axons, we used μSpikeHunter´s integrated spike sorting method (see [125]), in which spike events likely to come from single neurons are clustered together. When spike sorting, an estimate of the mean PV for each cluster is calculated with μSpikeHunter´s integrated cluster propagation velocity method (all PVs in the current experiment were obtained with this method). Upon completion, the sorted data, which included the spike times on each electrode, along with the estimated mean PV and PV confidence indices, for every sorted cluster, was saved.

To identify a STC suitable for stimulation, two criteria had to be met: (i) spike events could be detected within individual microtunnels; and (ii) after applying spike sorting to identify the signals likely to come from single neurons, the mean axonal PV for identified neurons could be calculated with confidence less than the estimated mean PV.

Based on these criteria, STC 4 was selected for stimulation. A paired pulse stimulation was applied to two microtunnels of STC 4 simultaneously, i.e. microtunnels 1 and 4, and the stimulation protocol was tailored to target one axon within each of these tunnels. Depending on the directionality of the detected spikes within each cluster, we defined a presynaptic and postsynaptic node for stimulation. These nodes corresponded to the electrodes located in the active zones, 100μm outside the microtunnels, one on each side (**Figure 11a**). An electrical pulse was first delivered to the presynaptic node (through the first electrode), and after a set time delay, an identical pulse was delivered to the postsynaptic node (through the target electrode). The time delay (in ms) was calculated based on the mean PV for the cluster in interest, taking into account the distance between the presynaptic and postsynaptic stimulation electrodes. Thus, the estimated delay was different depending on the axon of interest. The stimulation pulse was biphasic (negative first, +/- 200mV, phase duration 200μs), and pulses were delivered every 5s for 15min. Immediately after ended stimulation, spontaneous activity was recorded for 15min. A 15 min recording was also done three days after stimulation. The paired pulse stimulation protocol with respect to the different microtunnels of STC 4 is presented in **Figure 11** and **Table 2**.

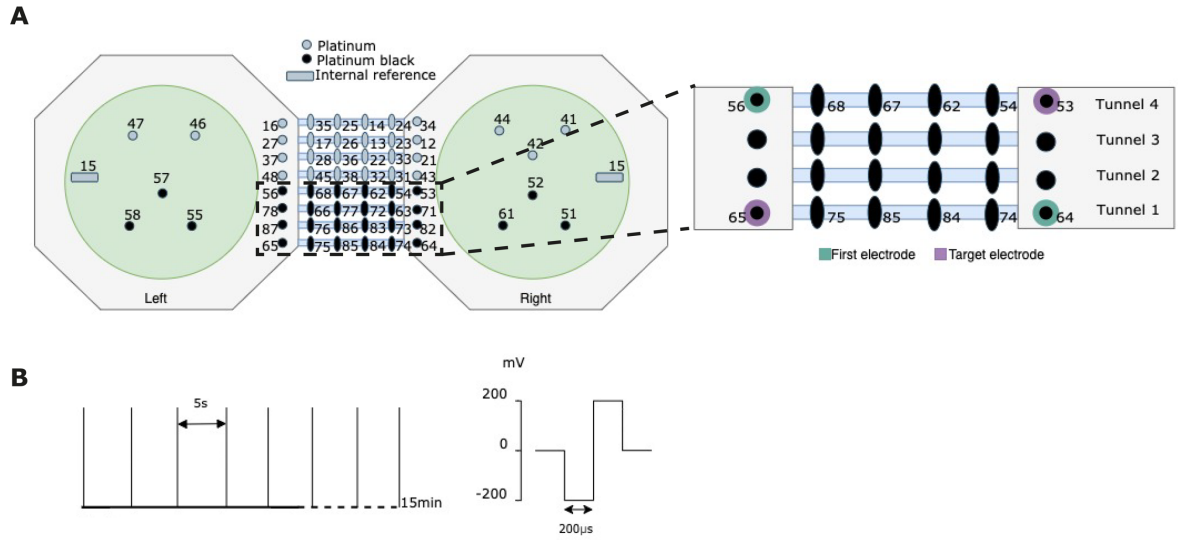


**FIGURE 11. STIMULATION PROTOCOL FOR THE CORTICAL NETWORK CULTURED ON STC 4**

**A)** STC design for reference. Boxed area is enlarged and show electrode arrangement and electrode numbering for the two microtunnels selected for stimulation (i.e. microtunnel 1 and 4). The paired pulse stimulation involved stimulating a presynaptic node (through the first electrode), and after a time delay (estimated specifically for each tunnel, see **TABLE 2**), apply an identical stimulation pulse to a postsynaptic node (through the target electrode). **B)** The stimulation pulse was biphasic (-/+ 200mV, negative first, pulse phase duration 200µs), and was delivered every 5s for 15min.

**TABLE 2.** OVERVIEW OF SELECTED MICROTUNNELS, STIMULATION ELECTRODES AND DELAY.

| STIMULATION | STC | MICROTUNNEL | FIRST ELECTRODE | TARGET ELECTRODE | DELAY (MS) |
|---|---|---|---|---|---|
| Paired pulse | 4 | 1 | 64 | 65 | 1.75 |
| | | 4 | 53 | 56 | 1.2 |

*Note.* See **FIGURE 11A** for an overview of the STC´s electrode arrangement and microtunnel numbering. First electrode and target electrode correspond to the electrode receiving the stimulation pulse first and last, respectively. Delay corresponds to the time delay (in milliseconds) between the delivery of the stimulation pulse to the first electrode and the target electrode.

### 3.5.3. DATA ANALYSIS

Due to time constraints, further data analysis was only carried out on one identified cluster (i.e. one identified neuron/axon), traced within microtunnel 1 of STC 4. Using µSpikeHunter´s spike sorting method, spiking data from the axon targeted by the stimulation was extracted for the different recording times, i.e. baseline/pre stimulation (Pre Stim), immediately post stimulation (Post Stim) and 3 days post stimulation (3 Days Post Stim). To investigate potential alterations in axonal information processing as a consequence of the stimulation, the sorted cluster´s mean PV and mean propagation delay were calculated for the different recording times. The propagation delay was calculated by taking the spike times of the first electrode from the spike times of the end electrode (the two outer electrodes in microtunnel 1) for every spike event. These were then used to calculate the mean axonal propagation delay. In short, the mean PV is calculated in µSpikeHunter by aligning all spike shapes within each identified cluster. The PV is then calculated by the distance between the two outer most electrodes of the microtunnels (in our case this distance is 0.6mm), over the time between the average peaks registered at these two electrodes (i.e. propagation delay). We decided to use the estimate of the mean propagation delay as an indication of axonal PV, as the effect of any potential outliers on the average of the delay would be exaggerated in the PV estimate, due to the inverse

proportional relationship between the two. We also obtained the peak spike amplitudes for each electrode using μSpikeHunter. For each time of recording, the mean peak spike amplitude was calculated for each of the four electrodes located within microtunnel 1. The graphs presenting the mean axonal propagation delay and mean spike amplitude were generated in Excel. A selected number of individual spike events within the cluster of interest were plotted in MATLAB to exemplify the data.

We further wanted to investigate if the paired pulse stimulation induced alteration in the connection strength between the stimulated pre- and postsynaptic node. To do this, a cross-correlation was applied to the spike train data obtained from STC 4 at the three different recoding times using MATLAB. The cross-correlations were performed with 5ms time bins, with a time offset up to +/-50ms. The difference in the average correlation between every electrode pair on the STC pre stimulation (averaged over 15min) vs. post stimulation (averaged over 15min) was then calculated by subtracting the average correlation of every electrode pair pre stimulation from post stimulation. From this analysis, the differences in average correlation between the electrode pair of interest (i.e. electrode 64 and 65) were extracted. All data analyses done in regard to experiment 2 were done in collaboration with Kristine Heiney (PhD Candidate) and Ola Huse Ramstad (PhD candidate).

### 3.6. IMAGING

A phase contrast microscope (*Zeiss Axio* Vert. 25) was used for imaging live cultures at different DIV, and imaging for immunoassay was obtained by using a fluorescence microscope (EVOS™ Microscope M5000 Imaging System). All images were processed using Fiji software and Adobe Illustrator.

# 4. RESULTS

## 4.1. EXPERIMENT 1 – AXOTOMY

### 4.1.1. NO AXONAL GROWTH THROUGH THE MICROTUNNELS

**FIGURE 12** displays the planned experimental setup for experiment 1, where the initial objectives were to assess cortical neuronal responses after *in vitro* axotomy, as well as investigate the effect of extracellular GABA addition immediately after axotomy. Six axotomy chips (axotomy chip 1-6), with the setup as shown in **FIGURE 12A**, were going to be used for the axotomy study, while the two remaining axotomy chips (with the setup as shown in **FIGURE 16A**) were going to be used for the purpose of ICC. Axotomy was to be performed when the neuronal networks reached ~35DIV.

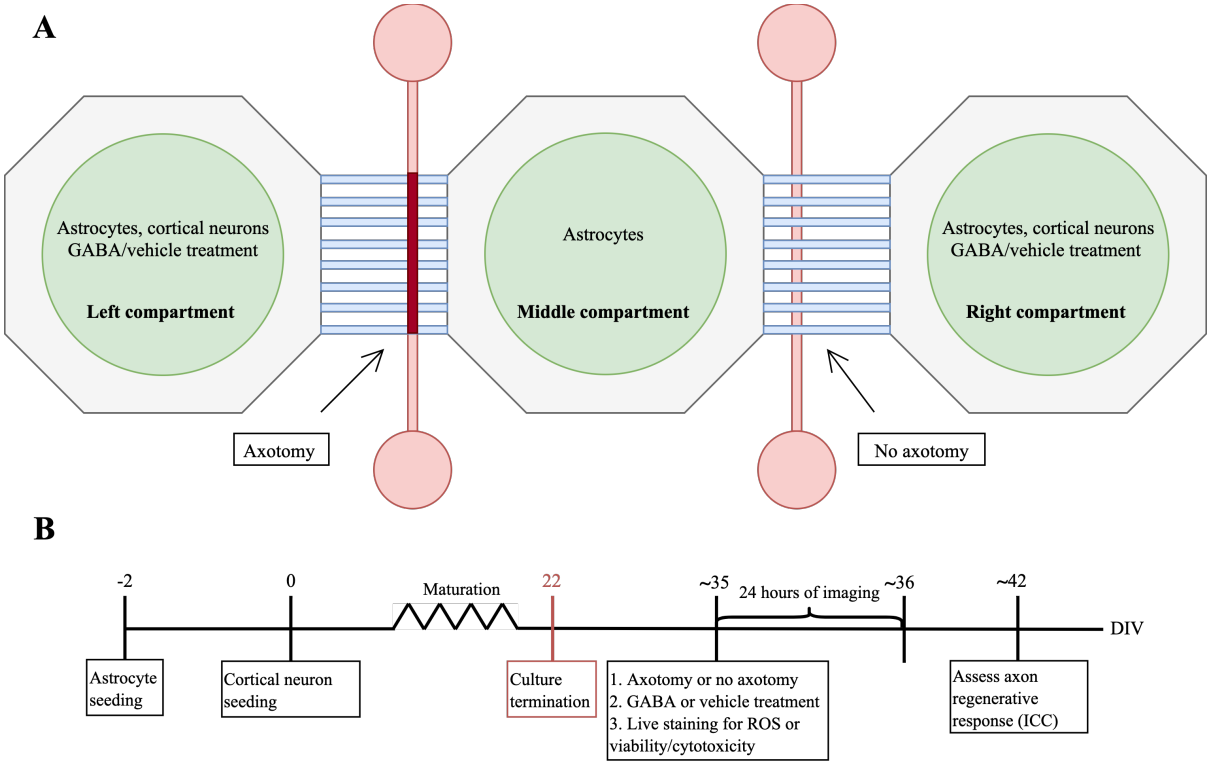


**FIGURE 12. DESIGN OF EXPERIMENT 1 – AXOTOMY.**

**A)** The original plan was to transect all axons elongating from neurons in the left compartment into the middle compartment, by air bubble-axotomy (indicated in dark red) at ~ 35DIV. All axons elongating from the right into the middle cell compartment of the same chip would not be transected; the network within the right cell compartment, and axons within the right tunnels would work as an internal control. Immediately after axotomy, the outer left and right compartments would either receive extracellular GABA or a vehicle treatment (cortical neuronal media). **B)** A step-by-step overview that indicates timepoints, treatments and assays of the planned experiment. Immediately after GABA/vehicle treatment, live staining for cellular production of ROS or live staining for cell viability/cytotoxicity would have been applied. After applying the live staining, imaging was to be carried out using florescence microscopy. The intention was to set the microscope to image all three cell compartments of one axotomy chip simultaneously every hour for 24 hours. All six axotomy chips would be imaged separately. The plan was to use the images to quantify and compare ROS production and cell viability over time, between neuronal networks of different experimental groups. 7 days later, axonal regenerative response would have been assessed through ICC. Culture termination, as a consequence of no axonal growth through the tunnels of any axotomy chips, is indicated in red (i.e. 22DIV).

When inspecting the axonal tunnels through light microscopy throughout the first three weeks *in vitro*, no cells were observed in close vicinity to the tunnels and no axons were

observed within the tunnels in any of the axotomy chips (**Figure 13**, images from 17DIV). We observed a high degree of debris around, and within, the tunnels. The debris, which is likely to be PDMS debris from chip production (at least the debris that appeared larger in size than potential cellular debris, indicated by arrows in **Figure 13**) appeared to block the microtunnels entrances. Smaller-sized debris was also observed within the axotomy channels (**Figure 13**, enlarged images). With no apparent axonal growth within the tunnels, we could not proceed with the original experiment.

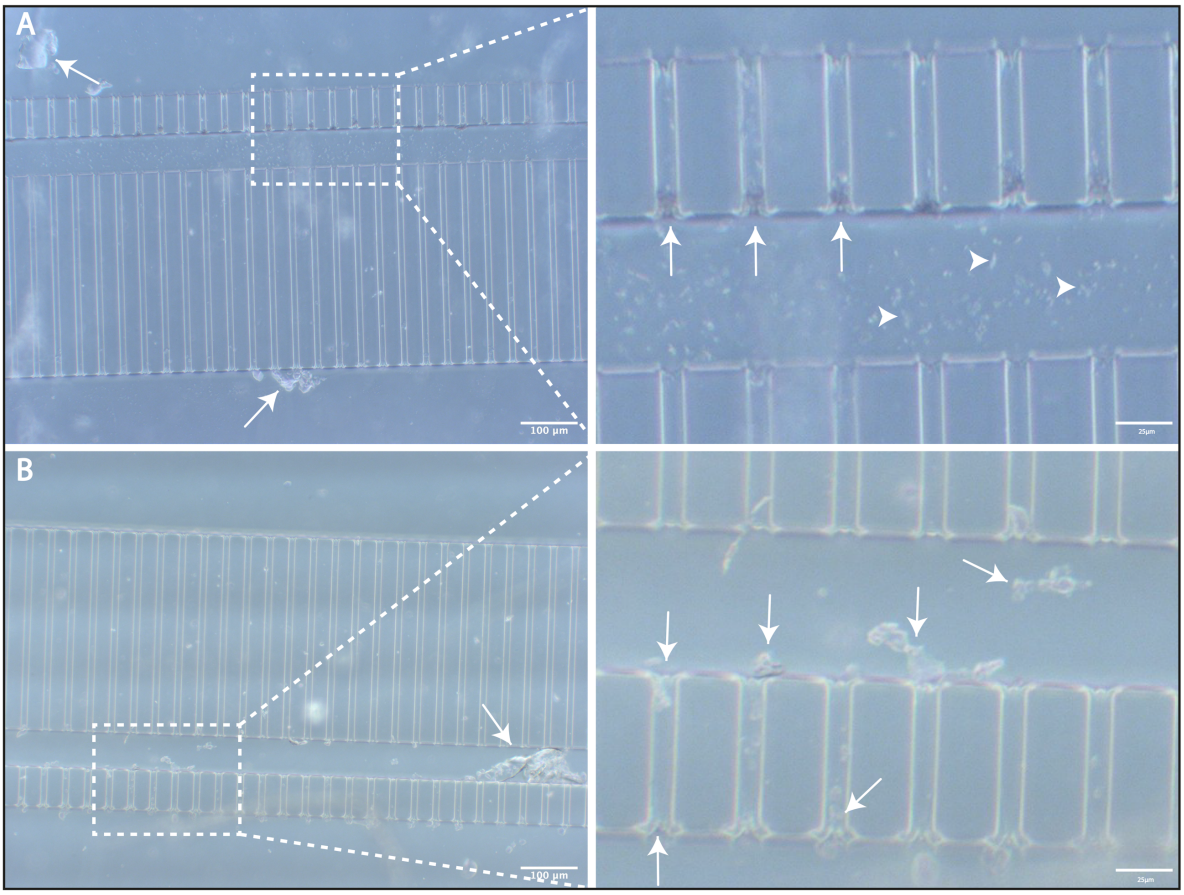


**Figure 13. Phase-contrast images of axon microtunnels at 17DIV.**

**A and B)** Representative images of axon microtunnels taken at 17DIV. (A) and (B) are images taken from two different axotomy chips. Notice that there are no signs of any cells in close vicinity to the microtunnels, and that no axonal growth through the microtunnels can be observed. Scale bar, 100µm. Magnification 10X. Boxed areas are enlarged; scale bar, 25µm. White arrows indicate noncellular debris, likely PDMS debris, around and inside the microtunnels. Arrowheads indicate debris within the axotomy microchannel.

Cortical network maturity within the separate cell compartments of the axotomy chips was assessed visually via light microscopy at 17DIV. **Figure 14B** and **C** depict phase contrast images of the left and right cell compartment of two representative axotomy chips, respectively. At 17DIV, we observed that neuronal networks had developed within the individual cell compartments of the chips. This was illustrated by the presence of attached cell bodies which appeared structurally connected to each other through neurite outgrowth (**Figure 14**, especially noticeable in the enlarged images).

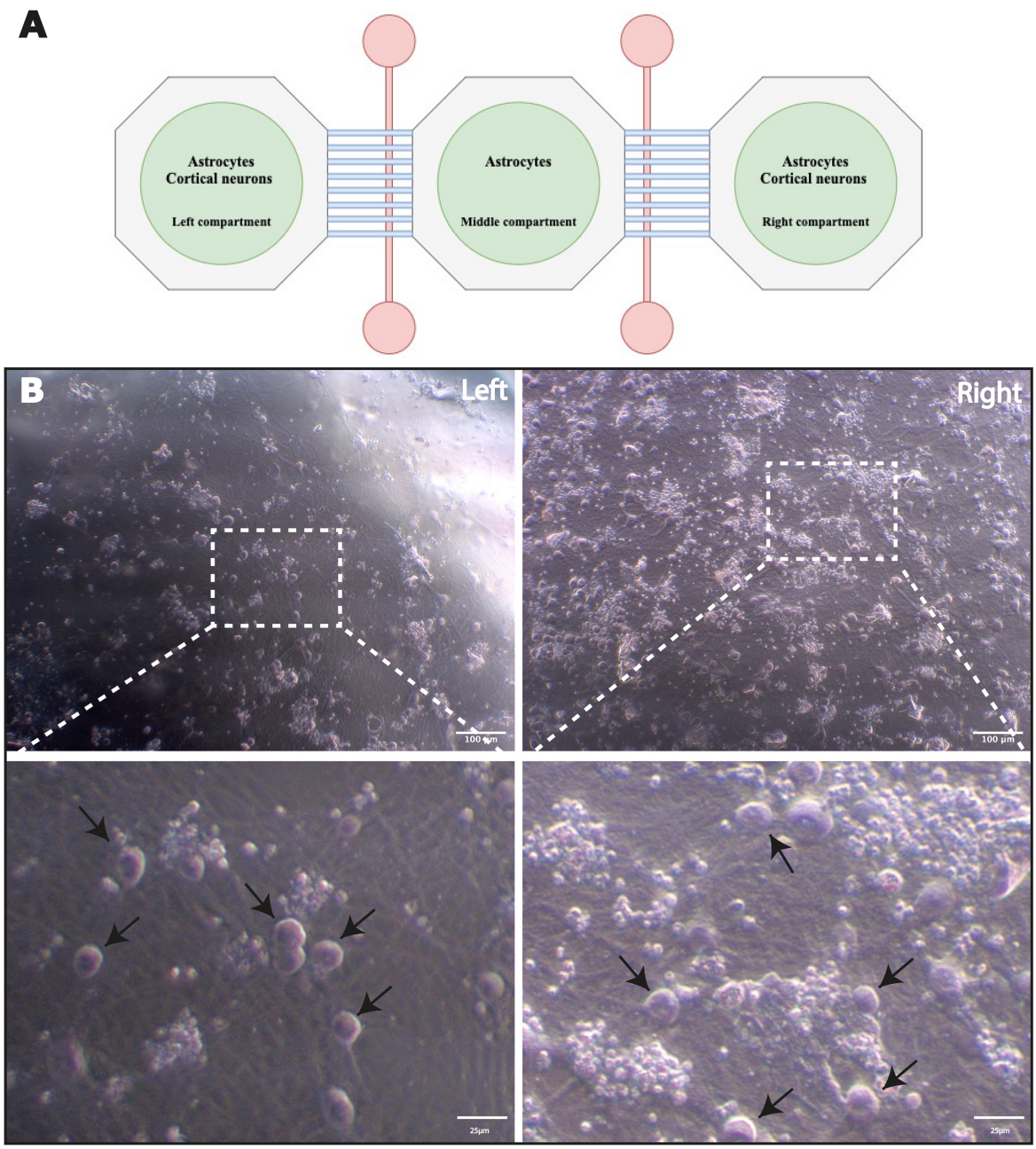
A
Astrocytes
Cortical neurons
Left compartment
Astrocytes
Middle compartment
Astrocytes
Cortical neurons
Right compartment
B
Left
Right
100 µm
100 µm
25µm
25µm

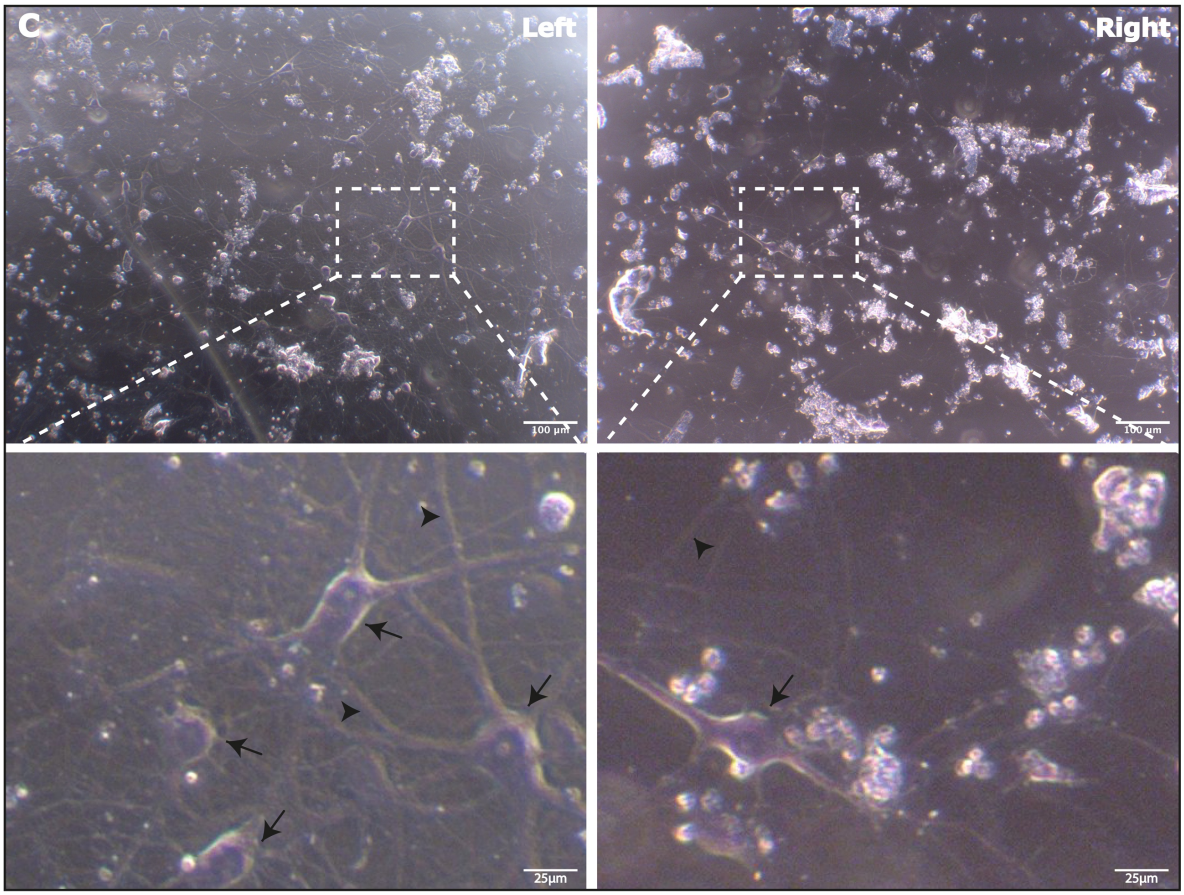


**FIGURE 14. REPRESENTATIVE PHASE-CONTRAST IMAGES OF CORTICAL NETWORKS IN INDIVIDUAL CELL COMPARTMENTS OF TWO AXOTOMY CHIPS AT 17DIV.**

**A)** Axotomy chip design and seeding overview for reference. The left and right cell compartment of six axotomy chips were seeded with astrocytes and cortical neurons. The middle cell compartment was seeded with astrocytes. **B)** Snapshots of cortical networks cultured in the left and right cell compartment, respectively, of one axotomy chip (i.e. Chip 6). Scale bar, 100µm. Magnification, 10X. Boxed areas are enlarged; scale bar, 25µm. Black arrows indicate attached cell bodies. **C)** Snapshots of cortical networks cultured in the left and right cell compartment, respectively, of another axotomy chip (Chip 2). Scale bar, 100µm. Magnification, 10X. Boxed areas are enlarged; scale bar, 25µm. Black arrows indicate attached cell bodies, and black arrowheads indicate neurites.

To examine the structural properties of the cortical networks cultured on the axotomy chips further, the networks were fixated at 22DIV for the purpose of ICC (see **FIGURE 12A** for culture termination relative to experimental timeline). We performed immunofluorescent labelling against the neuron-specific markers neurofilament heavy (NF-H) and synaptophysin. NF-H is a marker for intermediate filaments, a component of the neuronal cytoskeleton, which is especially prominent in axons[126]. Synaptophysin is a presynaptic marker which labels membrane proteins of synaptic vesicles. The immunoassay revealed extensive neurite outgrowth (NF-H), and the presence of presynaptic assemblies (synaptophysin) in close proximity to the NF-H positive neurites, within the individual cell compartments (**FIGURE 15**). This indicates that cortical neurons cultured together with astrocytes were able to form structurally connected networks within the individual cell compartments of the axotomy chips.

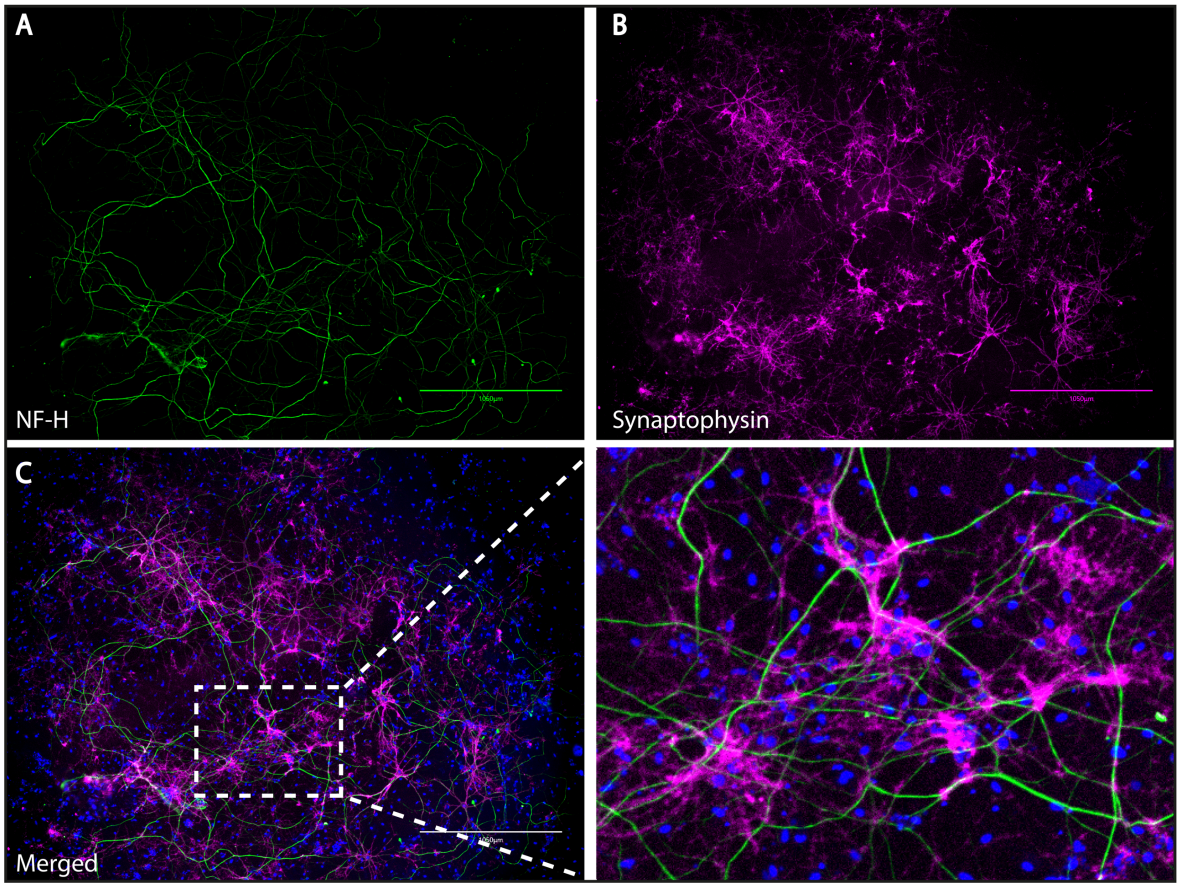


**FIGURE 15. IMMUNOLABELING OF CORTICAL NETWORKS WITHIN ONE CELL COMPARTMENT.**

**A and B)** Cortical neurons cultured together with astrocytes on axotomy chips expressed neurofilament heavy (NF-H) (A) and synaptophysin (B). C) Merged image with Hoescht dye for nuclear staining (blue). Scale bar, 1050µm. Magnification, 4X. Boxed area is enlarged; magnification 16X.

**FIGURE 16** depicts parts of the left cell compartment and the left tunnels of one representative axotomy chip. In this particular chip, all three cell compartments were seeded with astrocytes and cortical neurons (**FIGURE 16A**). It is clear that networks formed within the left cell compartment, visualised through immunofluorescent labelling against NF-H and synaptophysin (**FIGURE 16B** and **C**). As expected, the cell compartment area in front of the tunnels, and the area within the tunnels were largely negative for NF-H and synaptophysin. This suggests that networks formed within the central area of the cell compartment, but that there was limited network formation in close vicinity to the tunnels, and limited (possibly no) axonal growth through the tunnels. Surprisingly, within some of the tunnel entrances, immunofluorescent labelling against NF-H was positive (**FIGURE 16B** and **C,** especially noticeable in the enlarged images). The immunofluorescent labelling of cortical networks cultured on the IBIDI is presented in **SUPPLEMENTARY FIGURE 1**.

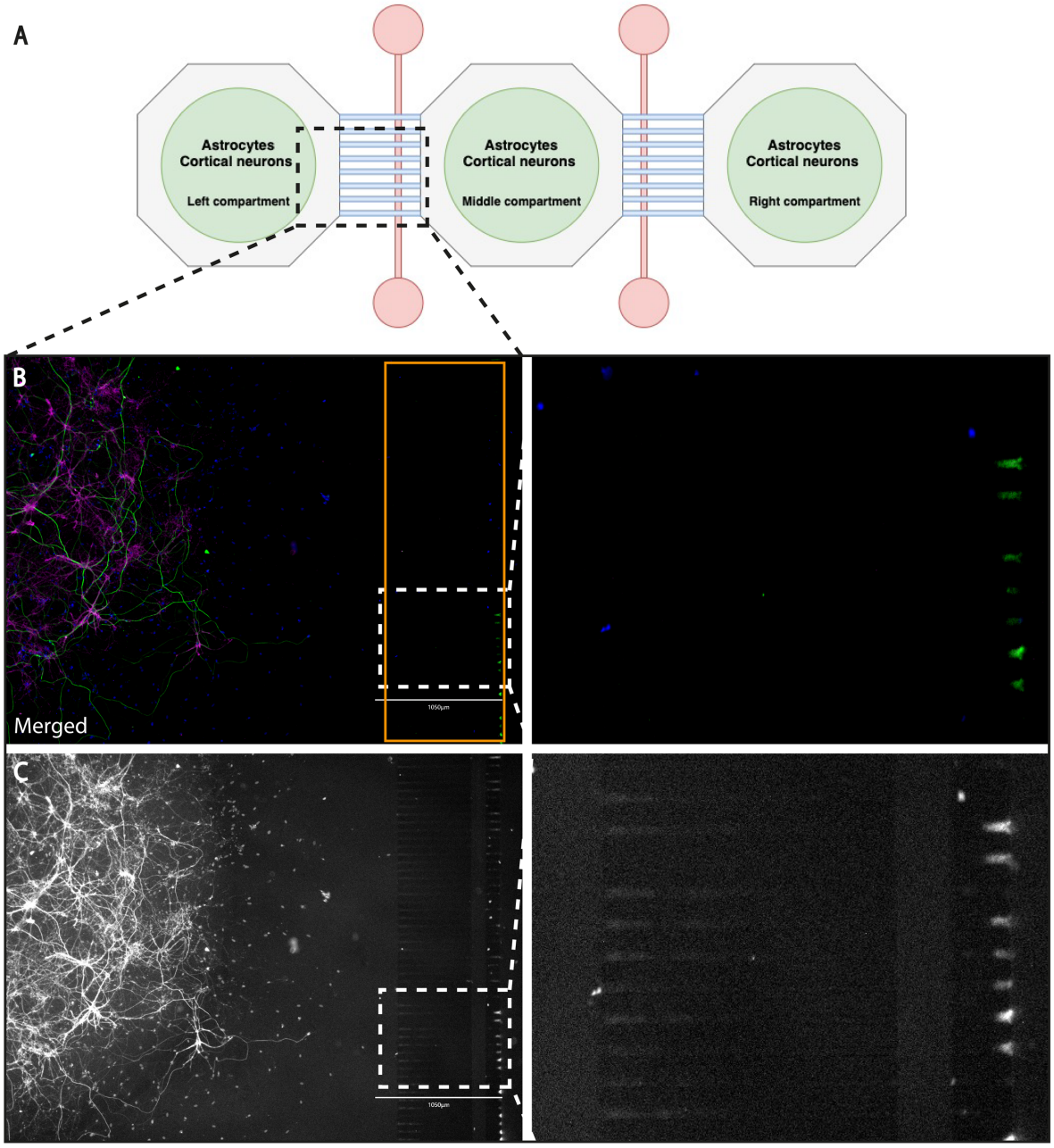


**FIGURE 16. IMMUNOLABELING OF CORTICAL NETWORKS IN ONE CELL COMPARTMENT AND ASSOCIATED MICROTUNNELS.**

**A)** Axotomy chip design and seeding overview for reference. Two axotomy chips were seeded with astrocytes and cortical neurons in all three cell compartments. The boxed area in (A) indicates the area of the axotomy chip which is imaged in (B) and (C). **B)** Notice that NF-H (green) and synaptophysin (magenta) are expressed within the left cell compartment, but that the area in front of the left tunnels, and the area within the tunnels (indicated by the orange bar) are largely negative for both immunolabels. Cell nuclei is visualized by Hoescht dye (blue). Scalebar, 1050µm. Magnification, 4X. Boxed area is enlarged: notice that within some of the tunnel entrances, immunofluorescent labelling of NF-H was positive. Magnification, 16X. **C)** The images are the same as displayed in (B). However, the images are converted from RGB to 8-bit grayscale and brightness and contrast are increased to visualize the microtunnels.

## 4.2. EXPERIMENT 2 – FUNCTIONAL PLASTICITY AT THE MESOSCALE

### 4.2.1. CORTICAL NETWORKS SELF-ORGANIZE, DEVELOP STRUCTURALLY RICH NETWORKS, AND ARE SPONTANEOUSLY ACTIVE

The cortical networks cultured in three separate wells of the MEA plate (well A1= network 1, A3 = network 2, and B3 = network 3) developed high interconnectivity over the experimental time course (0-60DIV). Images A-D in **FIGURE 17** show phase contrast images from a representative example network at different time points during development, indicating a more mature network with increased interconnectedness over time. This is especially noticeable when comparing the enlarged images in **FIGURE 17**, which display the same area of the network over time. After 1DIV, we observed that neurites had started to elongate from somata, but individual neurons appeared structurally independent of each other (**FIGURE 17A**). By 7DIV, the neurons had developed interconnections and appeared apart of a network (**FIGURE 17B**). Image **C** and **D** in **FIGURE 17** show a densely interconnected neuronal network with full neuronal confluence around the electrodes.

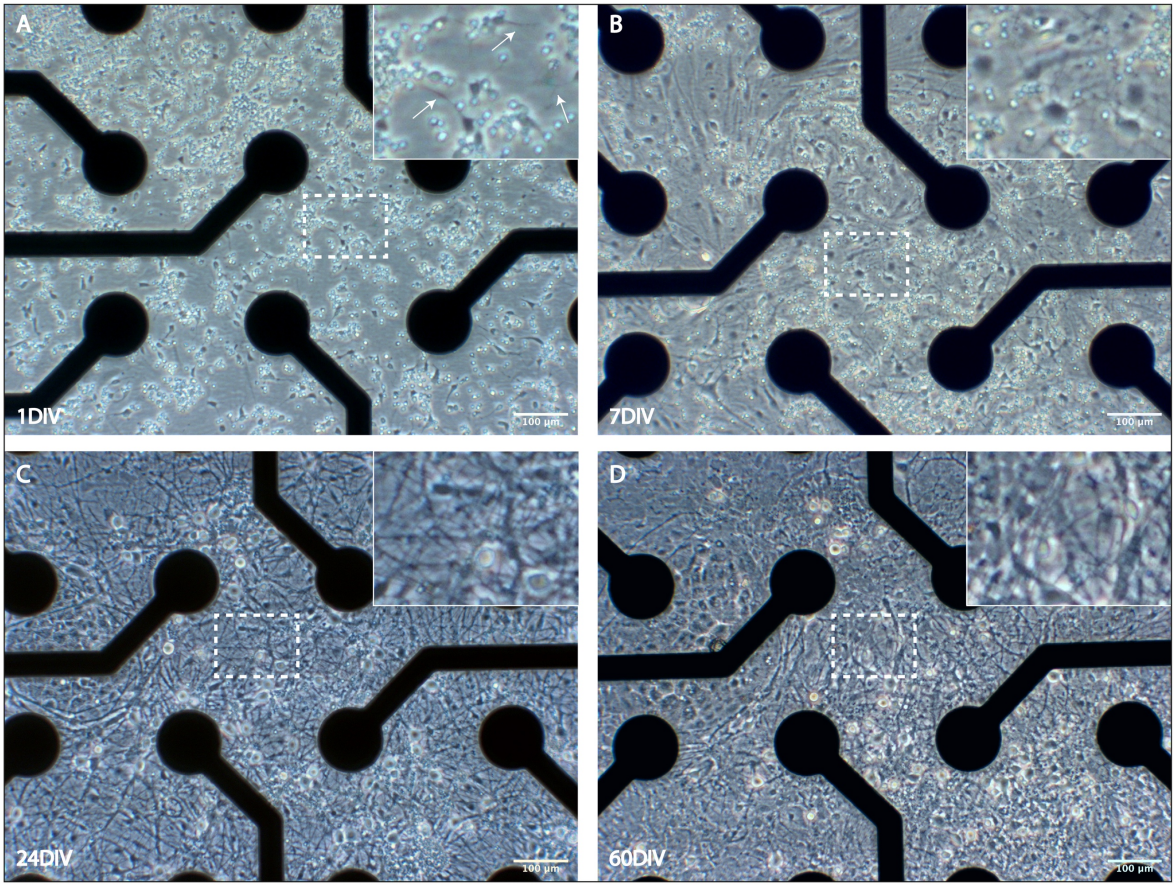


**FIGURE 17. PHASE CONTRAST IMAGES OF A CORTICAL NETWORK CULTURED ON THE MEA.**

**A-D)** Representative images of one cortical neuronal network at 1DIV (A), 7DIV (B), 24DIV (C) and 60DIV (D), at a density of 1 800 neurons/mm$^2$. All images are taken of network 1. Scale bar, 100µm. Magnification 10X. Boxed areas are enlarged, magnification 25X, and show the same area of the network over time. Image (A) shows that neurites (indicated by white arrows) have started to elongate from soma at 1DIV, but that individual neurons appear structurally independent of each other. Notice the increase in structural connectivity over DIV. When comparing (A), (B), (C) and (D), it is clear that the network develop progressively more interconnectivity.

To examine cortical network responses to TS, we used cortical networks of 55-56DIV. The networks expressed a mixture of spiking and bursting behaviour, and instances of

synchronized network activity occurring at some or most electrodes were observed (exemplified in **FIGURE 18**).

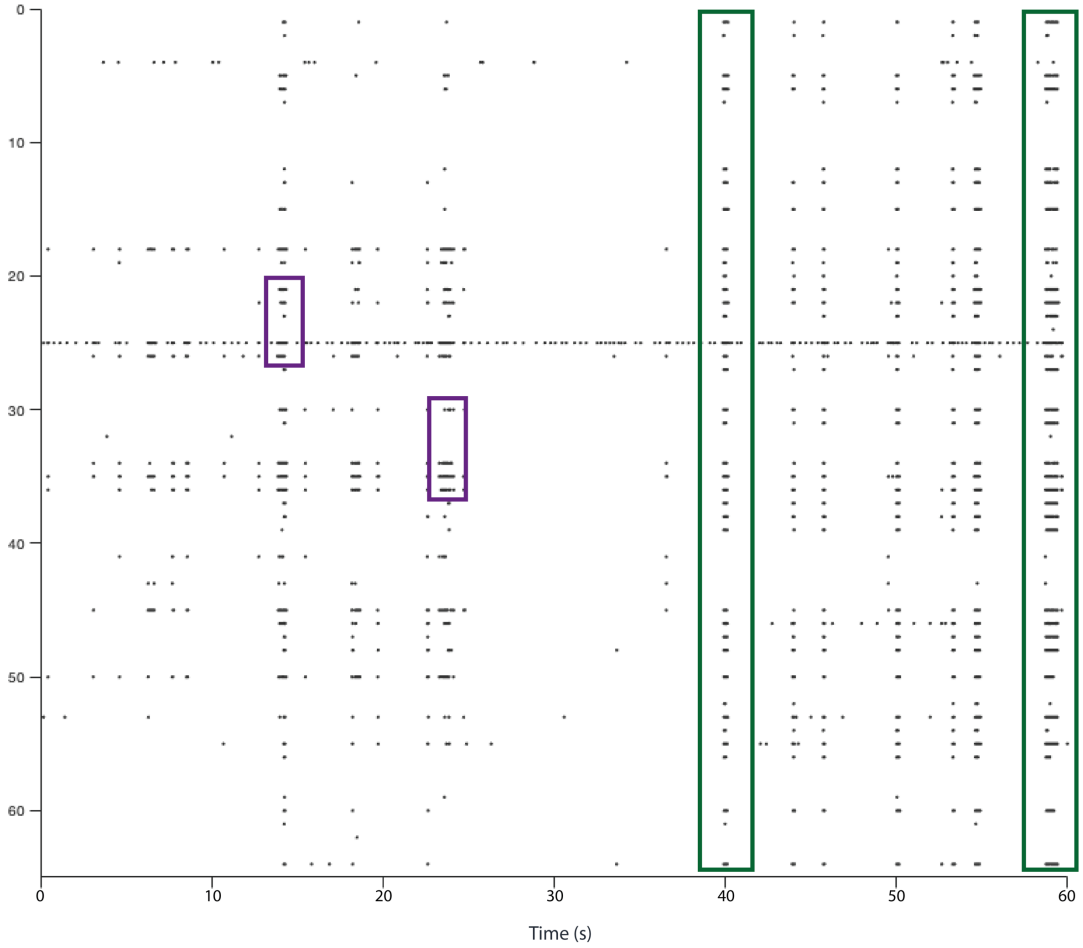


**FIGURE 18. RASTER PLOT SHOWING SPONTANEOUS ACTIVITY IN ONE OF THE CORTICAL NETWORKS AT 55DIV.**

Spikes are represented as single dots. The y-axis corresponds to the different electrodes on the MEA, and each horizontal line depicts the spike train recording obtained from the corresponding electrode. 60s of a 1h long recording is displayed in the figure. Several dots in rapid succession may be considered a burst. Bursting occurring at a few electrodes simultaneously are indicated by purple bars, and synchronized activity happening at most sites in the network are indicated by the green bars.

### 4.2.2. STABILITY OF CONNECTION STRENGHTS

To assess the stability of functional connection strengths in the cortical networks, we divided a 1h long recording of spontaneous activity, obtained at 55DIV, into two separate segments of 30 min each. The difference in the average correlation (*r)* between the first 30 min and the second 30 min of the same recording is displayed in **FIGURE 19**. Network functional connectivity appeared to be relatively stable over the course of 1h. The difference in average correlation between every possible electrode pair ranged from a maximum decrease of $r$ = -0.082 to a maximum increase of $r$ = 0.075.

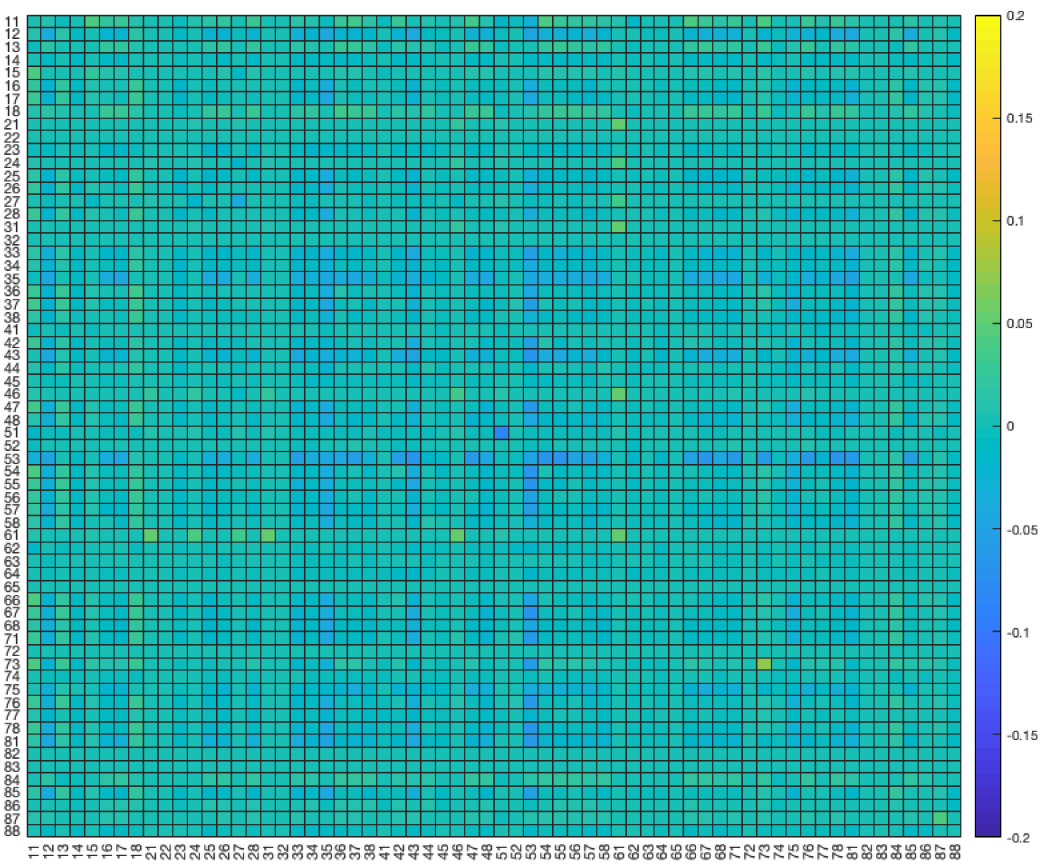


**FIGURE 19. ALTERATIONS IN NETWORK FUNCTIONAL CONNECTIVITY OVER 1H RECORDING OF SPONTANEOUS ACTIVITY.**

The difference in average correlation between the first 30min and the second 30min of a 1h long recording, at 55DIV, of spontaneous cortical network activity is displayed using a colour scale in a 64x64 matrix. The (*x,y*)th pixel represents the difference in the correlated activity pattern between the *x*th and *y*th electrode. The colour bar to the right ranges from -0.2 to 0.2. The difference in average correlation between every possible electrode pair ranged from a maximum decrease of $r$ = -0.082 to a maximum increase of $r$ = 0.075.

### 4.2.3. FOCAL TETANIC STIMULATION INDUCES CONNECTION SPECIFIC POTENTIATION AND DEPRESSION

TS was delivered through one arbitrary fixed central electrode in all three cortical networks at 56DIV (see **MATERIALS AND METHODS** for details on the stimulation protocol). Recorded cortical network responses during the 30min of stimulation, and spontaneous network activity during the subsequent 30min after stimulation are exemplified in **FIGURE 20**. When comparing the spontaneous network activity post stimulation with network activity during stimulation, it is clear that focal TS evoked network-wide responses, as illustrated by a global increase in spiking activity during the stimulation period.

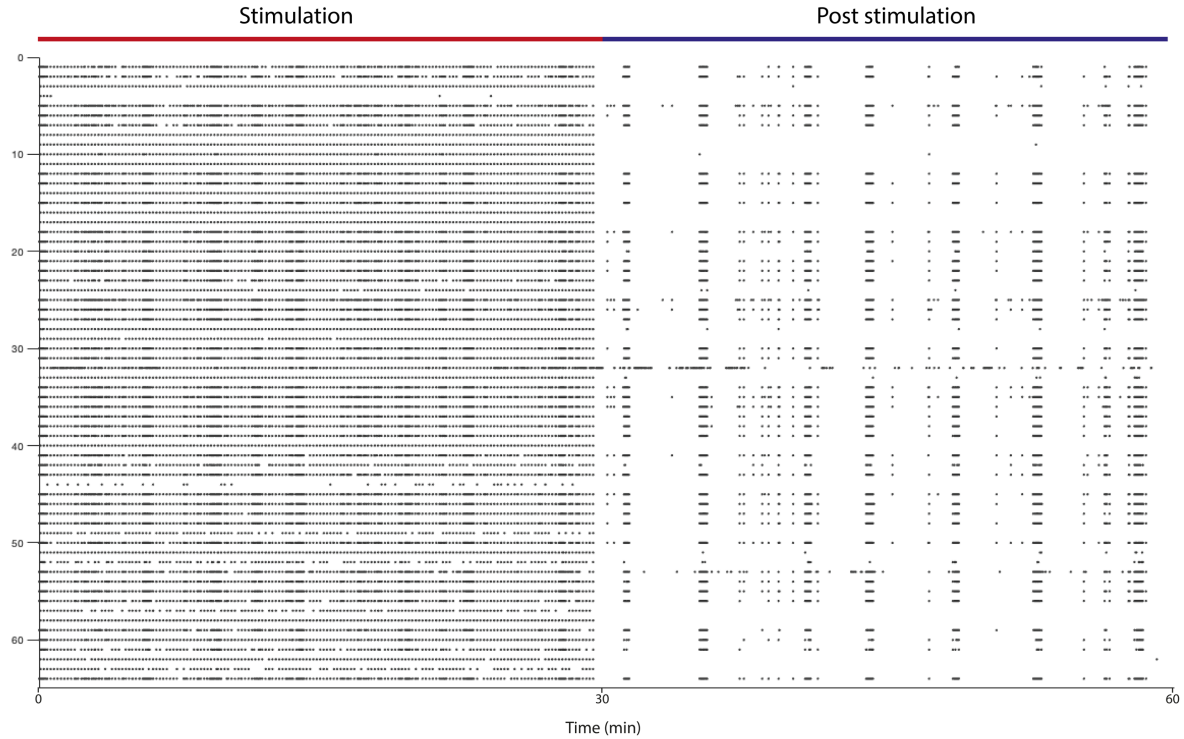


**FIGURE 20. RASTER PLOT OF CORTICAL NETWORK ACTIVITY DURING AND AFTER TS.**

Spikes are represented as single dots. The y-axis corresponds to the different electrodes on the MEA, and each horizontal line depicts the spike train recording obtained from the corresponding electrode. The x-axis represents time (min). The first 30 min display the network response to TS (indicated by the red line). The second 30 min display the recorded spontaneous activity after TS (indicated by the blue line). The presented data is from network 1.

The differences in the average correlation between each electrode/node pair pre and post stimulation, for all three networks respectively, are displayed in **FIGURE 21**. We defined an increase in functional connection strength between two nodes to be "significant" only if $r>0.1$, and a decrease to be "significant" only if $r<-0.1$. This criterion was set based on the estimate of the stability of functional connection strength over 1h of spontaneous activity, which revealed that an average increase/decrease between two nodes of $r>0.1/r<-0.1$ is unlikely to occur without manipulation (**FIGURE 19**). Depending on the cortical network evaluated, focal TS induced either both connection specific potentiation and depression (network 1, **FIGURE 21A**), or only connection specific depression (network 2 and 3, **FIGURE 21B** and **C**).

**A** **Network 1**

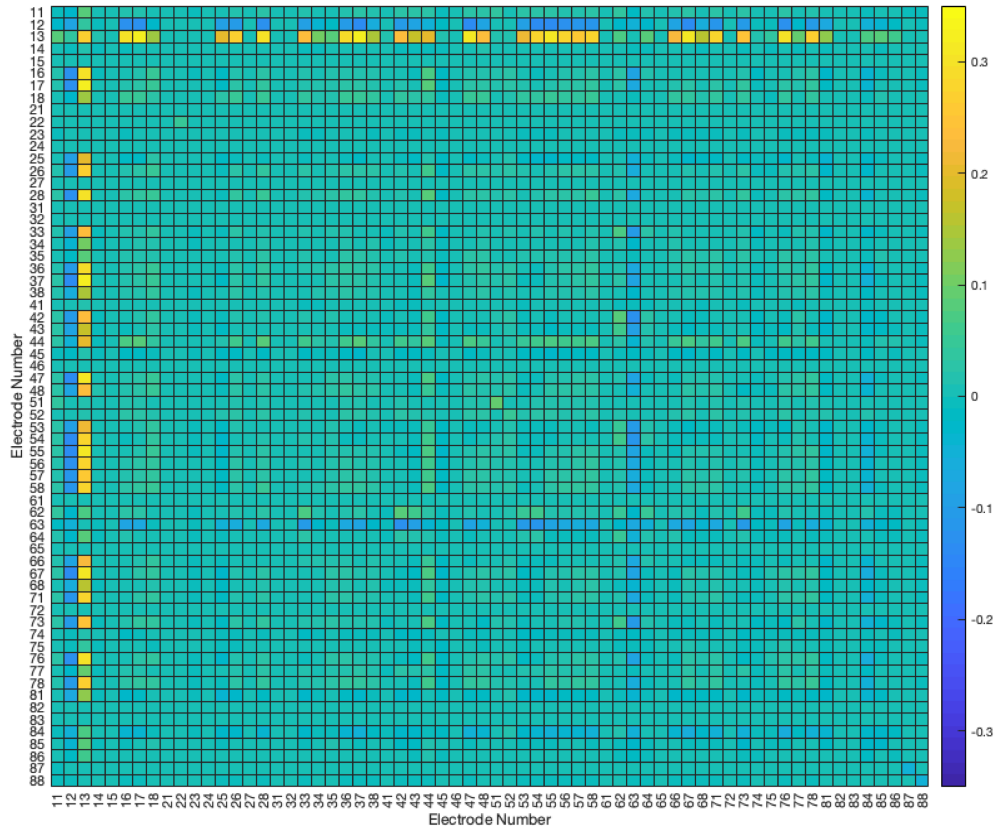


**B** **Network 2**

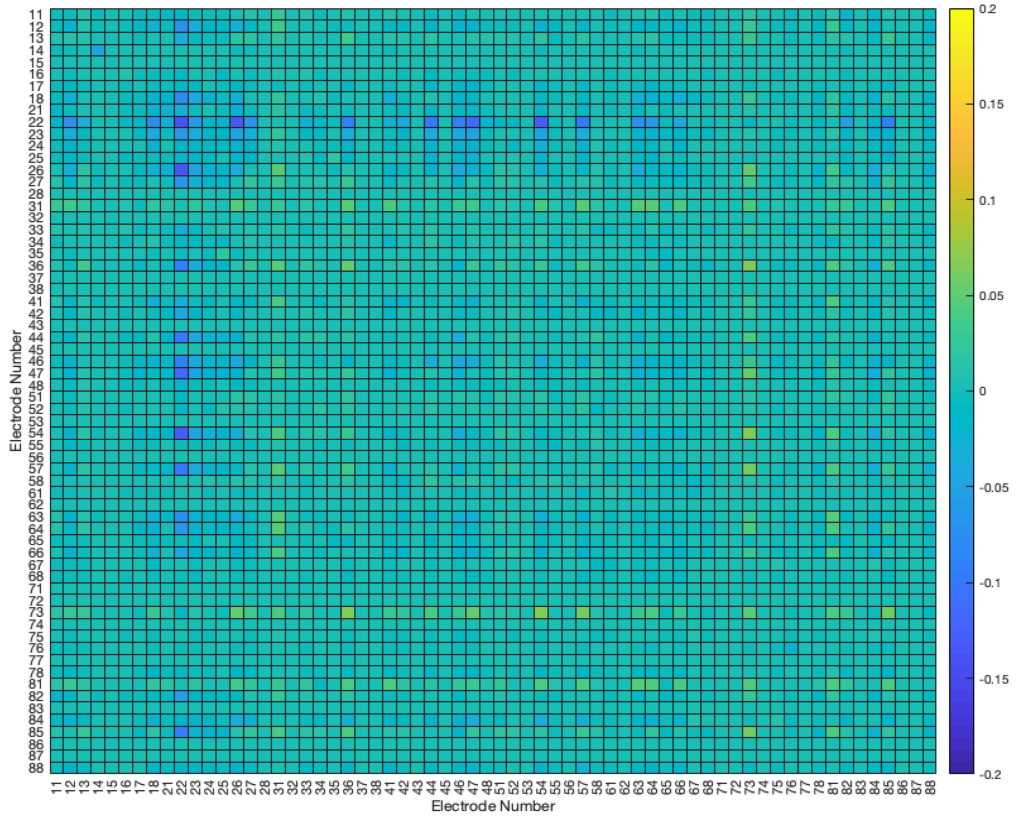

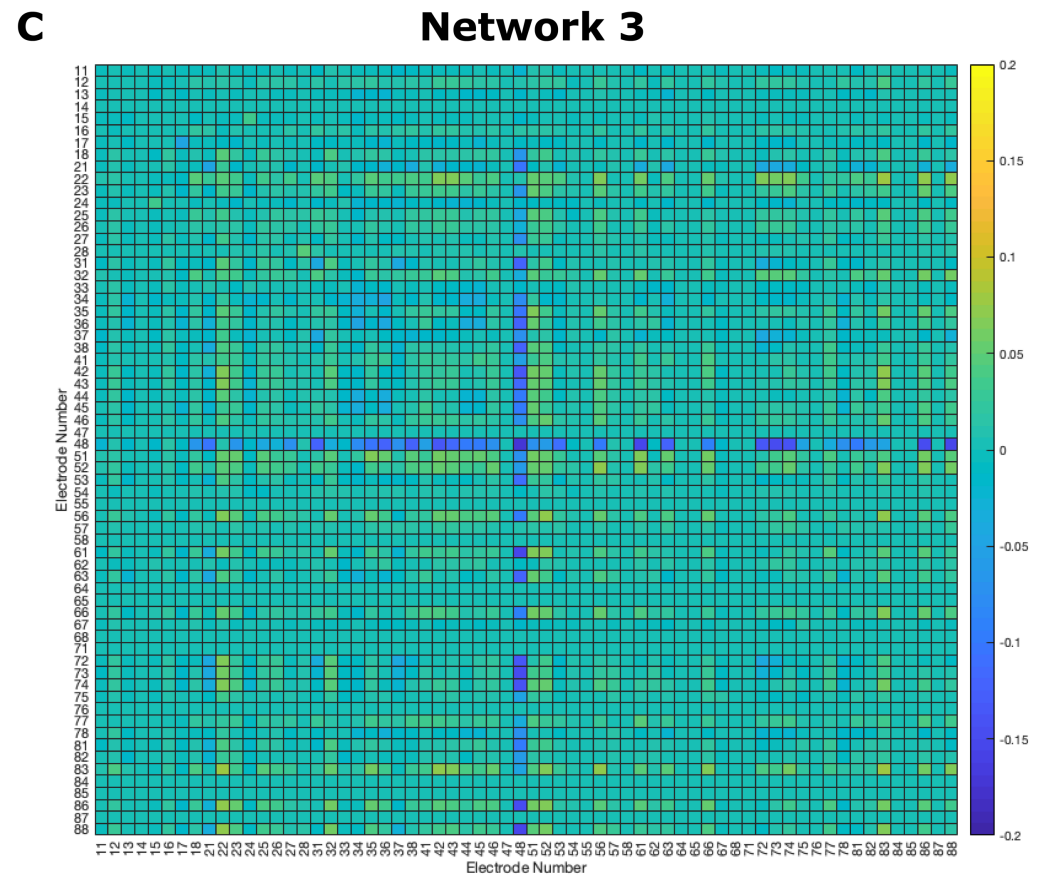


**FIGURE 21. CHANGES IN NETWORK FUNCTIONAL CONNECTIVITY AFTER FOCAL TS.**

**A-C)** The difference in average correlation between each electrode pair pre and post TS is displayed using a colour scale in a 64x64 matrix. The (*x*,*y*)th pixel represents the difference in the activity pattern between the *x*th and *y*th electrode pre and post TS. (A), (B) and (C) display the difference in average correlation between electrode pairs in network 1, 2 and 3, respectively. TS was delivered through electrode 44 in all instances. To clearly visualize the induced alterations, the colour bar to the right ranges from -0.35 to 0.35 in (A) and -0.2 to 0.2 in (B) and (C).

The magnitude of change in connection strength due to TS varied between the three cortical networks. Focal TS induced the greatest changes in network 1, i.e. in the number of connections that altered significantly (52 connections). In network 1, 30 connections increased in strength by $r>0.1$, of which 24 increased by $r>0.2$, and 7 by $r>0.3$. 22 connections decreased in strength by $r<-.01$ (peak potentiation: $r=0.33$ and peak depression: $r=-0.14$). Functional changes induced by TS in network 2 were limited, as no connections increased in strength by $r>0.1$, and only 3 connections decreased in strength by $r<-0.1$ (peak depression: $r=-0.13$). Similarly, in network 3, no connections increased by $r>0.1$, but 15 connections decreased by $r<-0.1$ (peak depression: $r=-0.15$). The results are summarized in **TABLE 3.**

**TABLE 3.** NUMBER OF FUNCTIONAL CONNECTIONS THAT ALTERED IN STRENGTH BY DEFINED *r*, AS A RESULT OF TS.

| NEURONAL NETWORK | NR. OF CONNECTIONS THAT ALTERED BY: | | | | | | | TOTAL |
|---|---|---|---|---|---|---|---|---|
| | *r*<-0.2 | *r*<-0.1 | *r*<-0.09 | *r*>0.09 | *r*>0.1 | *r*<0.2 | *r*<0.3 | |
| NETWORK 1 | 0 | 22* | 26 | 31 | 30* | 24* | 7* | 52* |
| NETWORK 2 | 0 | 3* | 7 | 0 | 0 | 0 | 0 | 3* |
| NETWORK 3 | 0 | 15* | 20 | 0 | 0 | 0 | 0 | 15* |

*Note.* * = significant alterations. Total = the total number of connections that altered in strength after TS. Except under "Total", some connections are counted multiple times, as connections that altered in strength by e.g. $r>0.3$, also altered by $r>0.2$ and $r>.01$.

The effects of TS on functional connectivity strengths on a network-level was limited. In all three networks, the modifications in functional connectivity were retained to relatively few connections, and most connection strengths stayed (fairly) unchanged (i.e. *r* was close to 0 for most connections in all three networks, see **FIGURE 21**).

## 4.3. EXPERIMENT 3 – FUNCTIONAL PLASTICITY ON THE MICROSCALE

### 4.3.1. AXONAL ELONGATION AND SPIKE DETECTION

Axons were observed to elongate into the tunnels of the STCs within the first week *in vitro* (data not shown). **FIGURE 22B** depicts a representative snapshot of three of the tunnels from STC 1 at 10DIV, clearly showing axonal growth within the tunnels. Spiking events, captured by the four electrodes within specific tunnels, were detected as early as 13DIV (exemplified in **FIGURE 22C**), indicating that at least a few axons had elongated all the way through the tunnels at this time point. Image **D** and **E** in **FIGURE 22** show representative snapshots of parts of the left cell compartment and the left active zone of STC 4 at 33DIV. Network structural interconnectedness can be observed in these images. We observed the presence of axons within the tunnels of the STCs throughout the entire experimental time period. As the structural interconnectedness of the cortical networks increased over DIV and new axons grew into the tunnels, individual axons got increasingly more difficult to capture using a phase contrast microscope (noticeable when comparing **FIGURE 22B** and **E).**

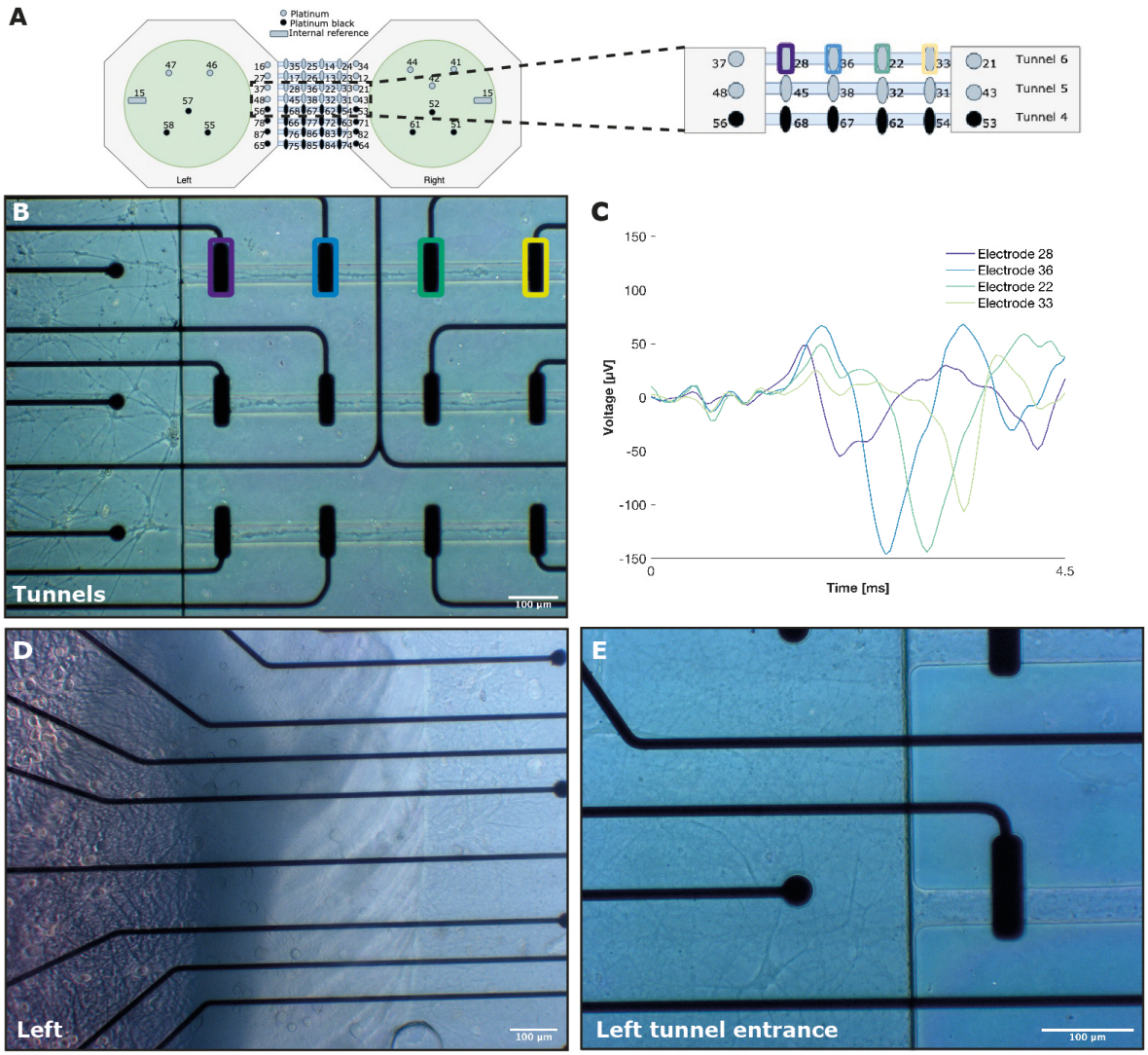


**FIGURE 22. AXON ELONGATION AND SPIKE TRACKING WITHIN MICROTUNNELS OF THE STC.**

**A)** STC design for reference. Boxed area is enlarged and depicts the tunnels imaged in (B). Electrodes are color-coded according to (C). **B)** Depicts axons elongating within three tunnels (tunnel 4-6) of STC 1 at 10DIV. Magnification 10X. Electrodes within tunnel 6 are color-coded according to (C). **C)** Illustrates a travelling spike moving along an identified axon (from left to right), picked up by the four electrodes within tunnel 6 of STC 1 at 13DIV. Y-axis = voltage (µV), x-axis = time (ms). **D)** Representative images of a part of the left cell compartment and the left active zone of STC 4 at 33DIV. Magnification 10X. **E)** Depicts the left active zone and a few of the microtunnel entrances of STC 4 at 33DIV. Notice the elaborate structural connectivity in the active zone. Magnification 20X. All scale bars are of 100µm.

### 4.3.2. STIMULATION-INDUCED DECREASE IN AXONAL PROPAGATION DELAY AND INCREASE IN SPIKE AMPLITUDE

All the presented results in this section were obtained from the spike data of one identified neuron, the axon of which was located within tunnel 1 of STC 4 (see **FIGURE 11A**). Spike events from this axon were monitored as spontaneous activity (Pre Stim) and as responses to stimulation, i.e. immediately post stimulation (Post Stim) and 3 days post stimulation (3 Days Post Stim). Before applying the paired pulse stimulation (see **FIGURE 23A** and **MATERIALS AND METHODS** for information regarding the stimulation protocol), the calculated mean axonal propagation delay for the identified axon was 0.98ms. Following the paired pulse stimulation, a decrease in mean axonal propagation delay was detected Post Stim

(0.68ms), with a further marginal decrease noticed at 3 Days Post Stim (0.61ms) (**FIGURE 23B**).

Furthermore, when comparing the mean peak spike amplitude detected at each of the four electrodes within tunnel 1 Pre Stim against Post Stim, a considerable increase was observed. An increase refers here to a more negative peak value as spike detection was done extracellularly. An even further increase was found 3 Days Post Stim (**FIGURE 23C** exemplifies the trend showing the mean peak amplitude detected at electrode 85 at the different recording times, Pre Stim = -141µV; Post Stim = -188µV; 3 Days Post Stim = -225µV). **FIGURE 23D** displays three representative single spike events captured along the axon at each recording day. When compared to Pre Stim, the figure clearly illustrates both the observed decrease in axonal propagation delay and the increase in peak spike amplitude for both recording times post stimulation.

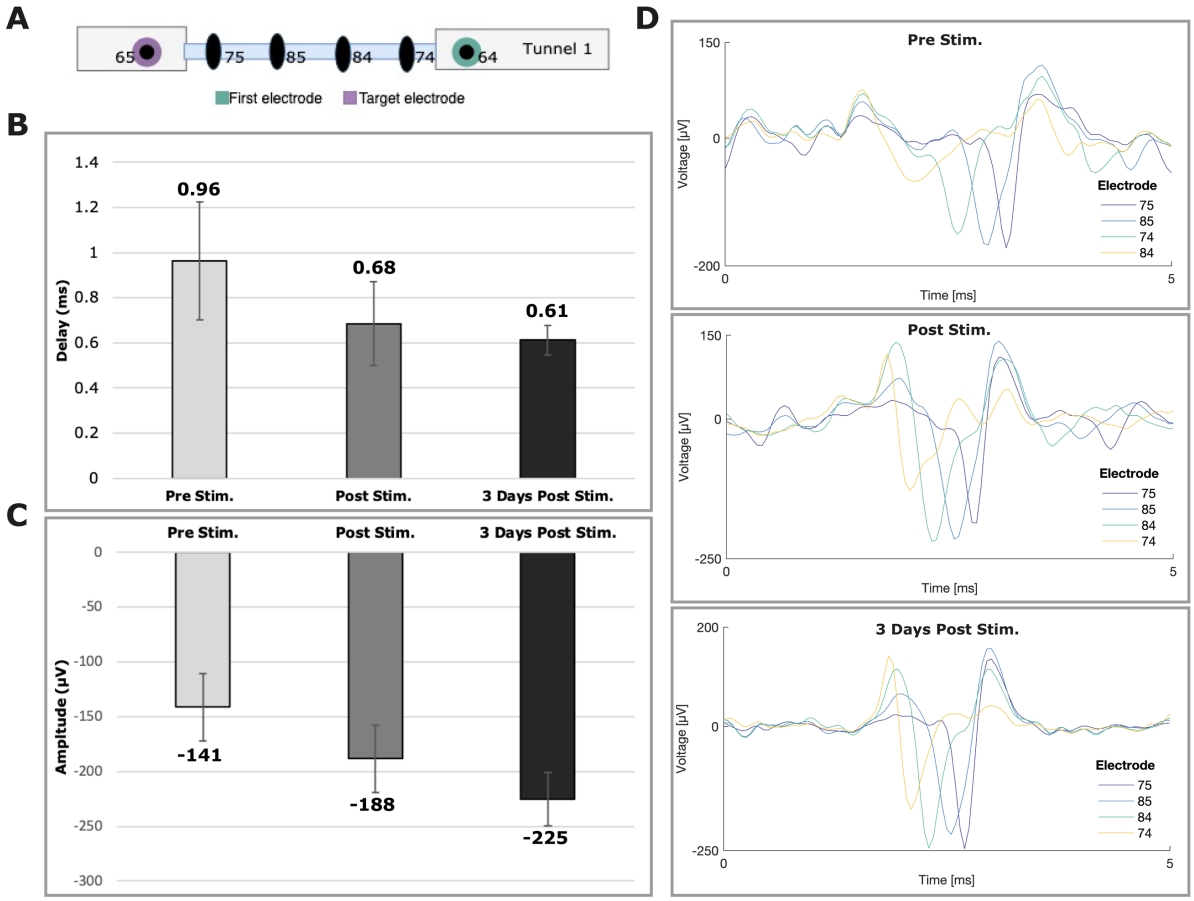


**FIGURE 23. STIMULATION-INDUCED DECREASE IN MEAN AXONAL PROPAGATION DELAY AND INCREASE IN MEAN SPIKE AMPLITUDE.**

**A)** Overview of electrode arrangement and numbering within microtunnel 1 of STC 4, together with the two electrodes located in the tunnel´s associated active zones. The paired pulse stimulation involved the delivery of a pulse through electrode 64 first, and after a time delay (estimated based on the calculated mean PV of the axon of interest), through electrode 65. **B)** Depicts the mean axonal propagation delay (ms) calculated based on all the detected spike events for the identified axon Pre Stim, Post Stim and 3 Days Post Stim, respectively. **C)** Shows the mean peak amplitude of spikes detected at electrode 84 within microtunnel 1 at the different times of recording. **D)** Depicts three representative spike events extracted from each of the different times of recording. Y-axis = voltage (µV), x-axis = time (ms). Notice that, when compared to Pre Stim, the spikes are detected with a decrease in time delay across the four electrodes Post Stim, with the delay decreasing even further at 3 Days Post Stim. The increase in peak spike amplitude after stimulation is also clearly visible. Error bars in (B) and (C) are of +/- 1 SD.

### 4.3.3. STIMULATION-INDUCED POTENTIATION OF ONE TARGETED CONNECTION

To assess if the paired pulse stimulation altered the connection strength between the stimulated node pair, we calculated the average correlation between the activity recorded at the corresponding electrode pair (electrode 64 and 65), Pre Stim, Post Stim and 3 Days Post Stim, respectively. The results are presented in **FIGURE 24**. An increase in average correlation of $r$ = 0.26 was observed from Pre Stim to Post Stim. Though a slight decrease in correlation was found 3 Days Post Stim, compared to Post Stim, the functional connection between the node pair was still potentiated, when compared to Pre Stim ($r$ = 0.18).

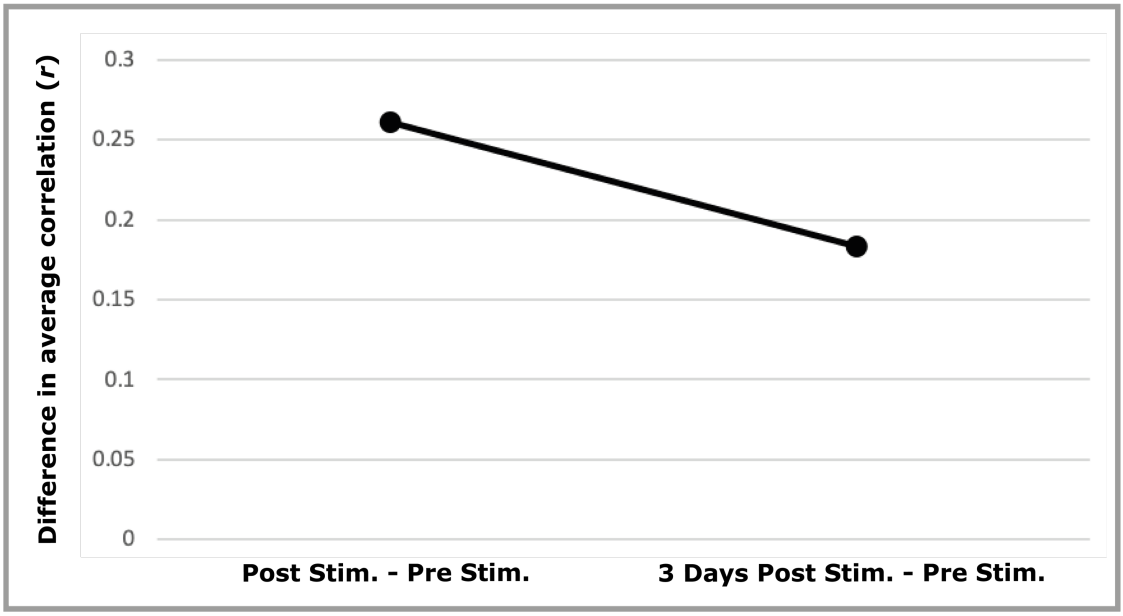


**FIGURE 24. STIMULATION-INDUCED POTENTIATION OF ONE TARGETED CONNECTION.**

The figure depicts the difference in the average correlation ($r$) between the activity of the stimulated electrode pair (electrode 64 and 65) located at either side of the entrances of tunnel 1, STC 4, pre and post stimulation. Compared to Pre Stim, an increase in the average correlation between the two electrodes were observed Post Stim ($r$=0.26). Though slightly dropping, the increase in average correlation was also maintained at 3 Days Post Stim ($r$=0.18).

# 5. DISCUSSION

The current project was divided into three main experiments. Experiment 1, where the original plan was to assess cortical neuronal responses to *in vitro* axotomy will be discussed first, and the focus will be on potential explanations for the observed lack of axonal growth within the microtunnels of the axotomy chips. Next, the results obtained from experiment 2 will be discussed, which suggest that focal TS can modify the functional connectivity of *in vitro* cortical networks by altering the strength of specific functional connections. Then, the results obtained from experiment 3 will be considered, which imply that targeted pre- and postsynaptic stimulation strengthens the connection between the stimulated node pair, both through altering axonal signalling, as well as inducing an increase in the functional connection strength between the two stimulated nodes. The last section of the discussion will address the significance of this project. There will be an emphasis on how a greater understanding of mechanisms of CNS neuroplasticity can facilitate the development of therapeutic strategies that aim to restore lost function after traumatic CNS injuries.

## 5.1. EXPERIMENT 1 – AXOTOMY

### 5.1.1. THE LACK OF AXONAL GROWTH THROUGH THE MICROTUNNELS

We were not entirely successful in establishing viable cortical networks on the axotomy chips. We observed both through light microscopy (**FIGURE 14**) and immunoassay (**FIGURE 15** and **FIGURE 16**) that cortical neurons, cultured together with astrocytes, survived and developed structural connectivity within the individual cell compartments. The immunolabeling against NF-H and synaptophysin demonstrated the presence of presynaptic assemblies in close vicinity to neurites, which suggests that the networks developed structures necessary for synaptic transmission within the cell compartments (**FIGURE 15**). However, no axonal growth through the tunnels connecting the compartments was observed in any of the eight chips (**FIGURE 13**). Surprisingly, NF-H was positively expressed within a few of the tunnel entrances (**FIGURE 16**). However, the NF-H positive elements appeared largely isolated and not a part of an integrated network, thus, it is reasonable to assume that these elements were some type of debris. Neurofilaments, though also present in dendrites, are especially abundant in axons[126]; it is therefore possible that axons did elongate from the cell compartments towards the tunnels, tried to enter, but fragmented. However, based on the immunoassay alone, it is difficult to judge what the NF-H positive elements within the tunnel entrances were. Notably though, our observations strongly suggest that no axons elongated all the way through the tunnels in any of the chips. With no axonal growth through the tunnels, we were unable to proceed with experiment 1, where the initial objectives included assessing cortical neuronal responses to *in vitro* axotomy, and cortical neuronal responses to extracellular GABA addition immediately after axotomy.

Cortical neurons cultured on microfluidic devices have been reported to start elongating axons into the tunnels of such devices already after 2-4 DIV[70,71,99]. Furthermore, our group has previously reported cortical axonal growth within microtunnels starting at a similar time *in vitro*[120]. A possible explanation for the lack of axonal growth observed in the current experiment might be linked with the high degree of non-cellular debris present in close vicinity and within the tunnels (**FIGURE 13**). This debris, which is likely to be PDMS debris from chip production (at least the debris that was larger in size than typical cell debris; **FIGURE 13**, indicated by arrows), can cause several issues. For one, it creates a physical barrier for exploring growth cones, by clogging the tunnel entrances. In addition, members

of our group have previously observed that neurons tend to avoid areas with PDMS debris, which could account for the lack of cells in close vicinity to the tunnels.

While the most obvious issue with PDMS debris blocking the tunnels would be the physical barrier it creates for exploring growth cones, let us assume that some axons did in fact manage to enter some of the tunnels. Then, PDMS debris could cause secondary issues by limiting the flow of culture media through the tunnels. To encourage survival and optimal growth conditions *in vitro*, the neuronal microenvironment needs to be artificially built to mimic the *in vivo* environment. The cell culture media, usually consisting of a combination of amino acids, vitamins, various salts, glucose and serum/supplements (such as growth factors and hormones)[127], are critical in providing cultured neurons with necessary nutrients and optimal growth conditions. Axons obtain some of their nutrients from soma-to-axon transport, and a substantial amount of the essential proteins for proper axonal function and survival is synthesised in the soma and transported to the axon[45]. The importance of soma-to-axon transport is for example illustrated by the fact that blocking it can lead to Wallerian-like degeneration (see [38] for a review). Yet, some nutrition may be absorbed locally, i.e. directly from the extracellular environment or through interactions with surrounding glia cells[45,128,129]. In addition, extensive research has indicated that axons and growth cones hold the necessary machinery for, and that they can perform, local protein synthesis. Local protein synthesis has been reported to play a role in axonal guidance, growth and survival during development, in the adult, and after injury (reviewed in [130]). Therefore, if PDMS debris blocks culture media from flowing through the tunnels, the tunnel-environment will lack the essentials for maintaining axonal energy homeostasis, and for facilitating axonal growth, function and survival, which potentially could lead to axonal degeneration.

In six out of the eight axotomy chips used in this study, cortical neurons were co-cultured with astrocytes in the two outer cell compartments, while the middle compartment was seeded with astrocytes only (see **Figure 12A**). In conventional cell culture models, neurons and growth cones are presented with a relatively homogenous milieu, while *in vivo*, growth cones navigate through pre-existing tissue and guidance cues are often expressed in gradients[9]. Therefore, in a reductionist *in vitro* environment, neurons tend to spread out somewhat evenly over the culture area, and unmanipulated axonal growth appears to be relatively random[12]. In our experimental model, axons were not presented with target neurons, and we did not provide a gradient of specific chemical guidance cues to encourage growth through the tunnels. As a consequence, another possible explanation for the lack of axonal growth through the tunnels could be a lack of specific guidance cues and synaptic targets in the middle compartment. However, this is unlikely. The first culture device able to separate neuronal soma from axons by providing tracks for axonal growth (i.e. the Campenot chamber) required the addition of growth factors to successfully accomplish this[131]. However, microfluidic chips, which are optimized versions of the Campenot chamber, provide sufficient structural guidance, i.e. the microtunnels, for axons without the addition of growth factors, and several research groups have reported axonal growth through the tunnels of microfluidic devices without providing axons with target neurons in a second compartment[70,71,100]. Notably though, neuronal survival depends on synaptic contact, thus, assuming axons had elongated through the tunnels of the axotomy chips, a lack of synaptic targets in the middle compartment could potentially have caused issues at later experimental time points, as axons might have retracted or neurons may have undergone apoptosis as a consequence of the lack of synaptic contact.

In summary, (i) we observed a systematic presence of non-cellular/PDMS debris in and around all the tunnels of all eight axotomy chips used in this study; (ii) we observed the structural development of cortical networks within the individual cell compartments of the axotomy chips; and (iii) axonal growth through tunnels of similar microfluidic devices have previously been reported in the literature. Therefore, the most likely explanation for the lack of axonal growth appears to be related to the tunnels themselves, i.e. blocked microtunnels entrances are likely to directly have prevented axons from entering. If some axons were in fact able to enter, PDMS debris may have blocked culture media from flowing through the tunnels, compromising the axonal microenvironment. Work towards an optimization of the axotomy chip fabrication process is likely to solve this issue.

## 5.2. EXPERIMENT 2 – FUNCTIONAL PLASTICITY AT THE MESOSCALE

### 5.2.1. NETWORK SELF-ORGANIZATION, SPONTANOUS ACTIVITY, STABILITY AND RESPONSIVENESS TO STIMULATION

When investigating and inducing activity-dependent plasticity by the use of dissociated neurons cultured on MEAs, four main prerequisites should be met: (i) the neurons must self-organize into interconnected networks; (ii) the networks must exhibit spontaneous activity; (iii) the stability of network activity should be assessed[110]; and (iv) the networks must respond to electrical stimulation[110].

We observed that the three cortical networks used in experiment 2 self-organized into increasingly more structurally interconnected networks over time (**FIGURE 17**). For assessing network responses to TS, we used mature cortical networks of 55-56DIV. In contrast to young developing networks, mature networks have reached a more stable activity pattern, characterized by a complex, nonperiodic, and synchronized pattern of bursts and spikes[108–110]. At 55DIV, the cortical networks exhibited what appeared as both spiking and bursting behaviour, and synchronized network events, occurring either on a few sites in the network or on a network-wide level, were observed (**FIGURE 18**).

As previously mentioned, the spontaneous network activity pattern is known to vary between similarly prepared *in vitro* cortical networks, and even between different recordings from the same network[110,111]. This makes it challenging to compare the activity between networks and recordings, and to differentiate between spontaneously occurring fluctuations in the network activity pattern and potential plastic alterations induced by stimulation protocols. However, without external input, cortical networks develop relatively stable connectivity after about three weeks *in vitro*[132], and the spontaneous activity pattern has been reported to be stable over short timescales (a few hours), but prone to fluctuations over longer timescales (hours-days)[111]. As we were interested in possible alterations in connection strengths as a consequence of TS, we assessed the stability of functional connections strengths over a 1h long recording of spontaneous activity. In line with previous research, we found the functional connectivity of *in vitro* cortical networks to be relatively stable over 1h (**FIGURE 19**). This gave us an indication that average alterations in connection strengths of $r>0.1$ and $r<-0.1$ were unlikely to occur without any manipulation.

Lastly, when investigating activity-dependent plasticity of *in vitro* cortical networks, it is crucial that electrical stimuli is able to produce responses in the network. In all three networks used in this study, we observed an overall increase in global network activity (i.e. increased spiking) during the 30 min of TS (**FIGURE 20**). This indicates that the

stimulation was able to activate and elicit responses in the cortical networks. That the electrical stimulation delivered through one central electrode produced responses in sites distal to the stimulation site suggests that the cortical networks were highly interconnected, and that the activity spread polysynaptically (indirectly) within the network. It should, however, be noted that the activity recorded during the stimulation period might be a stimulation artifact, i.e. reflect the stimulation pulse rather than actual network activity. Electrodes typically record on the scale of μV, while the stimuli delivered are on the order of mV, therefore, the stimulation pulse can easily swamp out the recorded spikes, even from sites distal to the stimulation site[133].

Taken together, the cortical networks used in the current study appeared to develop and behave in line with earlier observations on cortical networks cultured on MEAs. Thus, the data extracted from our networks should be comparable with similar data reported by other research groups.

### 5.2.2. DOES FOCAL TETANIC STIMULATION INDUCE ALTERATION IN THE STRENGTH OF FUNCTIONAL CONNECTIONS?

Of major interest was whether focal TS induced alterations in the functional connectivity of the *in vitro* cortical networks. More specifically, we wanted to investigate if the average connection strength between different network nodes plastically altered as a result of the stimulation. We assessed this by comparing the spontaneous activity of cortical networks, 1h pre and 30min post TS. Our results suggest that repetitive TS, delivered through a single electrode, does indeed modify the average connection strength between specific network nodes. The alterations revealed themselves as both potentiation and depression of specific connections within the networks (**FIGURE 21**), and the altered average strength was larger than what was expected to occur without manipulation (i.e. $r>0.1$ and $r<-0.1$, **FIGURE 19**). In network 1, the same stimulation led to both potentiation and depression of specific connections (**FIGURE 21A**) which is in line with Jimbo and colleagues[112] who reported that single-site TS can induce both increased neuronal firing (potentiation) and supressed neuronal firing (depression) in response to test stimuli delivered at different sites, within the same cortical network.

The underlying idea of Hebbian plasticity states that high frequency presynaptic neuronal activity eliciting a marked increase in postsynaptic excitation results in LTP, while prolonged low presynaptic activity eliciting moderate excitation in the postsynaptic neuron results in LTD[26]. It has previously been reported that within *in vitro* cortical networks, neurons develop extensive interconnectivity (which was also observed in the current study, **FIGURE 17**) and have a relatively low chance in forming monosynaptic (direct) connections with other neurons within the network[108,112]. Thus, if we assume that our networks developed random connectivity, and that there was a high chance of forming recurrent polysynaptic connections, as is the case in the intact cortex, focal TS is likely to induce a varying degree of excitation within the same network[112]. This might explain why some connections were potentiated while others depressed in network 1 (**FIGURE 21A**). From a functional perspective, Hebbian plasticity is generally accepted to be a cellular mechanism for learning. If (i) repetitive stimulation results in activity-dependent learning, and (ii) information processing within a neuronal network largely depend on the collective behaviour of neuronal assemblies, rather than just the independent behaviour of single neurons, the altered dynamics of a network after repetitive stimulation should reflect a dynamic state that is more effective at processing the delivered stimuli. This suggests that

in network 1, pathways important for processing the delivered stimuli were strengthened, while pathways less important for processing the stimuli were weakened.

It should, however, be emphasised that we investigated the electrophysiological responses to dissociated cortical networks over 30min of spontaneous activity post stimulation. It is commonly agreed upon that alterations in synaptic strengths/neuronal firing needs to be lasting for at least 3 hours to be considered LTP/LTD, and subsequently indicative of learning[96]. Thus, additional recordings at later time points post stimulation would have been needed to assess if the TS-induced alterations in fact were long-lasting. However, our results do suggest that TS resulted in altered strength of specific connections, and that these alterations were visible when averaging spontaneous network activity over 30min post stimulation, suggesting at least the presence of short-term plasticity mechanisms.

Interestingly, significant stimulation-induced potentiation only occurred in network 1, while in network 2 and 3, only significant depression of specific connections could be observed (**Figure 21B** and **C**). This was surprising as applying TS, specifically at 100Hz for 1s, is generally considered to be the standard stimulation protocol for inducing LTP. To get an indication on what caused depression in our networks we would have needed to perform additional assessments on the dynamics occurring in the pre and postsynaptic areas during and after the stimulation. However, such assessments were beyond the scope of this project, thus, we can only speculate.

Effective chemical synaptic transmission depends on presynaptic neurotransmitter release into the synaptic cleft, which subsequently reacts with receptors located on the postsynaptic neuron, leading to an alteration in the postsynaptic neurons´ membrane potential. Neurotransmitters are located within synaptic vesicles at the presynaptic terminal, and these vesicles are recycled for re-use; a mechanism that exists to avoid signal transmission failure during prolonged neuronal firing as a consequence of vesicle depletion[134]. Thus, the rate of local vesicle endocytosis vs. exocytosis determines how fast pools of presynaptic vesicles are depleted. It has been reported that vesicle depletion can occur in response to prolonged presynaptic activation, and subsequently lead to synaptic depression, as presynaptic signalling efficiency is reduced[95]. Initial studies investigating LTP commonly applied *one* train of stimulation at 100Hz for 1s to induce LTP[25]. In contrast, we repetitively stimulated the same network node with 100Hz for 1s, every 10s, for 30min. In theory, this should have led to the repetitive activation of the same correlated neurons and pathways within the network every time. Thus, it is possible that presynaptic vesicle depletion occurred at some persistently activated sites, which could account for the observed decrease in correlation (depression) between specific node pairs within our networks.

Furthermore, Hebbian plasticity has largely been studied with restriction to excitatory glutamatergic synapses[26], however, plasticity mechanisms can also alter the strength of inhibitory inputs[135]. As the firing of projection neurons is highly dependent on both excitatory and inhibitory inputs, activity within inhibitory circuits is likely to affect the input-output relationship between projection neurons. Dissociated cortical networks have been reported to sustain about the same distribution of inhibitory interneurons and excitatory projection neurons (10-25% are GABAergic) as in the intact *in vivo* cortex when plated[108]. Thus, since stimulation was delivered through an arbitrary central electrode in the current experiment, it is possible that TS mainly targeted one or several inhibitory

interneurons in some of our networks. Excitation of inhibitory neurons would be expected to cause local synaptic inhibition through the release of GABA[58], making the postsynaptic neuron(s) less likely to fire an action potential. This could potentially account for why only depression occurred in network 2 and 3; activated interneurons may repeatedly have supressed excitatory transmission, leading to depression of specific connections between projection neurons. Several reports have emphasised the importance of considering the dynamic interplay between inhibitory and excitatory synaptic inputs when studying synaptic plasticity in neuronal circuits[104,135,136]. In addition, support for potential stimulation of interneuron(s) comes from our immunolabeling against one of the two isoforms of the enzyme glutamate decarboxylase, i.e. GAD65, which is involved in GABA synthesis, and thus is a marker for GABAergic interneurons. The immunolabeling revealed the presence of a high number of interneurons expressing GAD65, distributed evenly throughout the *in vitro* cortical networks cultured on the IBIDI (**SUPPLEMENTARY FIGURE 1**).

It should also be noted that due to the fluctuating spontaneous activity within *in vitro* cortical networks, a challenge with such a platform for investigating stimulation-induced plasticity is that some evoked responses might be swamped by the ongoing spontaneous network activity [110,132]. Based on the performed stability test (**FIGURE 19**), we estimated that an average alteration in connection strengths of $r>0.1$ or $r<-0.1$ was unlikely to occur without manipulation. If this set limit was too strict, it is possible that the stimulation did induce mild potentiation in network 2 and 3, but that these alterations went unnoticed. On the contrary, if the stability estimate was too liberal, the lack of potentiation in networks 2 and 3 might indicate that the TS was unable to induce lasting changes in these networks. The observed significant depressions could then be a consequence of spontaneous fluctuations in activity patterns rather than depression induced by TS. In fact, a comprehensive study[137] involving 112 experiments on 18 dissociated cortical cultures, testing a number of tetani-based stimulation protocols, reported that all but one of these protocols were unsuccessful in inducing plastic alterations in neuronal activity. Among their suggestions on why eliciting plasticity in dissociated cortical networks potentially is challenging was that, due to a general high occurrence of spontaneous bursting activity within such networks, a great number of synapses might already be saturated. They conclude that supressing bursting activity prior to the delivery of TS is a necessity if wanting to induce plasticity[137,138]. While our results from network 1 does suggest that suppressing bursting activity prior TS is not required to induce potentiation in all instances, synaptic saturation might explain the lack of potentiation in networks 2 and 3 (**FIGURE 21)**.

As with the nature (potentiation vs. depression), the magnitude (i.e. the nr.) of altered connections also varied substantially between the three cortical networks. While 52 connections significantly altered in strength in network 1, in networks 2 and 3 only 15 and 3 connections altered, respectively (**TABLE 3**). The fact that we observed such varying responses between the three networks implies that the effect of TS is highly dependent on the individual network´s topology, such as the underlying organization of structural and functional connectivity at the time of stimulation. Due to the assumed random organization of *in vitro* cortical networks cultured on MEAs[108], the effect of stimulation is likely to depend on the stimulated node´s influence or efficiency in eliciting responses throughout the network. Therefore, it might be that the targeted node in network 1 had a more central function within the network (the node was highly interconnected with other nodes), when compared to the targeted nodes of networks 2 and 3. The underlying structural connectivity of a network largely determines the possible patterns of functional

connectivity[74], thus, different underlying patterns of structural connectivity is likely to influence the functional effects of the stimulation.

Even though there was an observed difference in the magnitude of alterations between the networks post TS, in all three networks, most connections strengths stayed relatively stable (**Figure 21**). If the networks were characterized by a high degree of synaptic saturation prior stimulation (as discussed above), this could potentially explain the limited network-wide effects of TS. Interestingly though, Chiappalone and colleagues[114] reported limited effects of TS (20Hz) in altering effective connectivity (effective connectivity refers to the influence one node has on another node within a network), but that the effect of TS could greatly be increased if paired with low frequency stimulation (1Hz) simultaneously delivered through a separate site. In addition, the difficulty in inducing plastic alteration by a variety of TS-based stimulation protocols reported by Wagenaar and colleauges [137] questions the effectiveness of TS in inducing plasticity in dissociated cortical assemblies. Chiappalone and colleagues[114] suggested that the increased effect of pairing TS with low frequency stimuli might imply that such associative stimulus is more physiologically relevant, a reasonable hypothesis given that TS is known to rarely occur in nature.

In summary, the results of the current experiment suggest that TS at 100Hz, delivered repetitively through the same central electrode on the MEA, alters the functional connectivity of *in vitro* cortical networks. However, the alteration in connectivity appears highly unpredictable and uncontrolled, i.e. both the nature (potentiation vs. depression) and magnitude of change (nr. of altered connections) vary greatly between similarly prepared and treated cortical cultures. Responses in network 1, i.e. both potentiation and depression of specific connections, are in line with earlier reports on the effect of focal TS [112]. An attractive hypothesis for the observed reconfiguration of functional connectivity strengths in network 1 is that focal TS resulted in a varying degree of excitation throughout the network, leading to the modification of synaptic strengths at different sites (i.e. Hebbian plasticity). The responses of network 2 and 3, i.e. only depressed connections, were surprising, and less intuitive. While many factors can contribute to synaptic depression, some which have been mentioned here, future investigations are necessary if wanting to establish which factors determine whether connections within *in vitro* cortical networks are potentiated or depressed in response to TS. Lastly, from a network-wide perspective, tetani-induced modifications in functional connectivity was limited, i.e. only a restricted number of specific connections were modified, which is in line with previous reports[114].

## 5.3. EXPERIMENT 3 – FUNCTIONAL PLASTICITY AT THE MICROSCALE

### 5.3.1. THE STC FACILITATES AXONAL GROWTH AND TRACKING OF TRAVELLING SPIKES ALONG INDIVIDUAL AXONS

With this experiment, we exploited the advancements in microfabrication and electrophysiological techniques to build a platform that successfully guided axons between compartments, enabled recordings, as well as offered possibilities for targeted stimulation of predefined pre- and postsynaptic network nodes. In contrast to our observations on the cortical networks cultured on the axotomy chips (see **Figure 13** and **Figure 16**), axonal growth through the tunnels of the STCs was observed within the first week *in vitro* (data not shown, but **Figure 22B** depicts axonal growth through the tunnels at 10DIV), which is in line with previous observations[70,71,100,120]. In addition, as four electrodes were placed within each microtunnel of the chip, we were able to track travelling spikes within the recorded data, and both signal directionality and signal source could be identified (**Figure**

**22B** and **C**). Together, these features make the STC platform a useful tool for studying axonal information processing and activity-dependent axonal and synaptic plasticity *in vitro*.

### 5.3.2. TARGETED AND TEMPORALLY ORDERED PRE- AND POSTYNAPTIC STIMULATION INDUCES ALTERATIONS IN AXONAL INFORMATION PROCESSING AND CONNECTION SPECIFIC POTENTIATION

In addition to establishing viable cortical networks on the STCs, our main objectives involved assessing neuroplastic responses to targeted and temporally ordered pre- and postsynaptic stimulation. Specifically, we wondered if a paired pulse stimulation, tailored based on the electrophysiological properties of single identified axons, could (i) modify axonal signalling, and (ii) strengthen the connection between the stimulated node pair. Our results indicate that axons can alter both their PV; measured indirectly as a decrease in mean axonal propagation delay, and their spike shape, i.e. peak spike amplitude (negative peak), as a function of the stimulation (**FIGURE 23**). In addition, compared to pre stimulation, we found an increase in the average correlation between the activity of the stimulated node pair post stimulation, suggesting connection specific potentiation (**FIGURE 24**).

Analyses of the spike data from one identified axon revealed both an immediate decrease in mean axonal propagation delay Post Stim (0.68ms), as well as a further marginal decrease at 3 Days Post Stim (0.61ms), when compared to Pre Stim (0.96ms) (**FIGURE 23B**). What mechanisms could account for this decrease? Axonal PV is known to depend on factors such as temperature and myelin thickness[8,103]. We used unmyelinated cortical axons so we can exclude this parameter. In addition, temperatures were kept constant at 37°C during the entire recording and stimulation period, so we can also exclude this parameter (however, some fluctuations may have occurred). Other factors that have been reported to influence axonal PV are axon morphology, such as axon diameter, and axonal ion channel density and kinetics[103,139].

Action potential propagation is highly dependent on the activation of voltage-gated sodium channels located along the axon membrane. After an action potential is initiated, propagation occurs by sodium currents depolarizing the axonal membrane ahead of the active site, while the repolarization phase of the action potential is determined by the opening of voltage-gated potassium channels, leading to potassium efflux[139]. Sodium channels exist in closed (rest), open and inactivated states[140]. Upon sufficient membrane depolarization, sodium channels transit from a resting to an open state; the channel´s pores open which leads to sodium influx and further depolarization of the axonal membrane. The open state corresponds to the rising phase of the action potential. At the peak of the action potential, sodium channels enter an inactive state; the channels inactivate themselves by closing their inactivation gate blocks, which stops further sodium influx. Importantly, repolarization of the membrane is required for sodium channels to re-enter a resting state, which will allow them to open again as a consequence of further depolarization[140]. The specifics of the sodium channel kinetics are important for the directionality of action potential propagation but do also influence action potential shape and propagation speed[102]. For example, studies have reported an activity-dependent decrease in both axonal PV[141] and spike amplitude[142] in unmyelinated axons in response to repetitive axonal electrical stimulation. This decrease has been suggested to reflect the proportion of sodium channels that are inactive, i.e. an activity-dependent decline in the

number of available sodium channels as a consequence of repetitive depolarization may result in decreased PV and spike amplitude[103,141].

Interestingly, it has been reported that the kinetics of sodium channels can alter in response to activity. Studying rat hippocampal neurons *in vitro*, Ganguly and colleagues[143] stimulated a postsynaptic neuron such that it fired in synchrony with a presynaptic neuron. The increased correlated neuronal firing resulted in LTP, but also in increased presynaptic excitability. The altered presynaptic excitability was thought to have occurred partly due to modifications of the gating kinetics of voltage-gated sodium channels. Both an increase in the probability of sodium channels to open (i.e. lower membrane depolarization necessary to trigger sodium channel activation) and a lower probability of sodium channels to enter an inactive state (i.e. inactivation occurred at a more positive membrane potential) were observed as a result of increased correlated firing between the pre- and postsynaptic neurons. Though Ganguly and colleagues[143] did not specifically look at axonal PV or spike amplitude, such alterations in the sodium channels' gating kinetics are likely to affect both. For example, inactivation at a more positive membrane potential can increase spike amplitude and will result in a higher number of sodium channels available during repetitive depolarization, thus, potentially also affect axonal PV. In addition, axonal PV will increase with a lower threshold for AP initiation; a lowering firing threshold would reduce the total propagation time between adjacent sites by reducing the time required to reach threshold at each site[8,144]. Indirect support that such alterations might have occurred in the current experiment comes from our results showing that repetitive paired pulse stimulation induced increased correlated firing between the stimulated pre- and postsynaptic node (**Figure 24**). Since sodium channels actively propagate action potentials, alterations in their kinetics could alter action potential shape and axonal PV within minutes, making alterations in sodium channel kinetics an attractive hypothesis for our observations Post Stim (**Figure 23b** and **c**). However, we did not look into potential alterations in the kinetics of sodium-channels in the current experiment, and short-term alterations in axonal PV and spike shape might occur due to other mechanisms, such as alterations in the kinetics of voltage-gated potassium channels[102,145] and/or modifications of axonal membrane composition[102,103].

Most research looking at plastic alterations in axonal PV and spike amplitude have focused on short-term dynamics. Interestingly, we found that the observed decrease in axonal propagation delay Post Stim was maintained, and even further marginally decreased at 3 Days Post Stim (**Figure 23b**). In addition, compared to Post Stim, mean peak spike amplitude had also increased further at 3 Days Post Stim (**Figure 23c**). These results suggest activity-dependent long-term modifications of axonal signalling. While short-term dynamics, such as the alterations in axonal signalling Post Stim discussed above, are likely to arise from axonal physical properties, and from ion channel mechanisms and modulation, at longer time scales, alterations may also be a result of modifications in the expression of axonal membrane proteins and/or morphology[102]. For example, increased axonal diameter will result in less electrical resistance, thus, facilitating a more rapid spread of the electrical current[139], potentially accounting for the observed decrease in axonal propagation delay 3 Days Post Stim. Synthesis and transport of new receptor proteins will increase the number/density of voltage-gated ion channels at specific sites along the axonal membrane. A larger number of sodium channels can facilitate a more rapid depolarisation[8], which can increase axonal PV and spike amplitude. It should however be noted that Habibey and colleagues[100] reported a positive correlation between axonal PV and age in culture. We did not control for age in the current experiment; thus,

we cannot rule out the alterations in axonal signalling observed at 3 Days Post Stim to be an age-related phenomenon.

As mentioned, not only alterations in axonal signalling were observed; we also found that the paired pulse stimulation induced an increase in the correlation of the firing pattern between the stimulated node pair (**Figure 24**). Assuming we correctly calculated the propagation delay for the targeted axon, the effect of the pulse delivered to the presynaptic node would be amplified by the pulse delivered to the postsynaptic node, thereby artificially increasing the influence the presynaptic node had on the postsynaptic node. In STDP, synaptic potentiation or depression depends on the temporal order of pre- and postsynaptic activation[92]. If the presynaptic neuron fires prior, within a short time interval, or at the same time as the postsynaptic neuron, synaptic potentiation occurs. If the temporal order is reversed, depression is favoured. Therefore, an attractive explanation for the observed potentiation between the two stimulated nodes are STDP.

In the current experiment, only one cortical network was stimulated, reducing the generalizability of the results. In addition, the spatial signal resolution of the STC is limited, making the number of neurons directly influenced by the paired pulse stimulation protocol unknown. Furthermore, we cannot be entirely sure that we in fact managed to target the identified axon with the stimulation as this would require us to know that the presynaptic neuron´s soma or axon were in close enough proximity to the first simulation electrode, and that the postsynaptic target neuron(s) were in close enough proximity to the target stimulation electrode. Due to time constraints, immunoassay labelling against neuron-specific markers was not performed, which would have provided additional information on the structural properties of the network. However, the stimulation was specifically tailored based on information processing of one identified axon, and the immediate alterations in the axon´s signalling properties strongly suggest that the stimulation in fact targeted the identified axon. Therefore, even though other neurons are likely to have been influenced by the stimulation, it is reasonable to assume that the observed potentiation between the stimulation node pair included connections of the neuron of interest.

### 5.3.3. FUNCTIONAL IMPACT ON NEURONAL NETWORKS

The results from the current experiment, as well as several other reports[8,103,139,146], stress the importance of considering the role of axons, and not only synapses and dendrites, in neuronal computation and plasticity. Axonal PV determines the timing of which neuronal networks communicate and consequently influences the relationship between pre- and postsynaptic activity. Therefore, alterations in axonal PV will have implications on the relative timing of presynaptic and postsynaptic spiking, with small changes potentially determining the nature of STDP-induced alteration in synaptic strength. In addition, the possibility of varying the timing and speed of information flow in neuronal circuits add diversity and extend the timescales at which computations can occur and information can be processed[139]. Furthermore, the possibility of axons to alter the shape of the action potential in response to activity, such as the signal amplitude, emphasises that the action potential is not an all-or-none event, but important for neuronal computation. The depolarization caused by an action potential arriving at a presynaptic terminal is directly linked with the amount of neurotransmitter release, and an increase in spike amplitude increases membrane depolarization and subsequent neurotransmitter release, which consequently determines the signal strength[103].

Furthermore, our results suggest a strong link between axonal plasticity and synaptic plasticity as the same paired pulse stimulation resulted in both alteration in axonal signalling as well as the strengthening of the connection between the stimulated nodes (**Figure 23** and **Figure 24**). Above, we focused on how activity-dependent alterations in axonal PV and action potential shape can effect synaptic transmission and plasticity, however, several studies have reported that alterations in axonal signalling[101] or presynaptic excitability[143] depend on synaptic transmission to occur (suggesting retrograde signalling from the postsynaptic neuron targeting the presynaptic neuron)[8]. This highlights an intricate relationship between axonal and synaptic plasticity, where alterations in one can induce alterations in the other. In addition, if the long-term alterations in axonal signalling observed in the current experiment were induced by the stimulation, this suggests that not only synapses, but potentially also axons, can store information, suggesting a role of axons in learning, memory, and recovery after injury.

### 5.4. HARNESSING CNS PLASTICITY TO RESTORE FUNCTION AFTER INJURY

Both rehabilitative training and electrical stimulation (both non-invasive and invasive) are currently used as strategies for restoring lost function after CNS injury and disease[147]. Many of these strategies are showing promising results and the functional gain associated with such strategies are commonly attributed to the underlying idea of activity-dependent neuroplasticity[147]; increased correlated neuronal firing results in learning while inactivity results in functional loss. However, neuroplasticity is complex, and several factors increase its complexity; injury, disease, age, maladaptive plasticity, area-dependent neuroplastic changes to mention a few[148]. Therefore, there is a great need for a better understanding of which exact mechanisms are essential for recovery, such that more accurate and targeted rehabilitation strategies can be developed.

For example, with this project we have shown that focal TS delivered to cortical networks through a fixed electrode results in functional alterations of specific connections, but that the cortical network responses are highly variable and unpredictable between different, but similarly treated, networks (i.e. experiment 2). This emphasises the complexity of neuroplasticity, and that the underlying structural and functional connectivity of a given cortical network, are highly important in determining the effects of electrical stimulation. In contrast, with the paired pulse stimulation used in experiment 3, which was designed based on the electrophysiological signalling properties of one identified axon, we successfully strengthened a targeted connection within the network. In the light of an incomplete SCI for example, such targeted strengthening could potentially increase the weight of spared connections between the brain and the spinal cord, potentially facilitating more efficient communication between the two areas. In addition, our results suggest that axons can alter their signalling and potentially also store information, which makes axons, and not only synapses a potentially relevant target in stimulation-induced rehabilitation.

# 6. CONCLUSION

Due to the complex pathophysiology of traumatic CNS injuries, and the limited intrinsic repair capacity of the adult CNS, successful therapies for TBI and SCI are likely to involve a set of different interventions targeting different aspects of such injuries. One such intervention is likely to involve limiting the spread of neurodegeneration after the initial injury. By the use of microfluidic axotomy chips, experiment 1 set out to investigate one injury aspect associated with TBI and SCI, namely axonal injury. Specifically, we wanted to assess the effects of GABA stimulation on cortical neuronal survival and oxidative stress response immediately after *in vitro* axotomy. However, no axonal growth was observed within the microtunnels throughout the experimental timeframe. As a consequence, we were not able to precede with the first experiment. Future investigations are left for assessing the effect(s) of extracellular GABA addition after *in vitro* axotomy.

Rehabilitative exercise and/or electrical stimulation, which harness the plastic CNS environment, have developed as strategies for restoring function after a traumatic CNS injury. To be able to enhance the functional gains of such strategies, there is a need for a greater understanding of mechanism of neuroplasticity. We approached this need with experiment 2 and 3.

Experiment 2 involved assessing the neuroplastic response of *in vitro* cortical networks to repetitive focal TS delivered through a fixed central electrode on the MEAs. We have shown through electrophysiological measures that focal TS appears to alter the strength of specific functional connections within the neuronal networks. Though the exact same electrical stimulation was delivered to all three cortical networks used in this experiment, the alterations in connection strengths were highly variable between the networks. This indicates that the underlying structural and function connectivity of each individual network at the time of stimulation are highly influential in determining both the nature (potentiation vs. depression) and the magnitude (nr. of altered connections) of tetani-induced modifications. Which mechanisms determine the magnitude and nature of a network´s responses to focal TS are left for future work.

Experiment 3 investigated functional *in vitro* neuroplasticity at the microscale, by the use of custom-designed microfluidic STCs. After identifying the signal properties of one cortical axon, we tailored a paired pulse stimulation protocol targeting this particular axon. We showed that axons can alter both their PV and spike amplitude as a function of the stimulation, and that the alterations were maintained and further altered several days after stimulation. In addition, the paired pulse stimulation induced increased correlated firing between the stimulated node pair, likely due to mechanisms of STDP. This indicates an intricate relationship between axonal and synaptic plasticity and emphasise the potential role of axons in both neuronal computation and plasticity.

The *in vitro* approach taken in this project has enabled the investigations of specific aspects of cortical neuroplasticity. The current findings add to the body of research aiming to increase our understanding of both micro- and mesoscale neuroplasticity. While the *in vitro* environment, healthy or injured, is unable to mimic every aspect of what´s occurring *in vivo*, *in vitro* models of neuroplasticity offer new insights into specific aspects of neuroplasticity, and may in that way facilitate the development of rehabilitation strategies aiming to promote lost function after CNS injury.

# 7. REFERENCES


1. Azevedo, F. A. C. *et al.* Equal numbers of neuronal and nonneuronal cells make the human brain an isometrically scaled-up primate brain. *J. Comp. Neurol.* **513**, 532–541 (2009).
2. Singer, W. The brain as a self-organizing system. *Eur. Arch. Psychiatry Neurol. Sci.* **236**, 4–9 (1986).
3. Sporns, O. Structure and function of complex brain networks. *Dialogues Clin. Neurosci.* **15**, 247–262 (2013).
4. Batista-García-Ramó, K. & Fernández-Verdecia, C. I. What we know about the brain structure-function relationship. *Behav. Sci.* **8**, (2018).
5. Park, H. J. & Friston, K. Structural and functional brain networks: From connections to cognition. *Science* **342**, 1238411 (2013).
6. Han, W. & Šestan, N. Cortical projection neurons: Sprung from the same root. *Neuron* **80**, 1103–1105 (2013).
7. Lodato, S., Shetty, A. S. & Arlotta, P. Cerebral cortex assembly: Generating and reprogramming projection neuron diversity. *Trends Neurosci.* **38**, 117–125 (2015).
8. Debanne, D., Campanac, E., Bialowas, A., Carlier, E. & Alcaraz, G. Axon physiology. *Physiol. Rev.* **91**, 555–602 (2011).
9. Stoeckli, E. T. Understanding axon guidance: Are we nearly there yet? *Development* **145**, dev151415 (2018).
10. Ming, G. L., Henley, J., Tessier-Lavigne, M., Song, H. J. & Poo, M. M. Electrical activity modulates growth cone guidance by diffusible factors. *Neuron* **29**, 441–452 (2001).
11. Bellon, A. & Mann, F. Keeping up with advances in axon guidance. *Curr. Opin. Neurobiol.* **53**, 183–191 (2018).
12. Gangatharan, G., Schneider-Maunoury, S. & Breau, M. A. Role of mechanical cues in shaping neuronal morphology and connectivity. *Biol. Cell* **110**, 125–136 (2018).
13. Munno, D. W. & Syed, N. I. Synaptogenesis in the CNS: An odyssey from wiring together to firing together. *J. Physiol.* **552**, 1–11 (2003).
14. Connors, B. W. & Long, M. A. Electrical Synapses in the Mammalian Brain. *Annu. Rev. Neurosci.* **27**, 393–418 (2004).
15. Südhof, T. C. Towards an understanding of synapse formation. *Neuron* **100**, 276–293 (2018).
16. Tessier, C. R. & Broadie, K. Activity-dependent modulation of neural circuit synaptic connectivity. *Front. Mol. Neurosci.* **2**, 8 (2009).
17. Tierney, A. L. & Nelson, C. A. Brain development and the role of experience in the early years. *Zero Three* **30**, 9–13 (2009).
18. Castellani, V. Building spinal and brain commissures: Axon guidance at the midline. *ISRN Cell Biol.* **2013**, 315387 (2013).
19. Goodman, C. S. & Shatz, C. J. Developmental mechanisms that generate precise patterns of neuronal connectivity. *Cell* **72 Suppl**, 77–98 (1993).
20. Katz, L. C. & Shatz, C. J. Synaptic activity and the construction of cortical circuits. *Science* **274**, 1133–1138 (1996).
21. Ganguly, K. & Poo, M.-M. Activity-dependent neural plasticity from bench to bedside. *Neuron* **80**, 729–741 (2013).
22. Carulli, D., Foscarin, S. & Rossi, F. Activity-dependent plasticity and gene expression modifications in the adult NS. *Front. Mol. Neurosci.* **4**, 50 (2011).
23. Wiesel, T. N. & Hubel, D. H. Single-cell responses in striate cortex of kittens deprived of vision in one eye. *J. Neurophysiol.* **26**, 1003–1017 (1963).
24. Le vay, S., Wiesel, T. N. & Hubel, D. H. The development of ocular dominance columns in normal and visually deprived monkeys. *J. Comp. Neurol.* **191**, 1–51 (1980).
25. Bliss, T. V. & Lømo, T. Long-lasting potentiation of synaptic transmission in the dentate area of the unanaesthetized rabbit following stimulation of the perforant path. *J. Physiol.* **232**, 357–374 (1973).
26. Sjöström, P. J., Rancz, E. A., Roth, A. & Häusser, M. Dendritic excitability and synaptic plasticity. *Physiol. Rev.* **88**, 769–840 (2008).

27. Wittenberg, G. F. Experience, cortical Remapping, and recovery in Brain Disease. *Neurobiol. Dis.* **37**, 252 (2010).
28. Chen, M. & Zheng, B. Axon plasticity in the mammalian central nervous system after injury. *Trends Neurosci.* **37**, 583–593 (2014).
29. Prins, M., Greco, T., Alexander, D. & Giza, C. C. The pathophysiology of traumatic brain injury at a glance. *Dis. Model. Mech.* **6**, 1307–1315 (2013).
30. Oyinbo, C. A. Secondary injury mechanisms in traumatic spinal cord injury: a nugget of this multiply cascade. *Acta Neurobiol. Exp.* **71**, 281–299 (2011).
31. Medana, I. M. & Esiri, M. M. Axonal damage: A key predictor of outcome in human CNS diseases. *Brain* **126**, 515–530 (2003).
32. Menon, D. K., Schwab, K., Wright, D. W. & Maas, A. I. Position statement: Definition of traumatic brain injury. *Arch. Phys. Med. Rehabil.* **91**, 1637–1640 (2010).
33. Hill, C. S., Coleman, M. P. & Menon, D. K. Traumatic axonal injury: Mechanisms and translational opportunities. *Trends Neurosci.* **39**, 311–324 (2016).
34. Smith, D. H. & Meaney, D. F. Axonal damage in traumatic brain injury. *Neuroscientist* **6**, 483–495 (2000).
35. Alizadeh, A., Dyck, S. M. & Karimi-Abdolrezaee, S. Traumatic spinal cord injury: An overview of pathophysiology, models and acute injury mechanisms. *Front. Neurol.* **10**, 282 (2019).
36. Kaur, P. & Sharma, S. Recent advances in pathophysiology of traumatic brain injury. *Curr. Neuropharmacol.* **16**, 1224–1238 (2018).
37. Rosell, A. L. & Neukomm, L. J. Axon death signalling in Wallerian degeneration among species and in disease. *Open Biol.* **9**, 190118 (2019).
38. Coleman, M. Axon degeneration mechanisms: Commonality amid diversity. *Nat. Rev. Neurosci.* **6**, 889–898 (2005).
39. Neukomm, L. J. & Freeman, M. R. Diverse cellular and molecular modes of axon degeneration. *Trends Cell Biol.* **24**, 515–523 (2014).
40. Wang, J. T., Medress, Z. A. & Barres, B. A. Axon degeneration: Molecular mechanisms of a self-destruction pathway. *J. Cell Biol.* **196**, 7–18 (2012).
41. Kerschensteiner, M., Schwab, M. E., Lichtman, J. W. & Misgeld, T. In vivo imaging of axonal degeneration and regeneration in the injured spinal cord. *Nat. Med.* **11**, 572–577 (2005).
42. Tsao, J. W., Brown, M. C., Carden, M. J., McLean, W. G. & Perry, V. H. Loss of the compound action potential: an electrophysiological, biochemical and morphological study of early events in axonal degeneration in the C57BL/Ola mouse. *Eur. J. Neurosci.* **6**, 516–524 (1994).
43. Waller, A. Experiments on the section of the glossopharyngeal and hypoglossal nerves of the frog , and observations of the alterations produced thereby in the structure of their primitive fibres. *Philos. Trans. R. Soc. London* **140**, 423–429 (1850).
44. Siddique, R. & Thakor, N. Investigation of nerve injury through microfluidic devices. *J. R. Soc. Interface* **11**, 20130676 (2014).
45. Maday, S., Twelvetrees, A. E., Moughamian, A. J. & Holzbaur, E. L. F. Axonal transport: Cargo-specific mechanisms of motility and regulation. *Neuron* **84**, 292–309 (2014).
46. Johnson, V. E., Stewart, W. & Smith, D. H. Axonal pathology in traumatic brain injury. *Exp. Neurol.* **246**, 35–43 (2013).
47. Lüscher, C. & Malenka, R. C. NMDA Receptor-Dependent Long-Term Potentiation and Long-Term Depression (LTP/LTD). *Cold Spring Harb. Perspect. Biol.* **4**, a005710 (2012).
48. Guerriero, R. M., Giza, C. C. & Rotenberg, A. Glutamate and GABA imbalance following traumatic brain injury. *Curr. Neurol. Neurosci. Rep.* **15**, 27 (2015).
49. Velasco, M. *et al.* Excitotoxicity: An organized crime at the cellular level. *J. Neurol. Neurosci.* **8**, 193 (2017).
50. Yi, J. H. & Hazell, A. S. Excitotoxic mechanisms and the role of astrocytic glutamate transporters in traumatic brain injury. *Neurochem. Int.* **48**, 394–403 (2006).
51. Cornelius, C. *et al.* Traumatic brain injury: Oxidative stress and neuroprotection.

*Antioxidants Redox Signal.* **19**, 836–853 (2013).
52. Ott, M., Gogvadze, V., Orrenius, S. & Zhivotovsky, B. Mitochondria, oxidative stress and cell death. *Apoptosis* **12**, 913–922 (2007).
53. Frati, A. *et al.* Diffuse axonal injury and oxidative stress: A comprehensive review. *Int. J. Mol. Sci.* **18**, 2600 (2017).
54. Bedi, S. S., Cai, D. & Glanzman, D. L. Effects of axotomy on cultured sensory neurons of Aplysia: Long-term injury-induced changes in excitability and morphology are mediated by different signaling pathways. *J. Neurophysiol.* **100**, 3209–3224 (2008).
55. Nagendran, T. *et al.* Distal axotomy enhances retrograde presynaptic excitability onto injured pyramidal neurons via trans-synaptic signaling. *Nat. Commun.* **8**, 625 (2017).
56. Ikonomidou, C. & Turski, L. Why did NMDA receptor antagonists fail clinical trials for stroke and traumatic brain injury? *Lancet Neurol.* **1**, 383–386 (2002).
57. Schwartz-Bloom, R. D. & Sah, R. γ-aminobutyric acid A neurotransmission and cerebral ischemia. *J. Neurochem.* **77**, 353–371 (2001).
58. Wu, C. & Sun, D. GABA receptors in brain development, function, and injury. *Metab. Brain Dis.* **30**, 367–379 (2015).
59. Galeffi, F., Sinnar, S. & Schwartz-Bloom, R. D. Diazepam promotes ATP recovery and prevents cytochrome c release in hippocampal slices after in vitro ischemia. *J. Neurochem.* **75**, 1242–1249 (2000).
60. Mazzone, G. L. & Nistri, A. Modulation of extrasynaptic GABAergic receptor activity influences glutamate release and neuronal survival following excitotoxic damage to mouse spinal cord neurons. *Neurochem. Int.* **128**, 175–185 (2019).
61. Zhou, C. *et al.* Neuroprotection of γ-aminobutyric acid receptor agonists via enhancing neuronal nitric oxide synthase (Ser847) phosphorylation through increased neuronal nitric oxide synthase and PSD95 interaction and inhibited protein phosphatase activity in cerebral is. *J. Neurosci. Res.* **86**, 2973–2983 (2008).
62. Hilton, B. J. & Bradke, F. Can injured adult CNS axons regenerate by recapitulating development? *Development* **144**, 3417–3429 (2017).
63. Akbik, F., Cafferty, W. B. J. & Strittmatter, S. M. Myelin Associated Inhibitors: A Link Between Injury-Induced and Experience-Dependent Plasticity. *Exp. Neurol.* **235**, 43–52 (2012).
64. Fawcett, J. W. The struggle to make CNS axons regenerate: why has it been so difficult? *Neurochem. Res.* **45**, 144–158 (2020).
65. Kawano, H. *et al.* Role of the lesion scar in the response to damage and repair of the central nervous system. *Cell Tissue Res.* **349**, 169–180 (2012).
66. Quraishe, S., Forbes, L. H. & Andrews, M. R. The extracellular environment of the CNS: Influence on plasticity, sprouting, and axonal regeneration after spinal cord injury. *Neural Plast.* **2018**, 2952386 (2018).
67. Koseki, H. *et al.* Selective rab11 transport and the intrinsic regenerative ability of CNS axons. *Elife* **6**, e26956 (2017).
68. Morrison, B., Saatman, K. E., Meaney, D. F. & McIntosh, T. K. In vitro central nervous system models of mechanically induced trauma: A review. *J. Neurotrauma* **15**, 911–928 (1998).
69. Park, J. W., Vahidi, B., Taylor, A. M., Rhee, S. W. & Jeon, N. L. Microfluidic culture platform for neuroscience research. *Nat. Protoc.* **1**, 2128–2136 (2006).
70. Taylor, A. M. *et al.* Microfluidic multicompartment device for neuroscience research. *Langmuir* **19**, 1551–1556 (2003).
71. Taylor, A. M. *et al.* A microfluidic culture platform for CNS axonal injury, regeneration and transport. *Nat. Methods* **2**, 599–605 (2005).
72. Shrirao, A. B. *et al.* Microfluidic platforms for the study of neuronal injury in vitro. *Biotechnol. Bioeng.* **115**, 815–830 (2018).
73. Park, H.-J. & Firston, K. Structural and functional brain networks: From onnections to cognition. *Science* **342**, 1238411 (2013).
74. Bullmore, E. & Sporns, O. Complex brain networks: Graph theoretical analysis of structural and functional systems. *Nat. Rev. Neurosci.* **10**, 186–198 (2009).

75. Witteveen, T. The effect of tetanic stimulation on functional connectivity. (University of Twente, 2011).
76. Bareyre, F. M. *et al.* The injured spinal cord spontaneously forms a new intraspinal circuit in adult rats. *Nat. Neurosci.* **7**, 269–277 (2004).
77. Weidner, N., Ner, A., Salimi, N. & Tuszynski, M. H. Spontaneous corticospinal axonal plasticity and functional recovery after adult central nervous system injury. *Proc. Natl. Acad. Sci. U. S. A.* **98**, 3513–3518 (2001).
78. Nudo, R. J. Recovery after brain injury: Mechanisms and principles. *Front. Hum. Neurosci.* **7**, 887 (2013).
79. Fouad, K., Pedersen, V., Schwab, M. E. & Brösamle, C. Cervical sprouting of corticospinal fibers after thoracic spinal cord injury accompanies shifts in evoked motor responses. *Curr. Biol.* **11**, 1766–1770 (2001).
80. Hylin, M. J., Kerr, A. L. & Holden, R. Understanding the mechanisms of recovery and/or compensation following injury. *Neural Plast.* **2017**, 7125057 (2017).
81. Torres-Espín, A., Beaudry, E., Fenrich, K. & Fouad, K. Rehabilitative training in animal models of spinal Cord injury. *J. Neurotrauma* **35**, 1970–1985 (2018).
82. Fouad, K. & Tetzlaff, W. Rehabilitative training and plasticity following spinal cord injury. *Exp. Neurol.* **235**, 91–99 (2012).
83. Vander Linden, C., Verhelst, H., Deschepper, E., Vingerhoets, G. & Deblaere, K. Cognitive training benefit depends on brain injury location in adolescents with traumatic brain injury: A pilot study. *Eur. J. Phys. Rehabil. Med.* **55**, 585–594 (2019).
84. Nudo, R. J., Milliken, G. W., Jenkins, W. M. & Merzenich, M. M. Use-dependent alterations in movement representations in primary motor cortex of adult squirrel monkeys. **16**, 785–807 (1996).
85. Hebb, D. O. *The organization of behavior: a neurophysiological theory*. (Wiley, 1949).
86. Ito, M. & Kano, M. Long-lasting depression of parallel fiber-Purkinje cell transmission induced by conjunctive stimulation of parallel fibers and climbing fibers in the cerebellar cortex. *Neurosci. Lett.* **33**, 253–258 (1982).
87. Malinow, R., Schulman, H. & Tsien, R. W. Inhibition of postsynaptic PKC or CaMKII blocks induction but not wxpression of LTP. *Science* **245**, 862–866 (1989).
88. Bliss, T.V.P. & Collingridge, G. L. A synaptic model of memory: LTP in the hippocampus. *Nature* **361**, 31–39 (1993).
89. Bear, M. F. Long-term depression in hippocampus. *Annu. Rev. Neurosci.* **19**, 437–462 (1996).
90. Tsumoto, T. Long-term potentiation and long-term depression in the neocortex. *Prog. Neurobiol.* **39**, 209–228 (1992).
91. Levy, W. B. & Steward, O. Temporal contiguity requirements for long-term associative potentiation/depression in the hippocampus. *Neuroscience* **8**, 791–797 (1983).
92. Bi, G. Q. & Poo, M. M. Synaptic modifications in cultured hippocampal neurons: Dependence on spike timing, synaptic strength, and postsynaptic cell type. *J. Neurosci.* **18**, 10464–10472 (1998).
93. Wang, H. X., Gerkin, R. C., Nauen, D. W. & Bi, G. Q. Coactivation and timing-dependent integration of synaptic potentiation and depression. *Nat. Neurosci.* **8**, 187–193 (2005).
94. Sjöström, P. J., Turrigiano, G. G. & Nelson, S. B. Rate, timing, and cooperativity jointly determine cortical synaptic plasticity. *Neuron* **32**, 1149–1164 (2001).
95. Hennig, M. H. Theoretical models of synaptic short term plasticity. *Front. Comput. Neurosci.* **7**, 45 (2013).
96. Ramiro-Cortés, Y., Hobbiss, A. F. & Israely, I. Synaptic competition in structural plasticity and cognitive function. *Philos. Trans. R. Soc. B Biol. Sci.* **369**, 20130157 (2014).
97. Lewandowska, M. K., Radivojević, M., Jäckel, D., Müller, J. & Hierlemann, A. R. Cortical axons, isolated in channels, display activity-dependent signal modulation as a result of targeted stimulation. *Front. Neurosci.* **10**, 83 (2016).

98. Lewandowska, M. K., Bakkum, D. J., Rompani, S. B. & Hierlemann, A. Recording large extracellular spikes in microchannels along many axonal sites from individual neurons. *PLoS One* **10**, e0118514 (2015).
99. Shimba, K., Sakai, K., Isomura, T., Kotani, K. & Jimbo, Y. Axonal conduction slowing induced by spontaneous bursting activity in cortical neurons cultured in a microtunnel device. *Integr. Biol.* **7**, 64–72 (2015).
100. Habibey, R. *et al.* A multielectrode array microchannel platform reveals both transient and slow changes in axonal conduction velocity. *Sci. Rep.* **7**, 8558 (2017).
101. Bakkum, D. J., Chao, Z. C. & Potter, S. M. Long-term activity-dependent plasticity of action potential propagation delay and amplitude in cortical networks. *PLoS One* **3**, e2088 (2008).
102. Bucher, D. & Goaillard, J. M. Beyond faithful conduction: Short-term dynamics, neuromodulation, and long-term regulation of spike propagation in the axon. *Prog. Neurobiol.* **94**, 307–346 (2011).
103. Debanne, D. Information processing in the axon. *Nat. Rev. Neurosci.* **5**, 304–316 (2004).
104. Marder, C. P. & Buonomano, D. V. Timing and balance of inhibition enhance the effect of long-term potentiation on cell firing. *J. Neurosci.* **24**, 8873–8884 (2004).
105. Jones, I. L. *et al.* The potential of microelectrode arrays and microelectronics for biomedical research and diagnostics. *Anal. Bioanal. Chem.* **399**, 2313–2329 (2011).
106. Poli, D., Pastore, V. P. & Massobrio, P. Functional connectivity in in vitro neuronal assemblies. *Front. Neural Circuits* **9**, 57 (2015).
107. Obien, M. E. J., Deligkaris, K., Bullmann, T., Bakkum, D. J. & Frey, U. Revealing neuronal function through microelectrode array recordings. *Front. Neurosci.* **8**, 423 (2015).
108. Marom, S. & Shahaf, G. Development, learning and memory in large random networks of cortical neurons: Lessons beyond anatomy. *Q. Rev. Biophys.* **35**, 63–87 (2002).
109. Giugliano, M., Arsiero, M., Darbon, P., Streit, J. & Lüscher, H. R. Emerging network activity in dissociated cultures of neocortex: Novel electrophysiological protocols and mathematical modeling. in *Advances in Network Electrophysiology* (eds. Taketani, M. & Baudry, M.) 221–251 (Springer, 2006). doi:10.1007/0-387-25858-2_10
110. Massobrio, P., Tessadori, J., Chiappalone, M. & Ghirardi, M. In vitro studies of neuronal networks and synaptic plasticity in invertebrates and in mammals using multielectrode arrays. *Neural Plast.* **2015**, 196195 (2015).
111. Stegenga, J., Le Feber, J., Marani, E. & Rutten, W. L. C. Analysis of cultured neuronal networks using intraburst firing characteristics. *IEEE Trans. Biomed. Eng.* **55**, 1382–1390 (2008).
112. Jimbo, Y., Tateno, T. & Robinson, H. P. C. Simultaneous induction of pathway-specific potentiation and depression in networks of cortical neurons. *Biophys. J.* **76**, 670–678 (1999).
113. Maeda, E., Kuroda, Y., Robinson, H. P. C. & Kawana, A. Modification of parallel activity elicited by propagating bursts in developing networks of rat cortical neurones. *Eur. J. Neurosci.* **10**, 488–496 (1998).
114. Chiappalone, M., Massobrio, P. & Martinoia, S. Network plasticity in cortical assemblies. *Eur. J. Neurosci.* **28**, 221–237 (2008).
115. Le Feber, J., Stegenga, J. & Rutten, W. L. C. The effect of slow electrical stimuli to achieve learning in cultured networks of rat cortical neurons. *PLoS One* **5**, e8871 (2010).
116. Kanagasabapathi, T. T., Ciliberti, D., Martinoia, S., Wadman, W. J. & Decré, M. M. J. Dual-compartment neurofluidic system for electrophysiological measurements in physically segregated and functionally connected neuronal cell culture. *Front. Neuroeng.* **4**, 13 (2011).
117. Takayama, Y. & Kida, Y. S. In vitro reconstruction of neuronal networks derived from human iPS cells using microfabricated devices. *PLoS One* **11**, e0148559 (2016).

118. Gladkov, A. *et al.* Design of cultured neuron networks in vitro with predefined connectivity Using asymmetric microfluidic channels. *Sci. Rep.* **7**, 15625 (2017).
119. Tong, Z. *et al.* A microfluidic neuronal platform for neuron axotomy and controlled regenerative studies. *RSC Adv.* **5**, 73457–73466 (2015).
120. van de Wijdeven, R. *et al.* A novel lab-on-chip platform enabling axotomy and neuromodulation in a multi-nodal network. *Biosens. Bioelectron.* **140**, 111329 (2019).
121. van de Wijdeven, R. *et al.* Structuring a multi-nodal neural network in vitro within a novel design microfluidic chip. *Biomed. Microdevices* **20**, 9 (2018).
122. Kim, G. H. *et al.* Recent progress on microelectrodes in neural interfaces. *Materials (Basel).* **11**, 1995 (2018).
123. Boehler, C., Stieglitz, T. & Asplund, M. Nanostructured platinum grass enables superior impedance reduction for neural microelectrodes. *Biomaterials* **67**, 346–353 (2015).
124. Wang, X. F. & Cynader, M. S. Effects of astrocytes on neuronal attachment and survival shown in a serum-free co-culture system. *Brain Res. Protoc.* **4**, 209–216 (1999).
125. Heiney, K. *et al.* µSpikeHunter: An advanced computational tool for the analysis of neuronal communication and action potential propagation in microfluidic platforms. *Sci. Rep.* **9**, 5777 (2019).
126. Yuan, A., Rao, M. V., Veeranna & Nixon, R. A. Neurofilaments at a glance. *J. Cell Sci.* **125**, 3257–3263 (2012).
127. Arora, M. Cell culture media: A review. *MATER METHODS* **3**, 175 (2013).
128. Simpson, I. A. *et al.* The facilitative glucose transporter GLUT3: 20 Years of distinction. *Am. J. Physiol. Endocrinol. Metab.* **295**, E242–E253 (2008).
129. Mergenthaler, P., Lindauer, U., Dienel, G. A. & Meisel, A. Sugar for the brain: the role of glucose in physiological and pathological brain function. *Trends Neurosci.* **36**, 587–597 (2013).
130. Jung, H., Yoon, B. C. & Holt, C. E. Axonal mRNA localization and local protein synthesis in nervous system assembly, maintenance and repair. *Nat. Rev. Neurosci.* **13**, 308–324 (2012).
131. Campenot, R. B. Local control of neurite development by nerve growth factor. *Proc. Natl. Acad. Sci. U. S. A.* **74**, 4516–4519 (1977).
132. Le Feber, J. *et al.* Conditional firing probabilities in cultured neuronal networks: A stable underlying structure in widely varying spontaneous activity patterns. *J. Neural Eng.* **4**, 54–67 (2007).
133. Potter, S. M., Wagenaar, D. A. & DeMarse, T. B. Closing the loop: Stimulation feedback systems. in *Electrophysiology: Using multi-electrode arrays* (eds. Taketani, M. & Baudry, M.) 215–252 (Springer, 2006). doi:10.1007/b136263
134. Fernández-Alfonso, T. & Ryan, T. A. The kinetics of synaptic vesicle pool depletion at CNS synaptic terminals. *Neuron* **41**, 943–953 (2004).
135. Tatti, R., Haley, M. S., Swanson, O., Tselha, T. & Maffei, A. Neurophysiology and regulation of the balance between excitation and inhibition in neocortical circuits. *Biol. Psychiatry* **81**, 821–831 (2017).
136. Chevaleyre, V. & Castillo, P. E. Heterosynaptic LTD of hippocampal GABAergic synapses: A novel role of endocannabinoids in regulating excitability. *Neuron* **38**, 461–472 (2003).
137. Wagenaar, D. A., Pine, J. & Potter, S. M. Searching for plasticity in dissociated cortical cultures on multi-electrode arrays. *J. Negat. Results Biomed.* **5**, 16 (2006).
138. Wagenaar, D. A., Madhavan, R., Pine, J. & Potter, S. M. Controlling bursting in cortical cultures with closed-loop multi-electrode stimulation. *J. Neurosci.* **25**, 680–688 (2005).
139. Alcami, P. & El Hady, A. Axonal Computations. *Front. Cell. Neurosci.* **13**, 413 (2019).
140. Bagal, S. K., Marron, B. E., Owen, R. M., Storer, R. I. & Swain, N. A. Voltage gated sodium channels as drug discovery targets. *Channels* **9**, 360–366 (2015).
141. De Col, R., Messlinger, K. & Carr, R. W. Conduction velocity is regulated by sodium channel inactivation in unmyelinated axons innervating the rat cranial meninges. *J.*

*Physiol.* **586**, 1089–1103 (2008).
142. Brody, D. L. & Yue, D. T. Release-independent short-term synaptic depression in cultured hippocampal neurons. *J. Neurosci.* **20**, 2480–2494 (2000).
143. Ganguly, K., Kiss, L. & Poo, M. M. Enhancement of presynaptic neuronal excitability by correlated presynaptic and postsynaptic spiking. *Nat. Neurosci.* **3**, 1018–1026 (2000).
144. Carp, J. S., Tennissen, A. M. & Wolpaw, J. R. Conduction velocity is inversely related to action potential threshold in rat motoneuron axons. *Exp. Brain Res.* **150**, 497–505 (2003).
145. Higgs, M. H. & Spain, W. J. Kv1 channels control spike threshold dynamics and spike timing in cortical pyramidal neurones. *J. Physiol.* **589**, 5125–5142 (2011).
146. Bucher, D. & Goaillard, J.-M. Beyond faithful conduction: short-term dynamics, neuromodulation, and long-term regulation of spike propagation in the axon. *Prog. Neurobiol.* **94**, 307–346 (2011).
147. Cramer, S. C. *et al.* Harnessing neuroplasticity for clinical applications. *Brain* **134**, 1591–1609 (2011).
148. Kolb, B. & Muhammad, A. Harnessing the power of neuroplasticity for intervention. *Front. Hum. Neurosci.* **8**, 377 (2014).

# 8. SUPPLEMENTARY

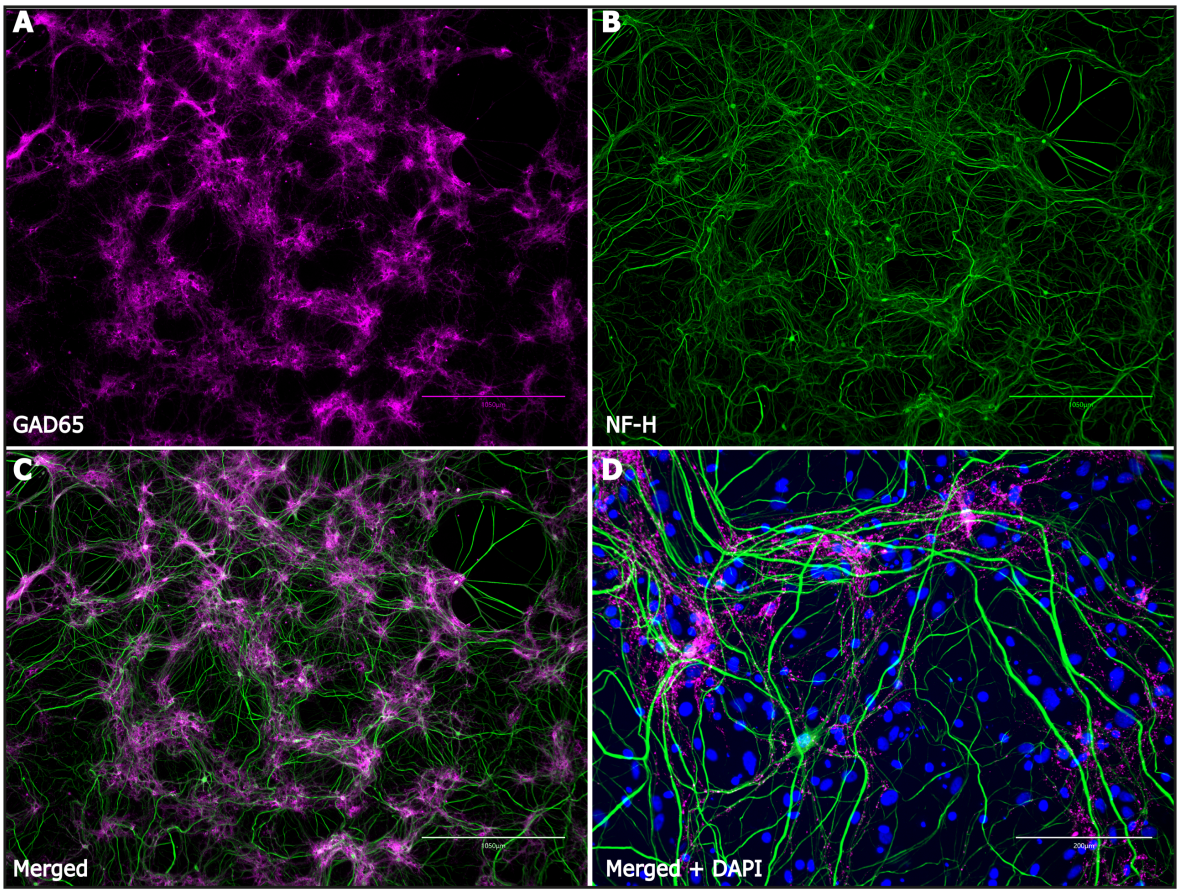


**SUPPLEMENTARY FIGURE 1. IMMUNOLABELING AGAINST GAD65 AND NF-H.**

Cortical neurons cultured on the IBIDI expressed GAD65 (magenta) and NF-H (green). **A and B)** show GAD65 and NF-H, respectively. **C)** is (A) and (B) merged. Scalebar 1050µm. Magnification 4X. **D)** DAPI nuclei stain is visualized in blue. Scalebar 200µm. Magnification 20X.

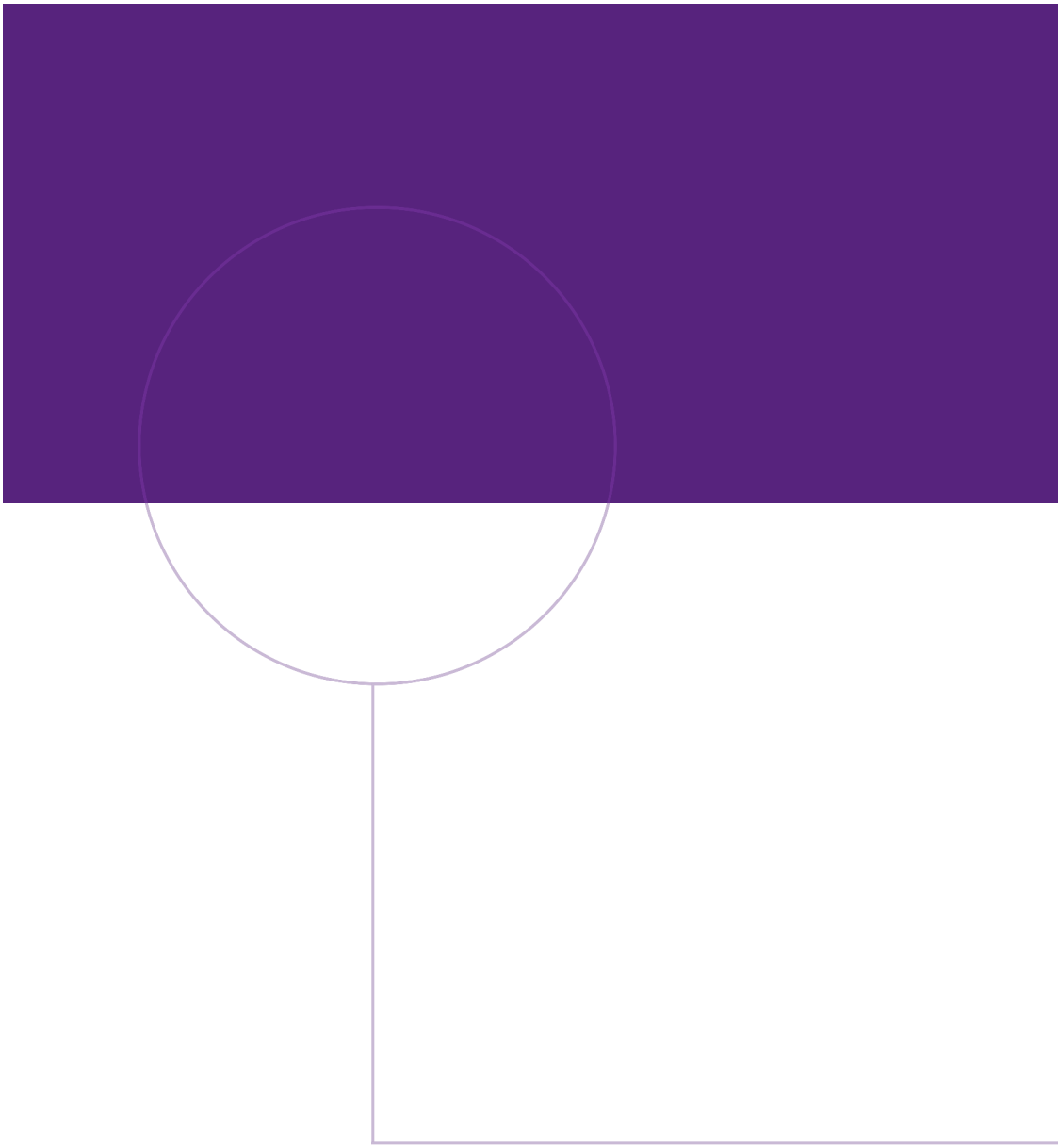

NTNU

Norwegian University of
Science and Technology